UNIVERSIDADE DE LISBOA

FACULDADE DE FARMÁCIA

Synthesis and evaluation of chemical probes to study the biology of liver stage malaria parasites

Joana Rita Leite Ribeiro

Dissertação orientada pelo Professor Doutor Rui Ferreira Alves Moreira e
Coorientada pela Doutora Rita Sofia Salvador Simões Capela

Mestrado em Química Farmacêutica e Terapêutica

2017

UNIVERSIDADE DE LISBOA

FACULDADE DE FARMÁCIA

Synthesis and evaluation of chemical probes to study the biology of liver stage malaria parasites

Joana Rita Leite Ribeiro

Dissertação orientada pelo Professor Doutor Rui Ferreira Alves Moreira e
Coorientada pela Doutora Rita Sofia Salvador Simões Capela

Mestrado em Química Farmacêutica e Terapêutica

2017

To the women of my life

Acknowledgements

Foremost, I would like to express my sincere gratitude to my supervisor Prof. Rui Moreira for the continuous support, immense knowledge and for this opportunity given to me to do the research in medicinal chemistry.

To Rita Capela, I would like to thank for your particular personality that made my days very different. I am also very grateful for scientific support, continuous guidance and encouragement. Without her, my lab work was not possible.

I would like to thank to everyone who helped me along this thesis in innumerous ways, in particular to all who are and were my laboratory colleagues in Faculdade de Farmácia.

A special thanks to Daniela Coutinho and Andreia Gonçalves who not only gave me enjoyable moments throughout my thesis as they supported all my difficult days and all my frustrations. I feel very privileged in having your friendship.

Finally, I must express my very profound gratitude to my mother, my daughter, my brother and all my friends for providing me with unfailing support and continuous encouragement throughout my years of study. This accomplishment would not have been possible without them.

Abstract

Malaria remains one of the most prevalent and life-threatening diseases. It is caused by infection with parasites of the genus *Plasmodium* and transmitted to humans through female *Anopheles* mosquitoes. Several species of *Plasmodium* cause malaria in humans but *P. falciparum* is the most lethal specie. Malaria parasites have a complex life cycle and in order to eradicate the disease, every stages should be considered for treatment. Due to the appearance and spread of resistant parasites to current therapies, it is urgent to discover novel antimalarial drugs that are effective against both blood and liver stages of infection by malaria parasites and endowed with the ability to block the transmission of the disease to mosquito vectors. Currently, artemisinin-based combination therapies are used for uncomplicated malaria. The endoperoxide bond of artemisinin plays a key role in the fight against disease. As it only activated by a high concentration of iron (II) that is present in the digestive vacuole of the parasites infecting erythrocytes, where they degrade host hemoglobin. In contrast, basal Fe (II) concentration in mammalian cells is very low. This particularity ensures the high selectivity of endoperoxide drugs. The goal of this work was to prepare an activity-based probe (ABP) designed to identify potential molecular targets of 1,2,4,5-tetraoxane-cyanopyrimidine hybrid antimalarials. Several of these hybrids have shown to be active against the blood and liver stages of malaria parasites, and thus identification of the molecular targets associated to this dual-activity profile may become relevant in the discovery of new antimalarial drugs to be used in eradication campaigns. A hybrid ABP combining the 1,2,4,5-tetraoxane core and a cyanopyrimidine containing an alkyne handle for click chemistry was designed and synthesized. The tetraoxane contained an adamantyl moiety to confer stability to the endoperoxide motif. The synthesis of a negative ABP tetraoxane-pyrimidine nitrile probe was performed. Finally, in order to monitor the distribution and accumulation of this compound, we coupled the ABP with a fluorescent NBD-based azide reagent via click (CuAAC) chemistry to give the corresponding hybrid fluorescent probe in moderate yields.

Keywords: malaria, tetraoxanes, cyanopyrimidine, activity-based probe

Resumo

A malária é uma das doenças infeciosas mais frequente em todo o mundo que afeta maioritariamente as regiões subdesenvolvidas. Segundo a Organização Mundial de Saúde, em 2015 surgiram cerca de 212 milhões de novos casos de malária e estima-se que no mesmo ano tenham ocorrido cerca de 429 mil mortes causadas pela malária. No entanto, não é possível conhecer-se o número exato de casos de malária porque a maioria das regiões endémicas de malária não possuem os recursos de diagnóstico necessários e ainda devido ao facto dos sintomas da doença serem bastante semelhantes a outras doenças existentes nas mesmas regiões.

Esta doença é causada por parasitas protozoários do género *Plasmodium* e sabe-se que existem pelo menos cinco espécies responsáveis pela infeção em humanos, o *P. vivax*, *P. falciparum*, *P. malariae*, *P. ovale* e *P. knowlesi*. Em conjunto com o *P. vivax*, o *P. falciparum* é também o responsável pela maioria de casos de malária. Apesar do *P. falciparum* ser a espécie responsável pela malária mais severa e por isso o responsável pela maioria das mortes, o *P. vivax* consegue gerar formas latentes, os hipnozoitos, que podem voltar à circulação levando à recorrência da doença.

Sendo parasitas, os *Plasmodium* necessitam de dois hospedeiros para se multiplicarem e desenvolverem, um mosquito e um humano. A malária é geralmente transmitida através da picada de uma fémea infetada do mosquito *Anopheles*, sendo que a espécie mais eficiente é o *Anopheles gambiae*. Assim que o mosquito se alimenta do sangue humano liberta esporozoítos presentes nas glândulas salivares que migram pela corrente sanguínea e se depositam nas células hepáticas. O ciclo de vida do parasita é complexo passando por uma fase hepática onde o parasita se reproduz assexuadamente nos hepatócitos, seguindo-se uma fase sanguínea. A fase hepática é assintomática surgindo apenas sintomas na fase sanguínea. É nesta segunda fase que também se formam as formas sexuais do parasita capazes de infetar outro mosquito continuando assim o ciclo de vida do *Plasmodium*.

Apesar dos diversos esforços, atualmente não existe nenhuma terapia eficaz no tratamento da malária. Esta ineficácia pode-se dever a diversos fatores como a biologia e ecologia complexa dos parasitas *Plasmodium* e dos vetores *Anopheles* e o aparecimento de estirpes de parasitas resistentes aos fármacos. O tratamento na fase hepática tem sido a maior preocupação já que nesta fase o numero de parasitas não é tão elevado como na fase sanguínea. O desenvolvimento de fármacos antimaláricos tem

sido maioritariamente focado na fase sanguínea do parasita da malária, mas a fase hepática da infeção do *Plasmodium* é um passo obrigatório para a maturação e replicação do parasita sendo por isso um alvo importante para a erradicação da malária. Durante a fase sanguínea da malária, os parasitas transportam hemoglobina para o vacúolo digestivo onde usam a hemoglobina como uma fonte essencial de aminoácidos. Esta degradação conduz à formação de ferro heme. O ferro heme é tóxico para o parasita, mas este consegue polimerizá-lo convertendo-o em hemozoína, um material biocristalino inerte.

Os primeiros compostos descobertos para o tratamento da malária foram as quinolinas. Após diversas alterações estruturais sintetizou-se um composto chamado cloroquina. A cloroquina tem sido utilizada no tratamento da malária desde os anos 60 e apesar das suas inúmeras vantagens como a eficácia, segurança e a possibilidade de administração a mulheres grávidas e crianças, o aparecimento de estirpes resistentes à cloroquina tornou necessária a procura de novos fármacos.

A descoberta do mecanismo de ativação da artemisinina pelo ferro do grupo heme e da importância do núcleo endoperoxídico para a atividade antimalárica levou à descoberta dos tetraoxanos como potenciais fármacos para o tratamento da malária. Após serem ativados pelo ferro, os endoperóxidos dão origem a radicais centrados no carbono e a espécies reativas de oxigénio capazes de causar stress oxidativo no parasita. Este método de ativação permite que os endopéroxidos sejam seletivos para o parasita já que são necessários elevados níveis de ferro heme no vacúolo digestivo que, em condições normais, não se encontram nas células mamíferas.

Atualmente, a artemisinina não é utilizada devido ao seu perfil farmacocinético fraco como o baixo tempo de semi-vida, a pobre solubilidade e a baixa biodisponibilidade tendo sido por isso sintetizados derivados semissintéticos. Estes derivados semissintéticos podem ser utilizados em terapias combinadas com outros agentes antimaláricos de longa ação permitindo a eliminação eficaz do parasita e evitando o aparecimento de casos de malária resistentes a esta terapia. No entanto, foram já documentados os primeiros casos de resistência à artemisinina. Um dos derivados semissintéticos da artemisinina, o arteméter, é atualmente utilizado em terapia combinada com a lumefantrina (Coartem©) para o tratamento da malária descomplicada em adultos e em crianças.

Devido ao aumento das espécies resistentes aos fármacos antimaláricos, a síntese de compostos híbridos com um mecanismo de ação duplo tem se tornado uma abordagem bastante promissora. Desta forma, sintetizou-se um tetraoxano que após ativação com o ferro leva à formação de dois compostos, uma molécula radicalar e altamente reativa

capaz de alquilar biomoléculas essenciais para a sobrevivência do parasita e aumentar o stress oxidativo e uma segunda molécula capaz de inibir enzimas como a falcipaína. A falcipaína é uma família de proteases de cisteína que se encontram no vacúolo digestivo e que desempenham um papel muito importante na hidrólise da hemoglobina. A inibição da falcipaína impede que o parasita consiga degradar a hemoglobina em aminoácidos conduzindo à sua morte. Diversos inibidores de proteases de cisteína têm sido sintetizados com bons resultados *in vitro* e *in vivo* com uma característica comum, um grupo eletrofílico capaz de reagir com o resíduo de cisteína.

Recentemente, foi descoberto um novo grupo de tetraoxanos híbridos ativados pelo ferro, capazes de inibir a falcipaína dentro do vacúolo digestivo do parasita, os tetraoxanos compostos por pirimidinas e nitrilos. O ataque nucleofílico pelos nitrilos no sítio ativo das proteases de cisteína resulta na inibição reversível e covalente das enzimas.

O objetivo deste trabalho foi preparar uma sonda baseada na atividade (*activity-based probe*, ABP), projetada para identificar potenciais alvos moleculares de 1,2,4,5-tetraoxanos híbridos antimaláricos. Para a obtenção do composto pretendido recorreu-se a um processo de síntese bastante extenso realizado em duas fases separadas. Primeiro realizou-se a síntese do tetraoxano e do núcleo pirimidínico e no fim, fez-se o acoplamento entre os dois. Os rendimentos de todos os passos de síntese realizados foram moderados a bons tendo-se conseguido sintetizar o composto pretendido.

De forma a monitorizar e observar a distribuição e acumulação do nosso composto dentro dos parasitas, decidiu-se acoplar a ABP a uma sonda fluorescente. Após a síntese da sonda, esta foi acoplada à ABP através de química click. Esta reação realizou-se por uma cicloadição catalisada por cobre entre a azida da sonda e o alcino do tetraoxano. O facto das azidas e dos alcinos serem inertes na maioria das condições biológicas e orgânicas permite que este acoplamento ocorra dentro do sistema vivo sem interferir com os processos bioquímicos naturais por reações bioortogonais. Apesar de ter ocorrido reação e de se ter sintetizado o composto pretendido, o rendimento deste acoplamento foi baixo tendo por isso a necessidade de ser otimizado. Neste projeto, pretendia-se ainda sintetizar um análogo do nosso tetraoxano inativo. A síntese deste análogo teve rendimentos moderados a altos mas não foi completa.

Palavras-Chave: malária, tetraoxanos, cianopirimidina, sonda baseada na actividade

Table of contents

Abbreviations

ABP – activity-based probes

ABPP – activity-based protein profiling

ACN – acetonitrile

ART – artemisinin

Boc – Boc *tert*-butoxycarbonyl

bs – broad singlet

COSY – correlation spectroscopy

CQ – chloroquine

CuAAC – cooper-catalyzed azide-alkyne cycloaddition

DCM – dichloromethane

DFO – desferrioxamine

DHA – dihydroartemisinin

DIPEA – N,N-diisopropylethylamine

DV – digestive vacuole

DMF – dimethylformamide

EtOH – ethanol

FP – falcipain

FPIX – ferriprotoporphyrin IX

H_2O – water

H_2O_2 – hydrogen peroxide

HCOOH – formic acid

HMBC – heteronuclear multiple bond correlation

HMQC – heteronuclear multiple quantum correlation

Hz – hertz

J – coupling constant

m – multiplet

MeOH – methanol

mp – melting point

MQ – mefloquine

MS-ESI – mass spectrometry-electrospray ionization

N_2 – nitrogen atmosphere

NaOH – sodium hydroxide

NBD – nitrobenzoxadiazole

NBD-Cl – 7-chloro-4-nitrobenzoxadiazole

NMR – nuclear magnetic resonance

ov – overnight

ppm – parts per million

PQ – primaquine

q – quartet

quint – quintuplet

Re_2O_7 – rhenium (VII) oxide

ROS – reactive oxygen species

rt – room temperature

s – singlet

SERCA – serca/endoplasmic reticulum membrane calcium ATP-ase

SN_2 – second-order nucleophilic substitution reaction

$SOCl_2$ – thionyl chloride

t – triplet

TBTU – O-(Benzotriazol-1-yl)-N,N,N',N'-tetramethyluronium tetrafluoroborate

USA – United States of America

List of Figures

List of Tables

List of Schemes

Chapter I

I. State of the Art

I.1 Malaria

Malaria was once a prevalent disease in most of the world but after the World War II, the use of chloroquine successfully[1] eliminated malaria from the United States of America (USA) and Canada, Europe and Russia.[2] Unfortunately, because of the rapidly increase an spread of antimalarial drug resistance[1,2], relaxation of control efforts, and insecticide resistance in the mosquito vectors, malaria resurged in tropical countries from the 1970s to the 1990s. More recently, the donor funding increased, the control was improved and the enthusiasm for elimination and eradication also increased, reducing malaria prevalence again.[2]

Human infections could be caused by five species of genus *Plasmodium*, *P. vivax*, *P. falciparum*, *P. malariae*, *P. ovale* and *P. knowlesi*.[1–4] *P. falciparum* is the species that causes most of the malaria deaths. *P. vivax* and *P. falciparum* are the species responsible the most of the cases of malaria.[2,4] *Plasmodium* parasites are eukaryotic organisms that require two hosts, a mosquito vector and a human, to multiply and develop. Malaria transmission occurs when an infected female *Anopheles* mosquito feeds from human blood.[2,5]

According with the World Health Organization (WHO), in 2015 there were 212 million new cases of malaria and it was estimated that there were 429 thousand malaria deaths, being children and pregnant women the most affected. Malaria disease is most prevalent in African countries (90%) followed by the South-East Asia countries (7%) and the Eastern Mediterranean countries (2%). Most of the malaria deaths occur in the African Region (92%) followed by the South-East Asia Region (6%) and the Eastern Mediterranean Region (2%). Despite this data, the incidence rates of malaria new cases fell by 21% and malaria mortality fell by 29% globally between 2010 and 2015. The malaria mortality rate among children under 5 years also fell by 35%.[6] In pregnancy, malaria causes indirect mortality from abortion and intrauterine growth retardation, which increases infant mortality.[2]

The real number of malaria cases is not precisely known because many of the malaria endemic countries lack appropriate diagnosis resources and there are rural settings where the clinical features of malaria are very similar to other diseases that may coexist in the

same geographical areas.[2] Due to the wide-scale development of malaria control interventions, the number of malaria endemic countries reduced from 108 to 91 between 2000 and 2016 as shown in **figure I.1**.

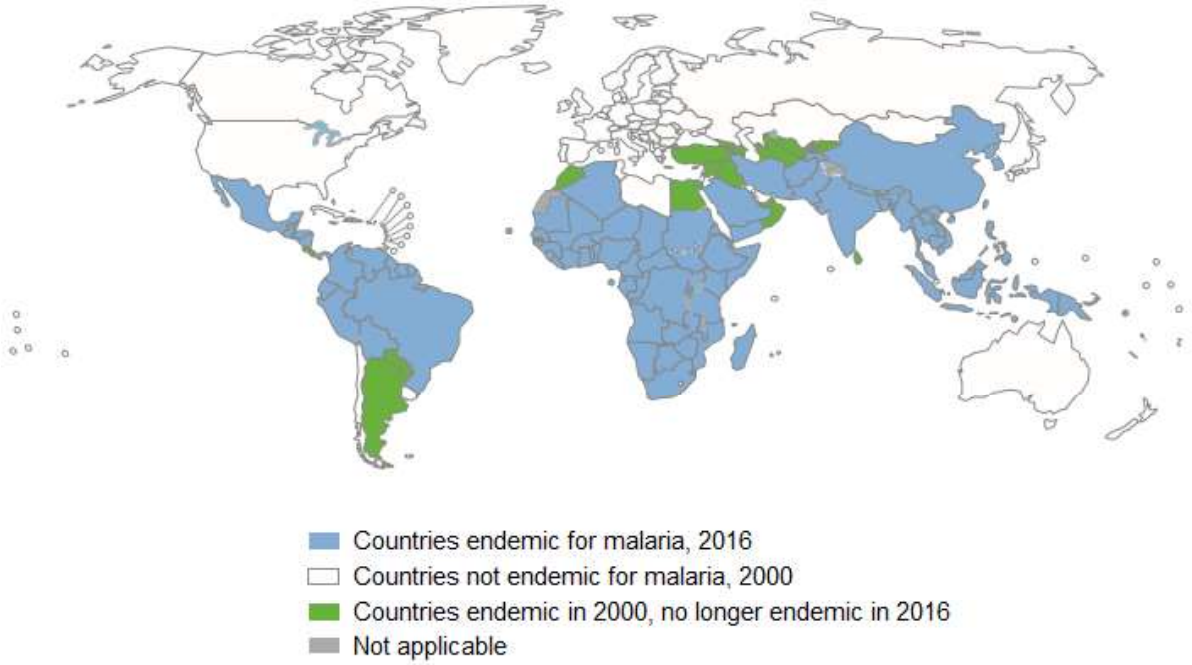

Figure I.1 – Countries endemic for malaria in 2000 and 2016 (adapted from [6])

The continent most affected by malaria is Africa due to several factors such as hot and humid climate, lack of resources and poverty. It is also in Africa that the most efficient species of vector, *Anopheles gambiae,* is found and where the species *P. falciparum* predominates, leading to more severe malaria.[2]

Together with tuberculosis and AIDS, malaria is one of the three most frequent infectious diseases in the world (the "Big Three").[1] Malaria is the most important protozoan disease of human beings and is transmitted by *Anopheles* mosquitoes.[2–4]

I.2 Life Cycle of *Plasmodium*

The parasite life-cycle begins (**figure I.2**) when a female *Anopheles* stings (A) a human and during a blood feeding injects saliva containing sporozoites that enter the host's bloodstream.[2,7] Then, the sporozoites travel to the liver (B), housed in functional units

called hepatocytes and reproduce asexually for a few days.[2] At this stage the disease is asymptomatic. After about a week, sporozoites mature into schizonts, which burst and release numerous identical daughter cells called merozoites to the red blood cells, initiating another asexual life cycle (C).[2] To hide from the immune system of the host, merozoites invades erythrocytes where the parasite develops into a blood schizont.[7,8]

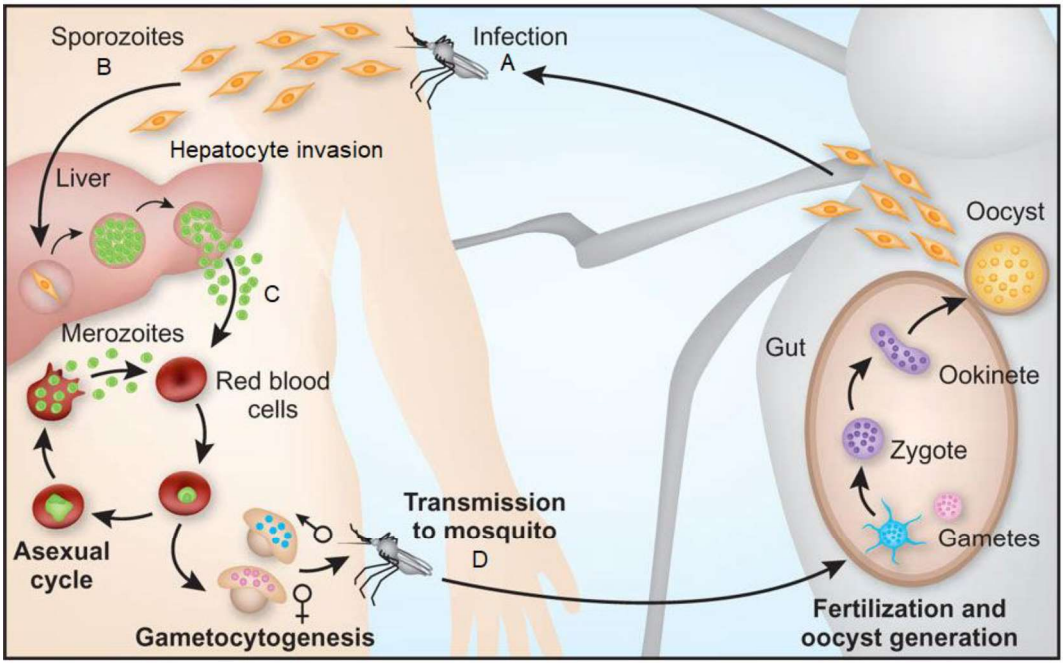

Figure I.2 – Life cycle of *P. falciparum* in human body and in anopheline mosquito. (A) Infection by *Anopheles*; (B) Sporozoites invades hepatocytes and multiplies; (C) Explosion of schizonts and release of merozoites; (D) Transmission to mosquito (adapted from [8])

When there are around 100 million asexual parasites in circulation, the symptoms of the disease begin to appear. Some parasites develop in sexual forms, the gametocytes. When the host is again bitten by an anopheline mosquito (D) the gametocytes are captured by the mosquito and reproduce sexually forming an ookinete and then an oocyst in the mosquito's gut. Finally, the oocyst explodes and release sporozoites, which migrate to the salivary glands of the insect from where they will be released during the next blood feed. This cycle can take about one month.[2]

In the cases of *P. vivax* and *P. ovale*, some sporozoites turn into hypnozoites, a form that can remain dormant in the liver cells, causing relapses months or even years after the initial infection.[7,9]

Symptoms of malaria usually develop in about 10-15 days after the infection and the most common malaria symptoms are fever, headache, and chills that difficult the diagnosis[4,10] because these symptoms are also found in other diseases like flu and viral infections.

When treatment is not initiated within the first 24 hours, the infection can progress to a more aggressive form called severe malaria, developing other symptoms such as anaemia and respiratory distress, or even cerebral malaria that often leads to death.[10]

Traditionally, the diagnosis of malaria is made by microscopic examinations that allow identifying and quantifying the degree of infection, through the detection of the malaria parasite's waste product, hemozoin.[4]

I.3 Antimalarial Drugs

Despite the many efforts already underway to control malaria, there are several factors that do not allow an effective therapy such as the complex biology and ecology of *Plasmodium* parasites and their anopheline vectors, drug-resistant strains of parasites, and the efficiency of immune evasion of the parasites during blood-stage replication.[3]

The treatment of the disease in its asymptomatic phase, the liver phase, has been a major concern because, at this stage, the number of parasites is not as high as in the blood stage. Due to the distinct metabolism between the two phases, the antimalarial drugs that work in the blood phase are not effective in the liver phase and, despite the efforts made in the last decades for treatment in the liver phase, there is still no totally effective antimalarial drug at this stage.[3]

I.3.1 Quinolines

I.3.1.1 Quinine

Quinolines are aromatic compounds with two fused hexagonal rings, wherein carbon in the first position is replaced by a nitrogen. The first quinoline compound used as an antimalarial drug was quinine, **1** (**figure I.3**).[11]

Quinine is an alkaloid extracted from the bark of cinchona tree and was found in the seventeenth century. According to a legend, an Indian was lost in an Andean jungle and with a high fever and thirsty drank from a pool of stagnate water surrounding by cinchona

trees. Surprisingly, his fever soon decreased, and he shared this accidental discovery with fellow villagers, who thereafter used extracts from the cinchona bark to treat fever.[12]

After several changes in obtaining and using the bark of the cinchona tree, in 1890s quinine began to be used for the treatment of malaria until the 1920s when a new drug appeared, chloroquine (CQ, **2, figure I.3**). Due to the appearance of resistance to CQ, quinine is still used for the treatment of severe malaria in combination with other drugs.[12]

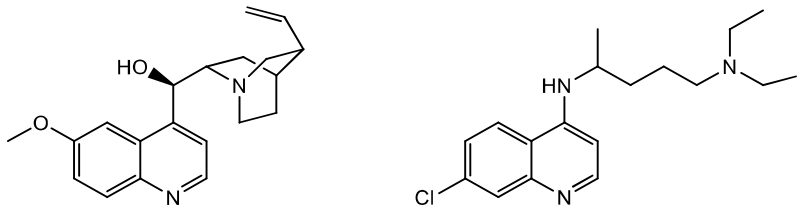

1 **2**

Figure I.3 - Structure of quinoline compounds, quinine **1** and chloroquine **2.**

The mechanism of action of quinine is still unknown, but it is known that its schizonticidal action against parasites of intra-erythrocytic malaria is rapid and also has gametocyte activity for *P. vivax* and *P. malariae*. Its oral and parenteral absorption is very rapid reaching maximum concentration within 1-3 hours and 80% of the drug is rapidly eliminated by hepatic biotransformation and 20% is excreted unchanged by the kidney. The half-life of quinine is between 11-18 hours.[12–15]

The first case of resistance to quinine was reported in 1910. Resistance to quinine is usually low grade, with the drug retaining some activity but having its action delayed or diminished.[12] After the second world war, CQ and pyrimethamine replaced quinine and the development of high-level resistance has been very slow.[11]

I.3.1.2 8-Aminoquinolines

The discovery of antimalarial activity of methylene blue **3** (**figure I.4**) led to the first attempts of synthetic antimalarial drugs. It was in 1891 that the first synthetic drug began to be used when Paul Ehrlich and Paul Guttmann cured two malaria patients with methylene blue.[7]

Replacement of the basic methyl side chains with a methyl side chain improved the activity of the compounds, so in the 1920s, Bayer Laboratories, connected methyl side chain with different heterocyclic systems such as the quinoline system leading the first synthetic antimalarial plasmoquine, later called pamaquine **4** (**figure I.4**) in 1925.[7,11] Pamaquine then began to be used in 1926 but was found to be very toxic, later synthesizing an analogue, primaquine (PQ **5, figure I.4)** in 1952.[7,11]

The mechanism of action of PQ is not yet clear but is known to be active in the liver stage of the parasite and against latent forms of *Plasmodium* (hypnozoites), especially in P. vivax infections. In addition, it can prevent the spread of the disease by preventing the transmission of gametocytes to naive mosquitoes.[7,16] Currently PQ is still used to eradicate the hypnozoites of *P. vivax* and *P. ovale*.[7,11,17]

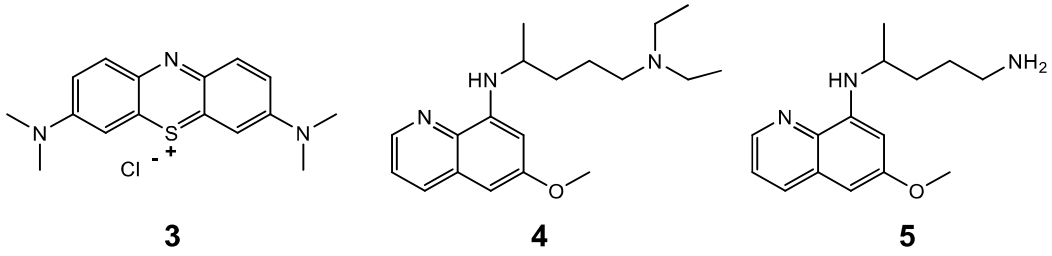

3 **4** **5**

Figure I.4 – Structure of methylene blue **3**, pamaquine **4**, primaquine **5.**

I.3.1.3 4-Aminoquinolines

Later, German scientists of IG Farben tried to associate the basic side chain of pamaquine to heterocyclic ring systems that leads to the synthesis of acridine **6 (figure I.5)** and resochin. Initially it was thought that the resochin would be too toxic and therefore was not used but later, after its re-evaluation, this compound was found to be safe at therapeutic concentrations. This finding led to resochin being called chloroquine and initiating clinical trials in 1943. CQ **2** has been used in the treatment of malaria since the 1960s. [7,11]

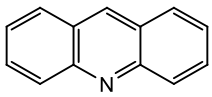

6

Figure I.5 – Structure of acridine **6**.

CQ is a dibasic compound (pka1 = 8.1, pka2 = 10.2) which in its unprotonated form is able to cross the erythrocyte membranes of the parasites that accumulate in the DV, once the

DV has a low pH (5.0 – 5.4).[18] This accumulation depends on the pH difference between the external environment and the DV and requires metabolic energy to occur. The passage of CQ through the membranes also implies the existence of sodium and hydrogen exchangers. CQ binds to the sodium-binding site and, when during the glycolysis the generated protons are released to the external medium of the vacuole, CQ can penetrate the vacuole.[11]

Iron is a required element for all living organisms and is the most abundant transition metal in the human body. Most of the iron present in the human body is in ferric form, Fe (III).[19] During the symptomatic phase of malaria, ferrous iron, Fe (II), is present in large quantities and can invade red blood cells.[19] After invasion, *Plasmodium* parasites transport hemoglobin to the digestive vacuole (DV).[11,19]

In DV, parasites use hemoglobin as source of essential aminoacids. Degradation of hemoglobin leads to a ferrous heme. This is a toxic byproduct called ferriprotoporphyrin IX (FPIX), but the parasite can convert it into an inert biocrystalline material containing heme oxidized Fe (III) called hemozoin by polymerizing the heme.[7,11,19,20] In hemozoin crystals, heme is present as β-hematin and the crystals are made of dimers of hematin molecules that are linked by hydrogen bounds forming a large structure with the ferric iron of each heme moiety chelated onto a carboxyl side chain of the adjacent moiety (**figure I.6**).[11,20] Although this form is less toxic, it is thought that the concentration of Fe (II) in the infected red blood cells is higher than the concentration present in healthy tissues and serum.[19]

Mechanism of action is not yet fully understood but is thought that after CQ penetration in DV, CQ forms a complex with FPIX and thereby prevents its polymerization into hemozoin leading to parasites death.[7,11] After treatment with CQ, swelling of the digestive vacuole of the parasite and accumulation of hemoglobin not ingested in endocytic vesicles is observed. These observations allowed us to conclude that CQ is only active in the blood stage of malaria during which degradation of hemoglobin in the parasite occurs, thereby interfering with its feeding process.[11]

CQ presents a lot of advantages like its efficacy and safety and can be administered to children and pregnant women.[21] Due to these advantages and the low cost of production, the use of CQ began to be abusive and combined with the high adaptability of *Plasmodium* parasites, the first cases of resistance began to appear. Today, more than 80% of wild isolates are resistant to CQ.[7] The mechanism of resistance to chloroquine is also unknown, but in some resistant strains, CQ apparently undergoes a mutation and is removed from DV. In chloroquine-resistant strains high levels of glutathione are observed and therefore

it is thought that glutathione reductase may be another target of the FPIX -chloroquine complex.[22]

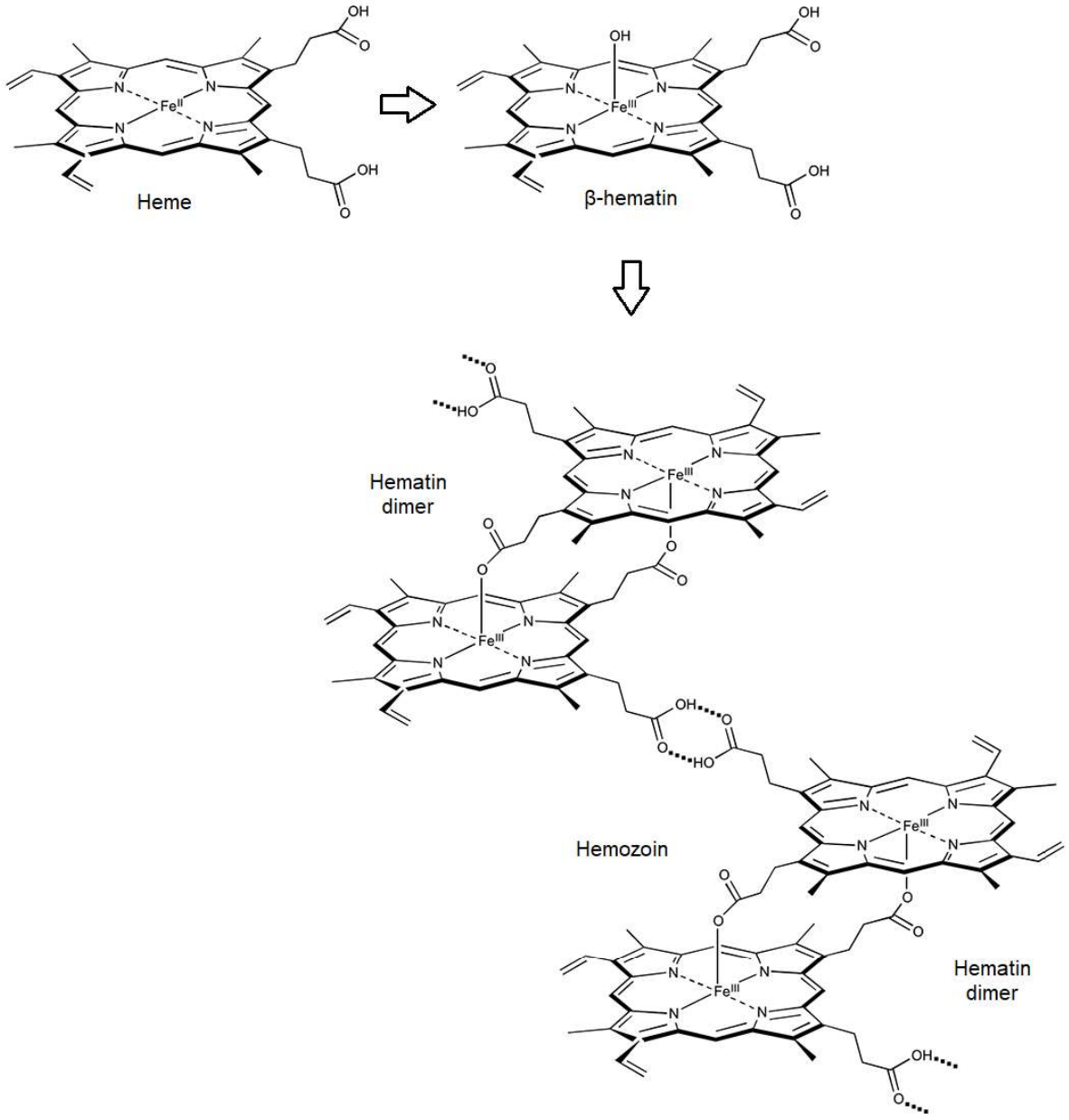

Figure I.6 – Chemical structures of heme, β-hematin and hemozoin. (adapted from [23])

I.3.1.4 Quinolinemethanols

Due to problems in Vietnam with CQ-resistant malaria in 1963, the Walter Reed Army Institute for Research (Washington, DC, USA) began large-scale screening for new potential antimalarial drugs. With this investigation, they found that 4-quinolinemethanols with analogue structures of quinine were the most promising group. In 1970, a new compound called mefloquine (MQ **7**, **figure I.7**) was synthesized. MQ showed an even more potent activity than CQ and its great advantage was the efficacy against CQ resistant strains of malaria parasites.[11]

Prophylactic use of mefloquine is prohibited for people who require unimpeded skills, such as air crew members, because mefloquine triggers some neuropsychiatric side effects such as insomnia, depression and panic attacks.[7]

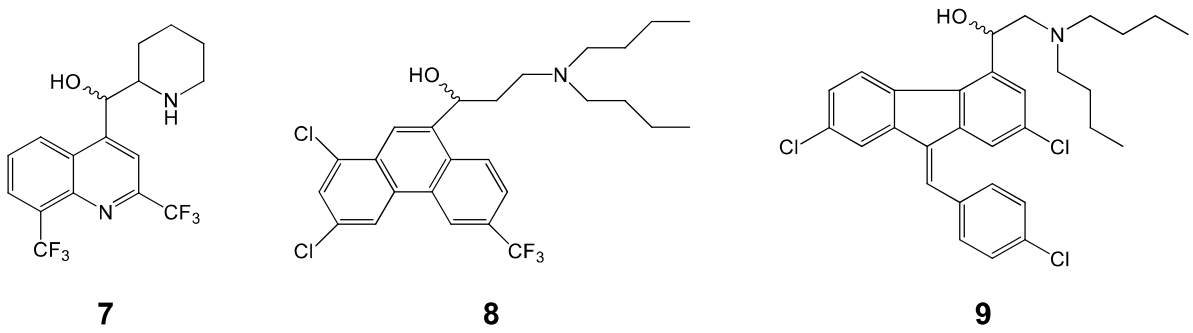

7 **8** **9**

Figure I.7 – Structures of 4-quinolinemethanols, mefloquine **7**, halofantrine **8** and lumefantrine **9.**

In addition to the 4-quinolinemethanols found, the Walter Reed Army Institute for Research (Washington, DC, USA) found that replacing the quinoline of 4-quinolinemethanols with a different aromatic system led to the formation of aryl(amino)carbinols. Of this group of compounds, halofantrine **8** (**figure I.7**) was the most promising and was introduced into the treatment of CQ-resistant malaria but its use was banned because of the serious cardiotoxic problems it triggered.[7,11]

Lumefantrine **9** (**figure I.7**) was developed in the 1970s by the Academy of Military Sciences in Beijing, China. Although lumefantrine exhibits less antimalarial activity than halofantrine, this drug has the advantage of not triggering cardiotoxicity problems of the halofantrine. Presently, lumefantrine is used in combination with endoperoxides drugs.[7]

I.3.2 Pyrimethamine/Sulfadoxine

Pyrimethamine **10** (**figure I.8**) was discovered during the World War II and in 1950s was being used as a monotherapy against malaria parasites. A decade later, sulfadoxine **11** (**figure I.8**) proved to be an effective, slow-acting blood schizontocide in clinical trials and the combination of pyrimethamine-sulfadoxine was later used as a treatment for *falciparum* and *vivax* malaria, including CQ-resistant strains.[24,25]

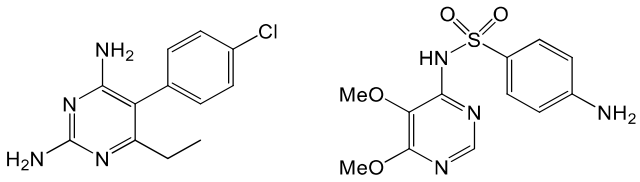

10 **11**

Figure I.8 – Structures of pyrimethamine **10** and sulfadoxine **11**.

Combination of these two drugs represent a major advantage when compared to monotherapy because pyrimethamine acts as dihydrofolate reductase inhibitor (DHFR inhibitors) while sulfadoxine acts as dihydropteroate synthase inhibitor (DHPS inhibitors).[26] These two enzymes are involved in the folate cascade to synthesize some nucleotides and aminoacids by malaria parasites and thus, inhibition of these two enzymes leads to synergism. DHFR enzyme converts dihydrofolate into tetrahydrofolate that is an essential cofactor in transfer reactions in the purine, pyrimidine, and amino acid biosynthetic pathways. DHPS is involved in the synthesis of folate, an essential substrate used in the folate cascade.[24,26]

I.3.3 Falcipain, as a validated target

Identification of the role played by cysteine proteases in the parasite life cycle has become essential for the discovery of new compounds capable of interacting with these enzymes.[27,28] Among the proteases found in DV involved in the hydrolysis of hemoglobin the most influential in this process are falcipains.[29]

Falcipains (FP) are a family of papain-family cysteine proteases that includes four isoforms of falcipains, falcipain-1 (FP-1), falcipain-2 (FP-2), falcipain-2' (FP-2') and falcipain-3 (FP-3).[30–32]

FP-2 and FP-3 contribute equally to the digestion of hemoglobin in digestive vacuole[33] and both enzymes are expressed during the erythrocyte stage of the parasite. FP-2 beginning in early trophozoites followed by expression of FP-3 in late trophozoites and schizonts.[34] Their inhibition results in inhibition of hemoglobin hydrolysis resulting in excess heme iron in the parasite that blocks parasite development.[31] FP-2 also plays a crucial role in the erythrocyte rupture affecting the merozoites release.[35]

Falcipains are dependent on a common catalytic triad constituted by cysteine, asparagine and histidine residues.[36] Active site of cysteine proteases enzymes is constituted by four pockets S1, S1', S2 and S3. S1 is the least defined pocket which normally keeps the glutamine in the "oxyanion hole". Tryptophan is the most conserved residue in the S1' pocket and participate in hydrophobic interactions with substrates.[37] S2 is the most well-defined pocket and it's the pocket responsible for the specificity.[38] Most of residues of S2 pocket are hydrophobic but sometimes a polar residue is present, like glutamic or aspartic acid. Finally, S3 pocket is a glycine rich region.[37] **Figure I.9** highlights the active site of FP-3 with the cysteine surrounded by four subsites (S1', S1, S2 and S3).

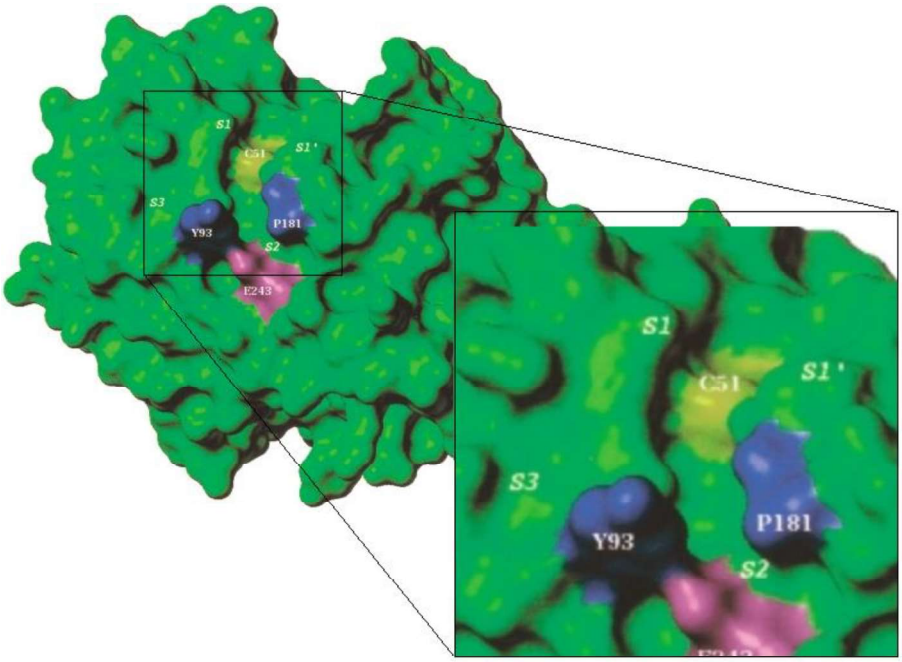

Figure I.9 – Representation of the falcipain-3 catalytic site surface showing the S1, S1', S2 and S3 pockets. (adapted from [37]).

Several cysteine protease inhibitors have been synthesized with good results *in vitro* and *in vivo* with a common feature, an electrophilic warhead capable of reacting with the cysteine residue.[33,38]

Alkyl and arylamines are well established inhibitors of cysteine proteases.[31,39,40] Coterón and co-workers developed a large library of cysteine protease inhibitors based on a general structure (**figure I.10**) with an electrophilic moiety for interaction with the cysteine residue of the enzyme and one or two series of substituents responsible for interactions with the different pockets of the protease.[31] FP-2 has been shown to have preference for substrates with a hydrophobic residue, particularly leucine, at position P2.[33,38] Leucine-like isobutyl moiety was the most potent derivative against FP enzymes.[31] Compounds with 5-bromopyrimidine and 5-chloropyrimidine scaffolds in P1 also proved to be the most promising, showing a clear advantage in terms of enzymatic activity over other nitriles.

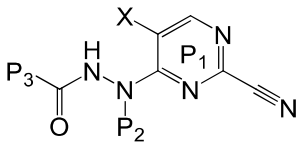

Figure I.10 – General structure of 2-pyrimidinecarbonitrile derivatives showing positions P1, P2 and P3.

I.3.4 Endoperoxides

An endoperoxide is a heterocyclic compound containing a peroxide (-O-O-) residue in the ring. It is accepted that this kind of compounds are activated by the iron or heme present inside the parasite by scission of the peroxidic bond. When this activation occurs, it leads to the formation of oxygen radicals that undergo a rearrangement resulting in carbon-centered radicals that can interfere with several targets. These are extremely reactive species and may alkylate the parasite biomolecules essential for his survival and simultaneously contributes to increase oxidative stress that makes very difficult for parasites to survive.[7]

In normal conditions, the concentration of free Fe (II) in mammalian cells is lower than inside the DV of *Plasmodium* parasites. Thanks to this difference, endoperoxides are essentially activated in the parasite providing a high degree of selectivity and safety of this group of drugs.[41,42]

Many parasitic proteins, such as falcipain (FP) proteases, and the heme itself responsible for activation of the endoperoxides can be alkylated by the formed radicals which may interfere with the elimination of the heme leading to the death of the parasite.[20] Lipophilic heme adducts can accumulate in neutral lipid bodies around the DV membrane and increase oxidative stress resulting in the oxidative degradation of phospholipids.[20,43]

I.3.4.1 Artemisinin

During the Vietnam War, Chinese government formed a research group to find drugs to defend the army against malaria infections. Due to its use to treat fevers, chills and convulsions, *Artemisia annua* was chosen to be investigated. Its active ingredient, artemisinin (ART **12**, **figure I.11**) was isolated for the first time in 1971.[7,44]

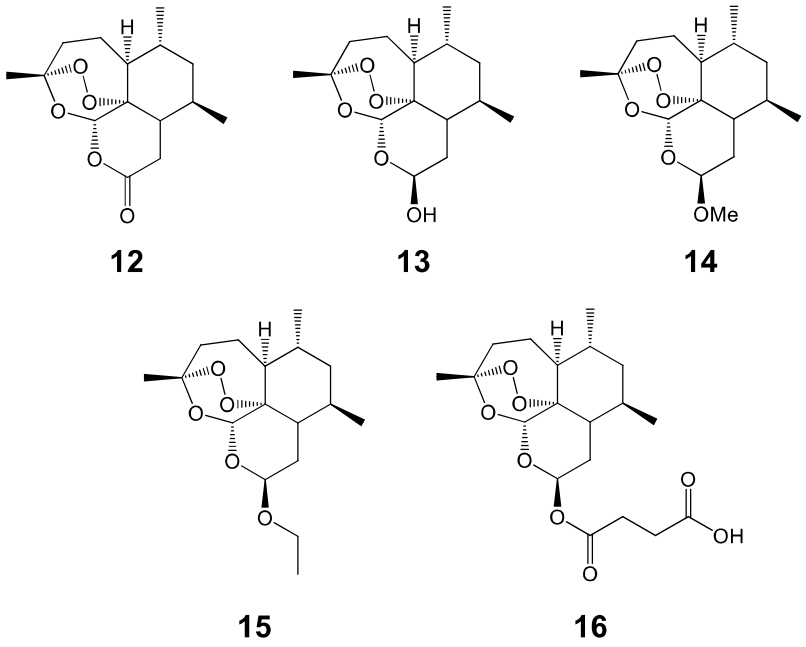

Figure I.11 – Structures of artemisinin **12** and its analogues, dihydroartemisinin **13**, artemether **14**, arteether **15** and artesunate **16**.

ART is a sesquiterpene lactone with a peroxidic bond fundamental for antimalarial activity and has been used in China for treatment of malaria since 1972.[7,20,45] It is an effective antimalarial drug in low nanomolar range against multiresistant strains of *P. falciparum* and is only active on blood stage.[7,20,44] There are some ART analogues with activity against

other types of parasites of the genus *Trypanosoma*, *Leishmania* and *Toxoplasma*[46] and also with antitumor[20] and antifungal activity[46].

Activation of ART by iron (II) can give rise to different types of radicals capable of alkylating the heme group and proteins resulting in the death of *Plasmodium*. ART activation leads to generation of carbon-centered free radicals or reactive oxygen species (ROS).[45] When Fe (II) binds to oxygen 1 of artemisinin (Route 1, **scheme I.1**), oxygen radicals are formed. Subsequently occurs an electron transfer inducing reductive scission of the C3-C4 bond giving rise to carbon radicals. On the other hand, when the iron binds to oxygen 2 (Route 2, **scheme I.1**) oxygen radicals are also formed and this process is then followed by an intramolecular 1,5-H migration leading to carbon radicals.[20,45,47] Selectivity of ART results from the fact that ferrous heme is present in high concentration inside the parasite.[48]

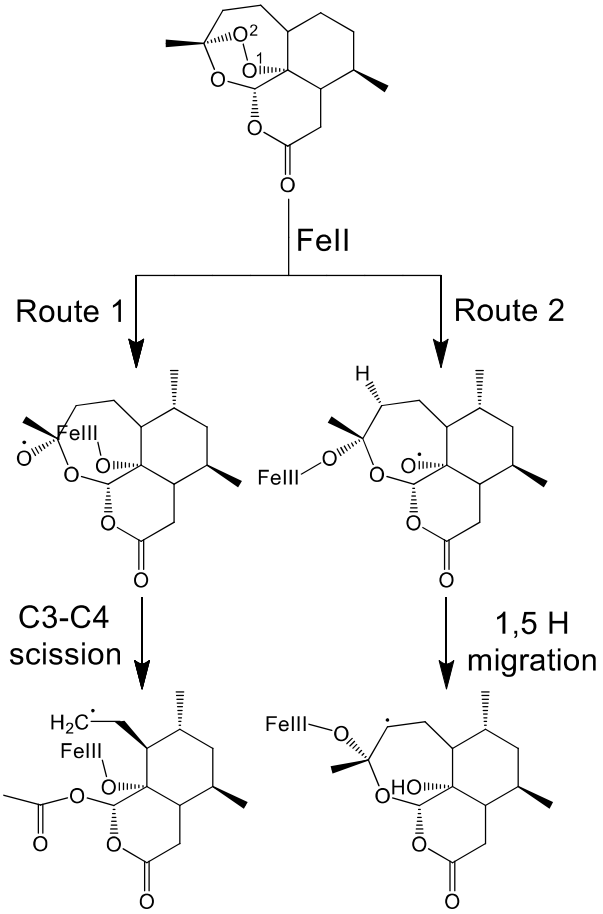

Scheme I.1 – Activation mechanism of ART by Fe (II).

Although many authors believe that the activation of ART occurs with heme iron there is also evidence that this activation may also occur with non-heme iron. Stocks and co-workers demonstrated that the presence of desferrioxamine (DFO) antagonize the

antimalarial activity of artemisinin *in vitro*. DFO is a chelating agent selective for Fe (III). This demonstrate that activation of ART is also dependent on non-heme iron.[49,50]

Several potential targets have already been proposed for the ART but its mechanism of action is still unclear. Meshnick *et al.* was the first to identify heme-drug adducts proving that ART is capable to alkylating heme. As result of this alkylation, heme polymerization and hemozoin formation are interrupt leading to the parasite death. Beyond heme alkylation, it was shown that ART is also capable of inhibit falcipains, a papain family cysteine protease involved in hemoglobin degradation.[20,51]

Currently ART is not used due to its poor pharmacokinetic profile as the short plasma half-life, limited bioavailability and poor solubility in water and oil, so the development of semisynthetic derivatives (**figure I.11**) such as dihydroartemisinin (DHA **13**), artemether **14**, arteether **15** and artesunate **16** was a breakthrough in malaria treatment.[44]

Although artemisinin derivatives have low half-lives, they are currently used in artemisinin combination therapies (ACT). In this strategy, ART and its semi-synthetic derivatives are combined with other long-acting antimalarial agents. This leads to effective parasite clearance and avoids the risk of resistance development.[46] WHO recommended the use of ACTs as first-line treatment of uncomplicated *falciparum* malaria in all malaria-endemic areas. The first signs of artemisinin resistance appeared on Thai-Cambodian border were the efficacy of ACT and artesunate monotherapy have decreased.[52–54] Currently the only artemisinin-based combination therapy available combines artemether with lumefantrine for treating uncomplicated *falciparum* malaria in adults and children (Coartem©).[7,45]

I.3.4.2 Tetraoxanes

As an alternative to artemisinin, several fully synthetic peroxidic analogues such as 1,2,4-trioxanes **17**, 1,2,4-trioxolanes **18** and 1,2,4,5-tetraoxanes **19** have been developed (**figure I.12**). These derivatives, are also activated by Fe^{2+} and exert their mode of action through the formation of radical species.[7]

Tetraoxanes are rapidly and effectively activated by heme iron inside the parasite by scission of the peroxidic bond generating carbon-centered radicals that lead to the formation of heme adducts and ketone byproducts.[29,55]

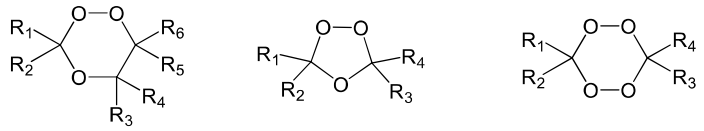

Figure I.12 – General structures 1,2,4-trioxanes **17**, 1,2,4-trioxolanes **18** and 1,2,4,5-tetraoxanes **19**.

In 1992, Vennerstrom and co-workers also synthesized molecules with two endoperoxide groups, dispiro1,2,4,5-tetraoxanes **20a-d** (**figure I.13**). These compounds proved to be equally effective as artemisinin and could be synthesized in only one step from cheap materials.[56–58] The efficacy and low production costs of tetraoxanes have made this type of compounds very promising in the treatment of malaria.[56,59] Like ART, despite its effectiveness, first-generation tetraoxane derivatives showed a poor pharmacokinetic profile due to its low lipophilicity and low bioavailability.[60]

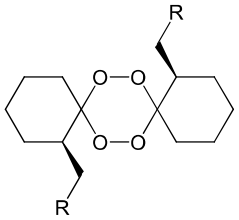

20a: R=H
20b: R=CCH
20c: R=CH_2COOEt
20d: R=COOEt

Figure I.13 – Compounds synthesized by Vennerstrom.

I.4 Hybrid drugs based on tetraoxanes

Due to the increase of resistant strains to most of the available antimalarial drugs, combination of two or more drugs has become a very interesting approach.[61,62] Hybrid drugs consist of the binding of two pharmacophores with different mechanisms of action covalently linked to each other.[62,63]

Compared to combination therapy, hybrids compounds only have a single active pharmaceutical ingredient and therefore the associated costs of production and purification are lower.[64] As the administration is done with only one tablet or one injection, patients acceptance of this therapy is also greater. In addition to increasing efficacy and consequently decreasing the risk of treatment failure, the hybrid drugs can be more effective due to the synergism than drug combination allowing the use of smaller doses

and hence a greater margin of safety and a low toxicity. The hybrid combination of two drugs is limited to a fixed ratio of 1:1 in which the pharmacophores share the same pharmacokinetic and pharmacodynamic profile.[62]

This approach also has some limitations. When the volume of the hybrid reduces the penetration of the drug into the parasite cell the efficacy of treatment may decrease.[62] Another disadvantage of hybrid drugs is the difficulty of adjust the ratio of activities at different targets.[61]

The molecular properties of the hybrid compounds should be studied *in silico* for drug-likeness assessment based on Lipinski's rule of five. It states that poor absorption or permeability of a compound is more likely when there are >5 hydrogen-bond donors, the molecular mass is >500, calculated log *P* is >5, and the sum of nitrogen and oxygen atoms in a molecular is greater than 10.[65]

I.4.1 Tetraoxane-pyrimidine nitrile hybrids

A class of covalent inhibitors that have been used are nitrile-based inhibitors.[66] Nucleophilic attack of nitriles at the active site by cysteine protease results in the formation of a reversible and covalent thiomidate intermediate leading to its inhibition.[27,28,66] In order to inhibit the protease, an inhibitor must possess an electrophilic fraction for the cysteine residue in the active site of the enzyme and within hydrogen bonding distance to a histidine residue (His).[31,66] **Scheme I.2** shows the reaction mechanism of cysteine protease with nitrile inhibitors.

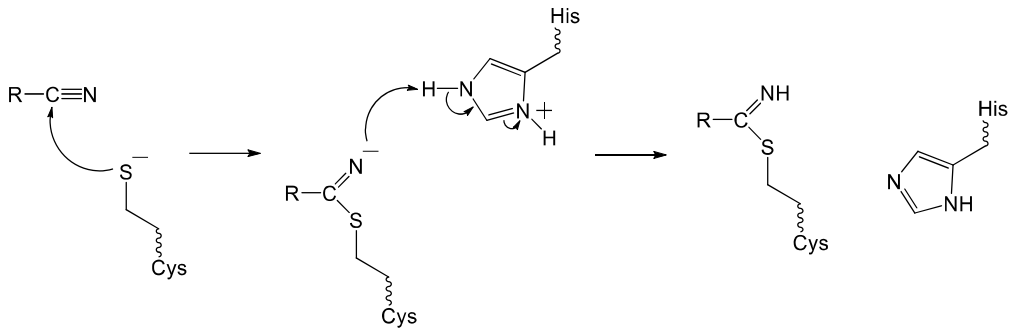

Scheme I.2 – Reaction mechanism of cysteine protease with nitrile inhibitors.

O'Neill and co-workers have shown that tetraoxane-pyrimidine nitrile hybrids **21** (**figure I.14**) are activated by Fe (II) and are able to inhibit FP within the DV of the parasite. They studied their activity against blood and liver stages of malaria infection in murine models. These new compounds showed to have higher FP-2 inhibitory activity with IC_{50} values between 3.4 and 978 nM (**table I.1**).[28]

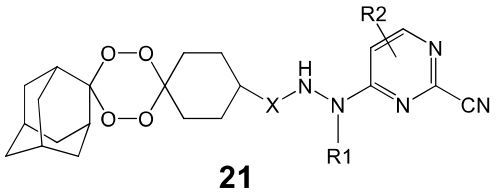

21

Figure I.14 – Tetraoxane-pyrimidine nitrile hybrids **21**.

Vennerstrom and co-workers showed that 1,2,4-trioxolanes substituted with an adamantane ring are not only chemically stable but active against *P. falciparum* in the low nanomolar range.[7,67,68] Recently, O'Neill and co-workers concluded that adamantyl group is responsible for increasing the lipophilicity and stability of the endoperoxide motif and its presence seems to be essential to increase the activity of tetraoxane-based chemical hybrids.[28,29,69,70]

Table I.1 – Falcipain-2 inhibition and antiplasmodial activity of tetraoxane-pyrimidine nitrile hybrids **21.** (adapted from [28])

				IC_{50}[nM]
Compound	X	R1	R2	FP-2
21a	CO	$-CH_2CH(CH_3)_2$	5-Br	16.4±4.2
21b	CH_2CO	$-CH_2CH(CH_3)_2$	5-Br	95.1±0.4
21c	CO	$-CH_2CH(CH_2)_4$	5-Br	112±9
21d	CO	$-CH(CH_2)_5$	5-Br	25.3±7.1
21e	CO	$-CH_2CH(CH_3)_2$	5-Cl	3.4±0.6
21f	CO	$-CH_2CH(CH_3)_2$	5-H	909±93
21g	CO	$-CH_2CH(CH_3)_2$	6-Cl	978±205

I.5 Activity-based probes and click reaction

Activity-based proteomics has been developed to characterize protein activity and directly monitor the functional regulation of enzymes in complex proteomes. This method utilizes small molecule activity based probes (APBs) which covalently modify the enzyme active site and enable detection and affinity purification of a target enzyme population.[71] ABPs can be viewed as chemical antibodies to report on the expression of a protein, but at the same time as probes to detect the target active enzymes in a living system.[72]

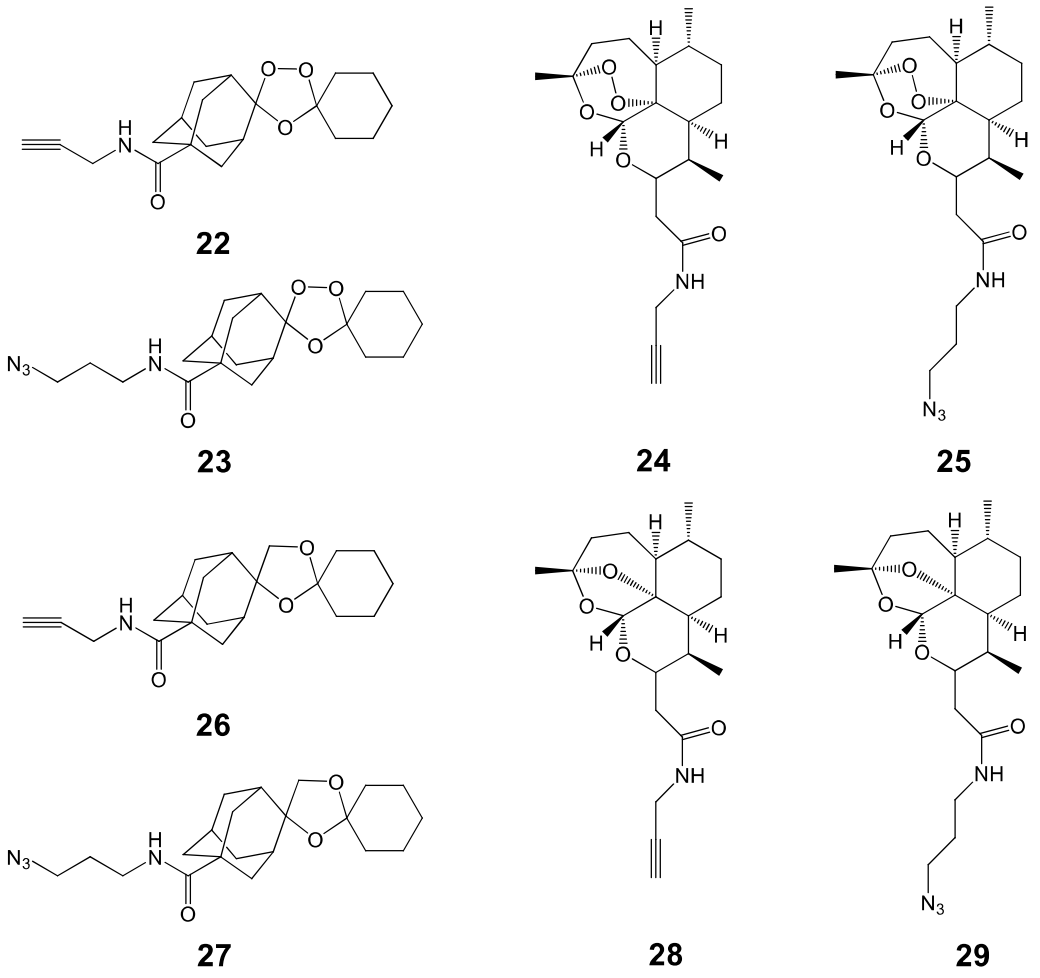

Figure I.15 – 1,2,4-trioxolanes-ABPPs and artemisinin-ABPPs compounds.

In spite of the recent increase in endoperoxide antimalarials under development, it remains unclear if all these chemotypes share a common mechanism of action. Activity-based protein profiling (ABPP) is a proteomic technique that use ABPs. O'Neill *et al.* synthesized activity-based protein profiling probes (ABPPs) based on a 1,2,4-trioxolane antimalarial

core (**22** and **23**, **figure I.15**) and artemisinin core (**24** and **25**, **figure I.15**) in order to characterize their malaria parasite protein alkylation fingerprint. They verified that the active probes containing azide/alkyne functionality retained potent antimalarial activity as determined by their IC_{50} *in vitro* against *P. falciparum* parasites while the non-peroxidic negative control probes (**26** to **29**, **figure I.15**) had not appreciable activity in these assays, confirming the essentiality of the endoperoxide-bridge for drug activity.[73,74]

The click chemistry reactions allows the use of small size of the functional groups like alkyne groups to provide fluorescence *in situ*.[75] Since Sharpless and co-workers introduced the so called click chemistry concept, this tool has become very powerful in biomedical research. These reactions should be fast, simples, stereospecific and give products in very high yields with formation of inoffensive byproducts that can be removed by nonchromatographic methods. Huisgen 1,3-dipolar cycloaddition like cooper-catalyzed azide-alkyne cycloaddition (CuAAC) (**scheme I.3**) is the most widely used.[76,77] In this reaction, azides and alkynes react with one another to form a triazole. A "clickable" handle often does not hinder the permeability of an ABP, but isolation depends on efficiency of the click reaction and subsequent isolation steps.[78]

Alkyne groups were used as surrogate groups for later addition of reporter tags by click chemistry to reduce adverse interactions between bulky tags and the target enzymes.[79] Azides and alkynes are inert to most biological and organic conditions, molecular oxygen, water, and the majority of common reaction conditions in organic synthesis.[76] This property allows highly bioorthogonal fluorescent labeling in living and complex samples.[75]

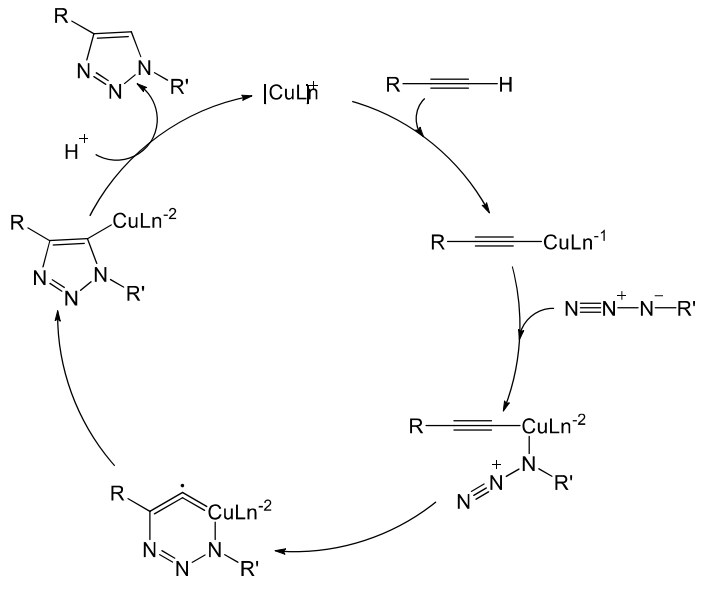

Scheme I.3 – Catalytic cycle of CuAAC. (adapted from [80])

I.7 Goals of the project

As mentioned earlier, the parasites use hemoglobin as a source for the synthesis of essential amino acids. The high selectivity of endoperoxide drugs is one of its most important characteristics since they are only activated by a high concentration of iron (II) that is not present in mammalian cells.

The main goal of this project is to synthesize new tetraoxane-pyrimidine nitrile hybrids ABPs **30** (**scheme I.4**) with an adamantyl group as part of a larger project to identify the molecular targets of antimalarial hybrid drugs. The resulting tetraoxane-pyrimidine nitrile hybrid **30** should be activated by iron (II) and release a potent falcipain inhibitor byproduct inside the parasites (**scheme I.4**).

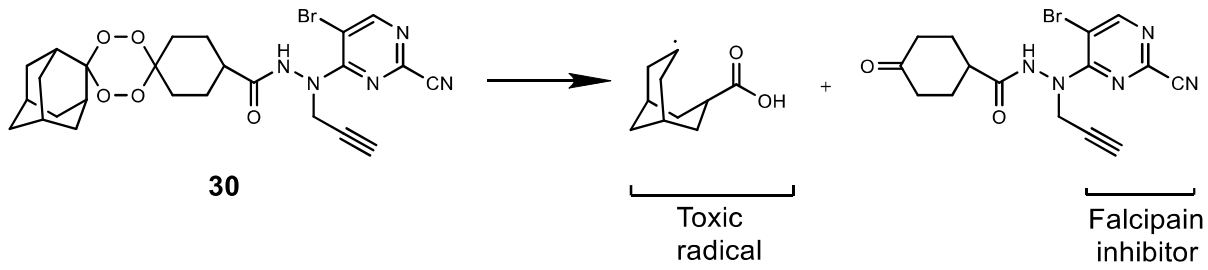

Scheme I.4 – Structure of tetraoxane-pyrimidine nitrile hybrid **30** and release of potent FP-2 inhibitor.

Moreira lab recently identified a low molecular weight pyrimidine nitrile that inhibits both liver and blood stages. This validated drug-like hit is a potent inhibitor of falcipain-2, a cysteine protease involved in host heme degradation in the blood stage but absent in the liver stage of the parasite.

This work should be accompanied by an inactive close analog (“negative” ABP) of our tetraoxane-pyrimidine nitrile hybrid **30**. We decide to use the dioxane-pyrimidine nitrile hybrid **31** (**figure I.16**) as a negative control.

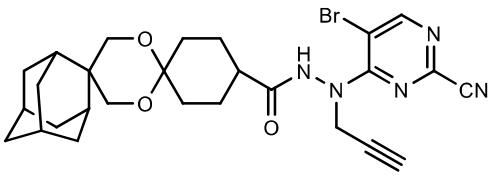

31

Figure I.16 – Structure of "negative" ABP **31**.

To monitor and observe our tetraoxane-pyrimidine nitrile hybrid **30** and compound **31** inside the parasites, we decided to couple both compounds to a fluorescent probe.

The fluorescent tag selected for this assay was nitrobenzoxadiazole (NBD) once it was previously used in *Plasmodium* to visualize accumulation of endoperoxides and could be visualized using confocal microscopy. This will lead us to chemical probes **32** and **33** (**figure I.17**).

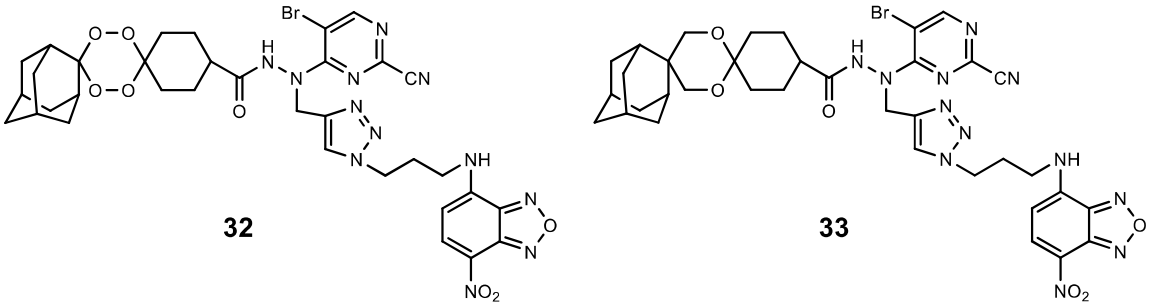

32 **33**

Figure I.17 – Structure of chemical probes **32** and **33.**

Chapter II

II. Methods, results and discussion

All the NMR results used for the characterization of synthesized compounds are presented in **Chapter VI**.

II.1 Tetraoxane-pyrimidine nitrile hybrid

We used a convergent synthetic approach to prepare the tetraoxane-pyrimidine nitrile hybrid ABP **30**. Tetraoxane and pyrimidine nitrile intermediates were synthesized separately and coupled in the final step. **Scheme II.1** illustrates the retrosynthetic analysis of tetraoxane-pyrimidine nitrile hybrid **30**.

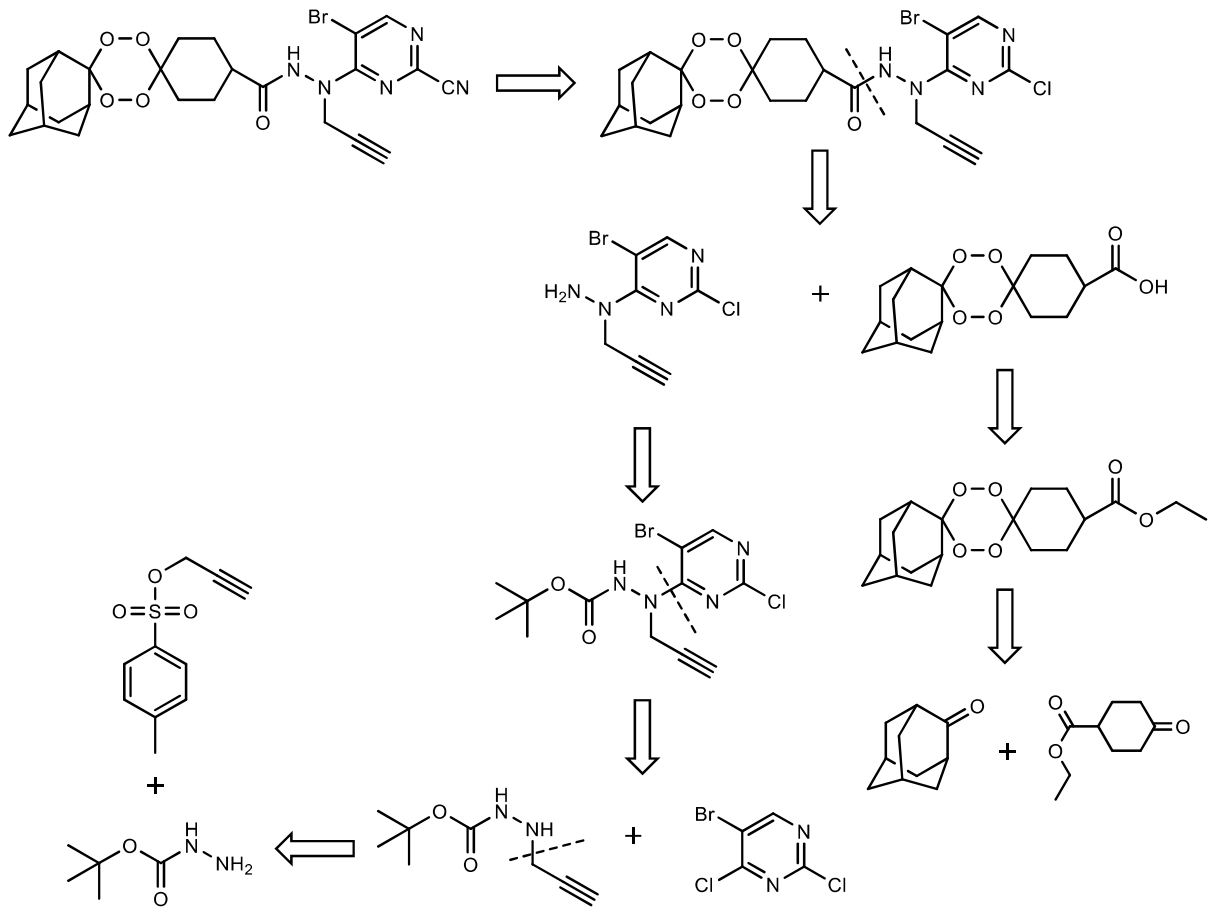

Scheme II.1 – Retrosynthetic analysis pathway for the synthesis of hybrid **30**.

Synthesis of intermediate pyrimidine nitrile **37** (**scheme II.2**) started with the alkylation of Boc-hydrazine **34** by a second-order nucleophilic substitution (SN_2) reaction with propargyl *p*-toluenesulfonate as the electrophile.

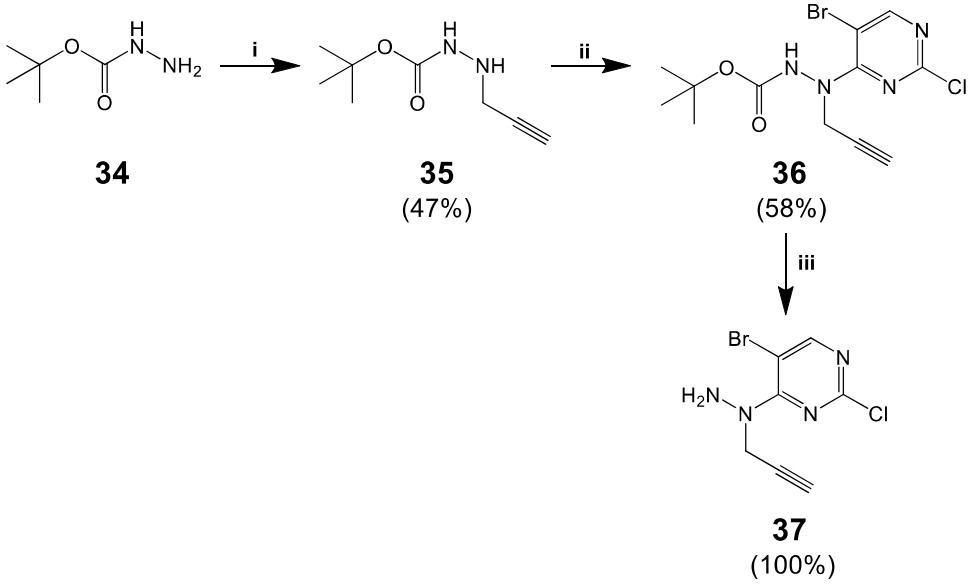

Scheme II.2 – Synthesis of intermediate pyrimidine nitrile **37**. Reagents and conditions: (i) propargyl *p*-toluenesulfonate, DIPEA, dry DCM, 0ºC, 4h, N_2; (ii) 5-bromo-2,4-dichloro pyrimidine, DIPEA, dry EtOH, reflux, ov, N_2; (iii) *p*-toluenesulfonic acid, ACN, rt, ov.

To avoid dialkylation of Boc-hydrazine **34** to a minimum, the temperature was maintained at 0ºC. The product **35** was identified by ^{1}H-NMR (**figure VI.1**). The triplet at 2.25 ppm integrating to one hydrogen and the dublet at 3.63 ppm integrating to two hydrogens correspond to alkyne hydrogen and to CH_2 adjacent to the sp carbon of the alkyne, respectively.

Compound **36** was obtained from a nucleophilic aromatic substitution between hydrazine **35** and 5-bromo-2,4-dichloro pyrimidine. In basic conditions, this substitution occurs preferentially in position 4 of the pyrimidine.[31] The appearance of a singlet integrating to one hydrogen at 8.35 ppm in ^{1}H-NMR spectrum (**figure VI.2**) corresponds to the aromatic proton and proved the product formation. In IR spectrum (**figure VI.7**) was observed a broad band at 3300 cm^{-1} which corresponds to the primary amine and a band at 1726 cm^{-1} which corresponds to the carbonyl of carbamate.

Deprotection of compound **35** with *p*-toluenesulfonic acid and subsequent neutralization with sodium carbonate 1M led to the synthesis of compound **37**. The formation of this compound was proved by the disappearance of the singlet at 1.49 ppm correspondent to

the Boc group and the appearance of a broad singlet integrating for two hydrogens correspondent to NH_2 at in ^{1}H-NMR spectrum (**figure VI.8**).

In IR spectrum of compound **37** (**figure VI.9**) was observed the disappearance of the band at 1726 cm^{-1} which means that Boc group was removed and the peaks 3308 and 3273 cm^{-1} corresponds to the primary amine.

Synthesis of tetraoxane **42** was made four steps (**scheme II.3**). Tetraoxane ester **40** was prepared from **38**, by an acid-catalyzed cyclocondensation procedure described by O'Neill *et al*. (**scheme II.4**).[59]

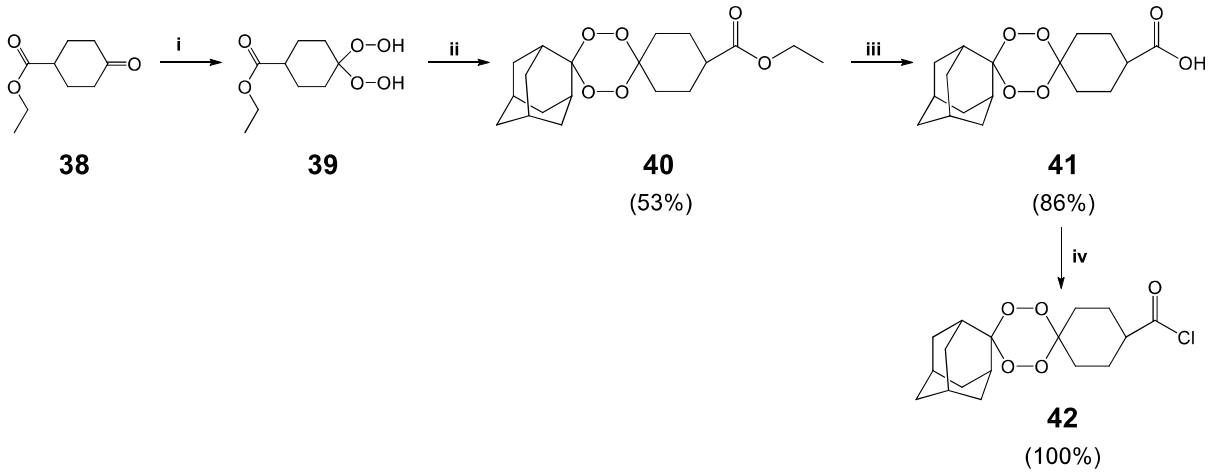

Scheme II.3 – Synthesis of intermediate tetraoxane **42**. Reagents and conditions: (i) HCOOH, H_2O_2 50%, dry ACN, rt, 1h, N_2; (ii) 2-adamantanone, Re_2O_7, dry DCM, rt, 3h, N_2; (iii) MeOH, NaOH, H_2O, reflux, 1h; (iv) $SOCl_2$, DMF, reflux, 6h.

Reaction of ethyl-4-oxocyclohexane-1-carboxylate **38** with hydrogen peroxide (H_2O_2) and formic acid (HCOOH) leads to the corresponding *gem*-dihydroperoxide **39**. Tetraoxane ester **40** was achieved by cyclization of the *gem*-dihydroperoxide **39** with 2-adamantanone using rhenium (VII) oxide (Re_2O_7) catalyst. Re_2O_7 in DCM offers a mild and highly efficient catalysis for the condensation of carbonyl groups with 1,1-dihydroperoxides to form 1,2,4,5-tetraoxanes.[81]

In ^{1}H-NMR spectrum (**figure VI.10**) was verified that CH_2 and CH_3 of ester group appeared as a quartet at 4.13 ppm integrating to two hydrogens and a triplet 1.24 ppm integrating to three hydrogens, respectively. The signal at 174.60 ppm in ^{13}C-NMR spectrum (**figure VI.12**) confirms the presence of the carbonyl carbon of ester function and the tetraoxane core was identified through two characteristic signals for C1 and C2 at 110.5 ppm and 107.2 ppm, respectively.

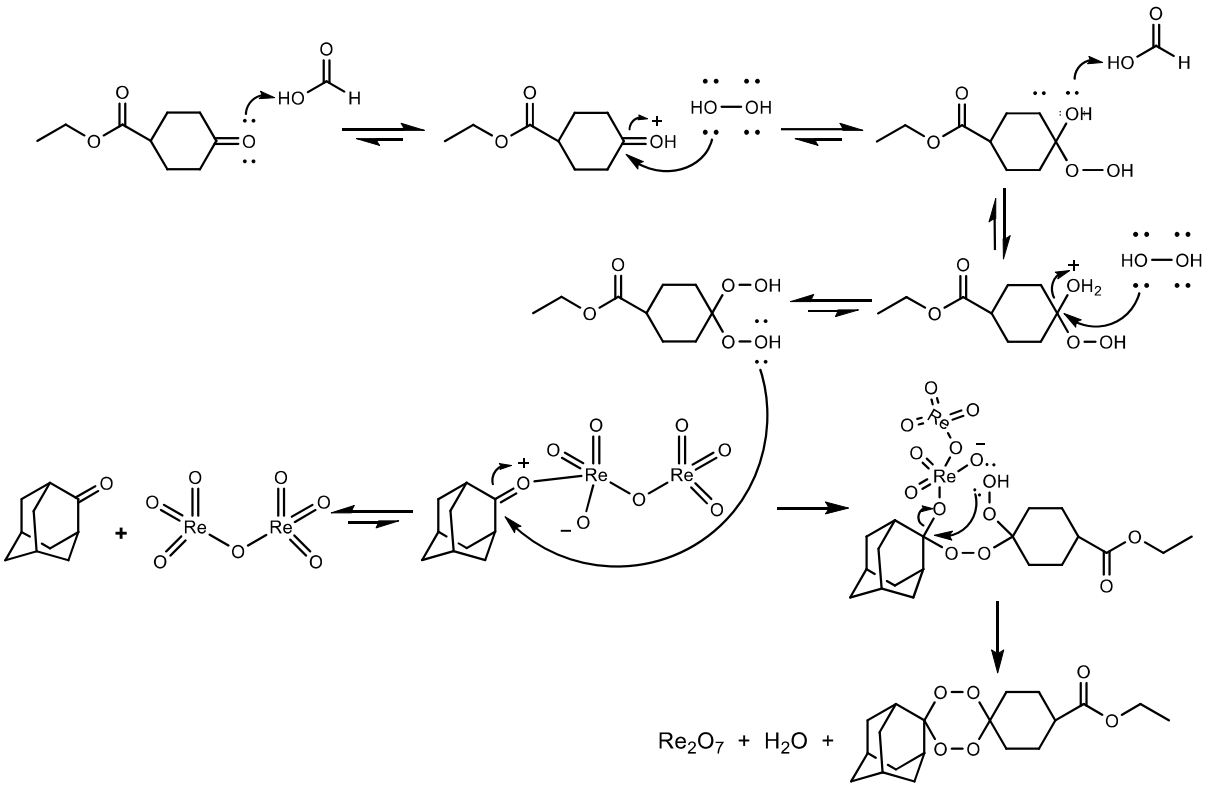

Scheme II.4 – Proposed reaction mechanism for the synthesis of tetraoxane ester **40**.

Tetraoxane ester **40** was subsequently hydrolyzed to tetraoxane acid **41** using sodium hydroxide (NaOH). In ^{1}H-NMR spectrum (**figure VI.16**) was observed the disappearance of the triplet at 1.24 ppm and the quartet at 4.13 ppm of the CH_3 and CH_2, respectively.

Reaction of the tetraoxane acid **41** with thionyl chloride and catalytic dimethylformamide (DMF) led to the formation of the final tetraoxane intermediate **42** (**Scheme II.5**). DMF reacts with thionyl chloride giving the iminium intermediate that subsequently reacts with the carboxylic acid resulting in the acid chloride formation.

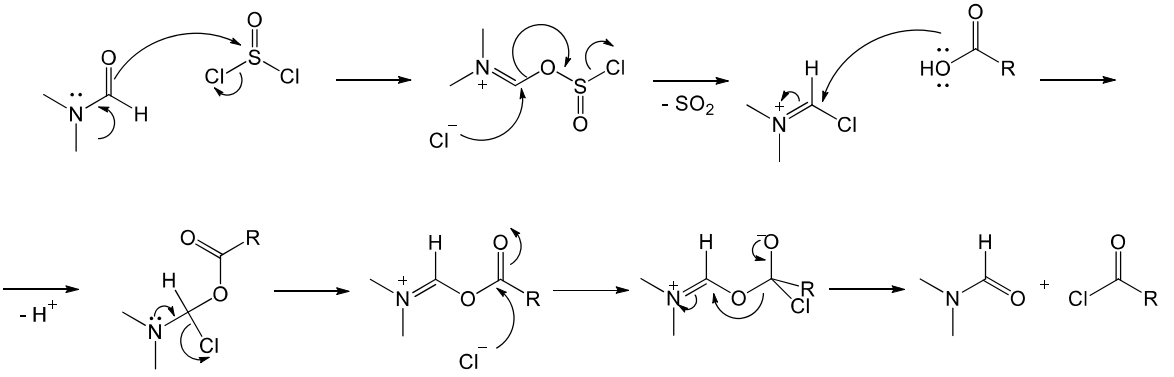

Scheme II.5 – Mechanism of reaction of an acid with thionyl chloride catalyzed by dimethylformamide.

Synthesis of the final tetraoxane-pyrimidine nitrile hybrid **30** followed the mechanism represented in **scheme II.6**.

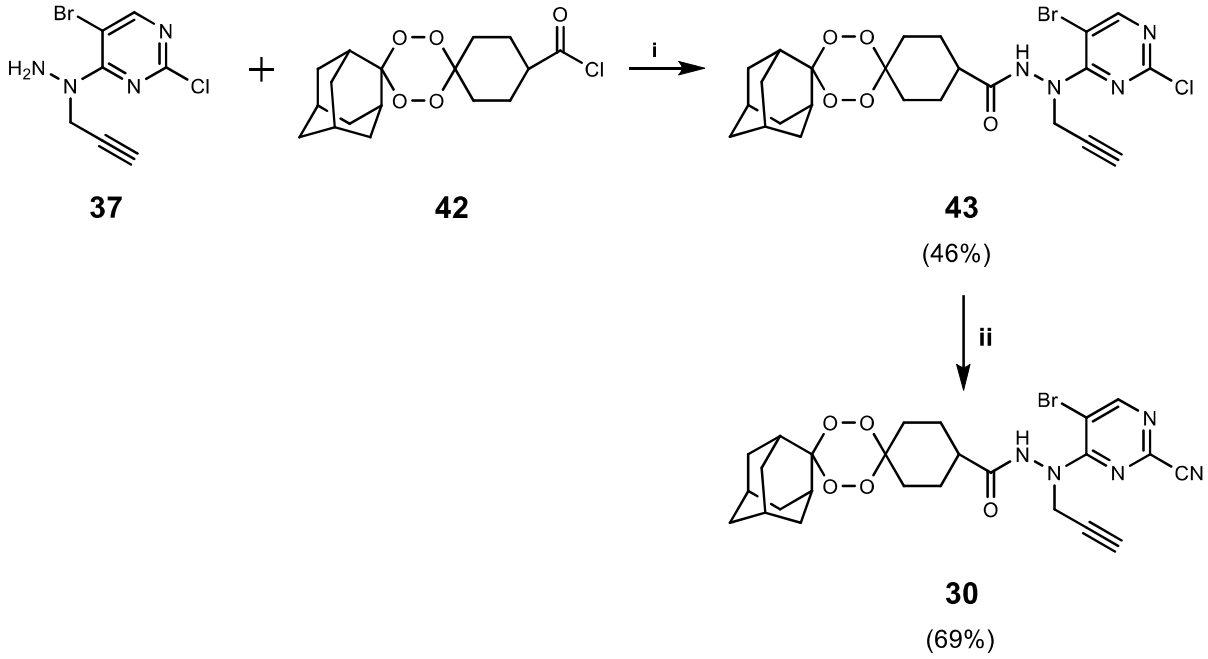

Scheme II.6 – Synthesis of tetraoxane-pyrimidine nitrile hybrid **30**. Reagents and conditions: (i) DIPEA, dry THF, rt, ov, N_2; (ii) DABCO, KCN, DMSO/H_2O, rt, 4h30.

First, the coupling of deprotected pyrimidine **37** and tetraoxane **42** was performed in basic conditions with DIPEA and under nitrogen atmosphere. This step led to the formation of tetraoxane-pyrimidine hybrid **37** in moderate yields. In ^{1}H-NMR spectrum (**figure VI.18**) was observed two moieties in 1:1 ratio and the conversion of the primary amine at 4.30 ppm to a secondary amide at 7.79 ppm.

Finally, tetraoxane-pyrimidine hybrid **43** was treated with potassium cyanide in basic conditions to give the final tetraoxane-pyrimidine nitrile hybrid **30**. The conversion of compound **43** in compound **30** is observed by the displacement of the pyrimidine hydrogen from 8.33 ppm to 8.53 ppm in ^{1}H-NMR spectrum (**figure VI.24**) and the appearance of the peak of CN at 115.14 ppm in the ^{13}C NMR (**figure VI.26**).

II.2 Tetraoxane-pyrimidine nitrile probe

To synthesize the tetraoxane-pyrimidine nitrile probe **32** first was prepared the fluorescent tag **46** (**Scheme II.7**).

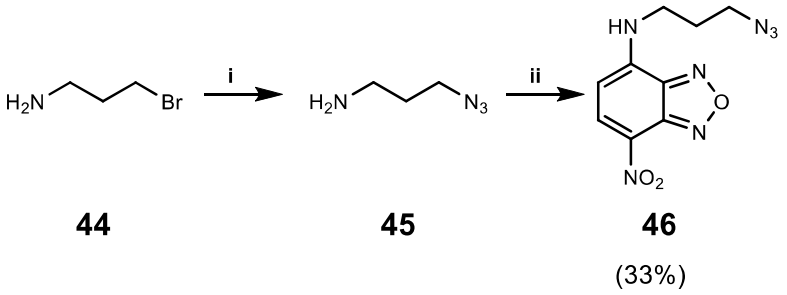

44 **45** **46**

(33%)

Scheme II.7 – Synthesis of fluorescent tag **46**. Reagents and conditions: (i) NaN_3, KI, THF:H_2O (3:1), reflux, ov; (ii) NBD-Cl, $NaHCO_3$, MeOH, reflux, 3h.

First, sodium azide was added to the halogenated carbon chain **44**. The resulting mixture was added to 7-chloro-4-nitrobenzoxadiazole (NBD-Cl) in basic conditions to afford compound **46**. ^{1}H-NMR spectrum (**figure VI.30**) was consistent with the structure.

The final tetraoxane-pyrimidine nitrile probe **32** was prepared from tetraoxane-pyrimidine nitrile hybrid **30** and the fluorescent tag **46** (**scheme II.8**) by a cooper-catalyzed alkyne-azide 1,3-dipolar cycloaddition described by Ruivo *et al*.[82]

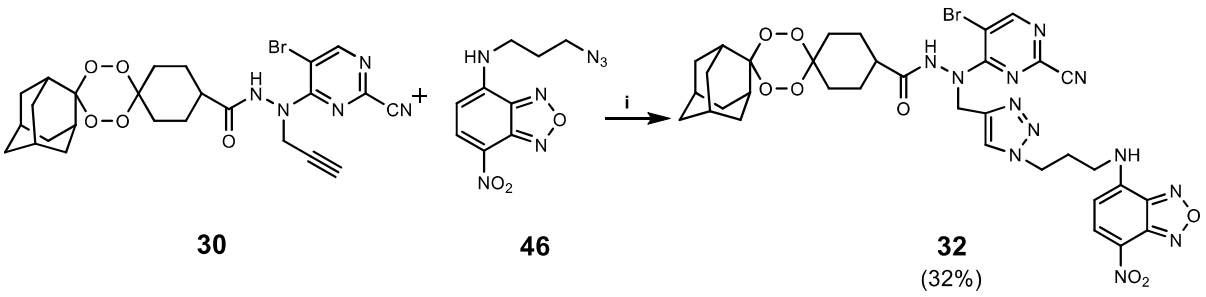

30 **46** **32**

(32%)

Scheme II.8 – Synthesis of tetraoxane-pyrimidine nitrile probe **32**. Reagents and conditions: (i) $CuSO_4$, sodium ascorbate, DMF, TEA, rt, 25h.

The click reaction was proceeded at room temperature in basic conditions with triethylamine. Sodium ascorbate was used as a reducing agent to prevent the oxidation of the copper sulphate and to produce copper (I) *in situ*.[83,84] The product was obtain with low

yield. The formation of cyclic 1,4-triazole was confirmed by ^{1}H-NMR due to the presence of a singlet at 9.13 ppm and the absence of propargyl CH signal (**figure II.1**).

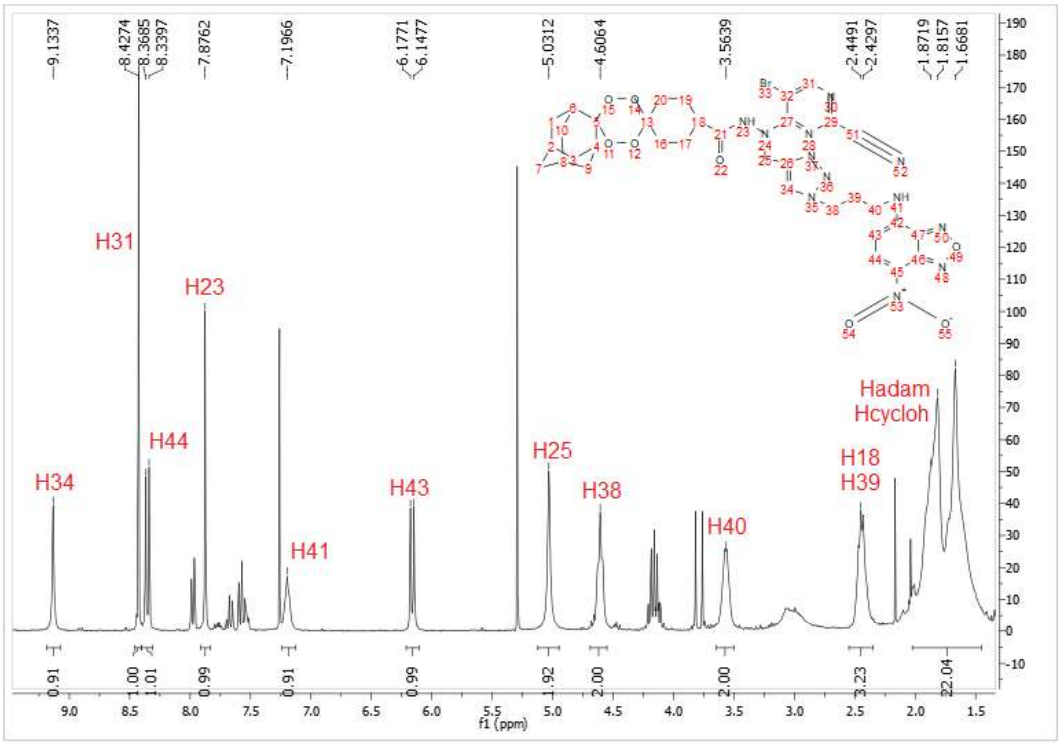

Figure II.1 - ^{1}H-NMR spectrum ($CDCl_3$) of tetraoxane-pyrimidine nitrile probe **32**.

II.3 Dioxane-pyrimidine nitrile hybrid

As tetraoxane-pyrimidine nitrile hybrid **30**, synthesis of dioxane-pyrimidine nitrile hybrid **33** was made in two separately steps. Intermediates, dioxane and pyrimidine nitrile, were separately synthesized and in the end, were coupled. **Scheme II.9** illustrates the retrosynthetic analysis of dioxane-pyrimidine nitrile hybrid **31**.

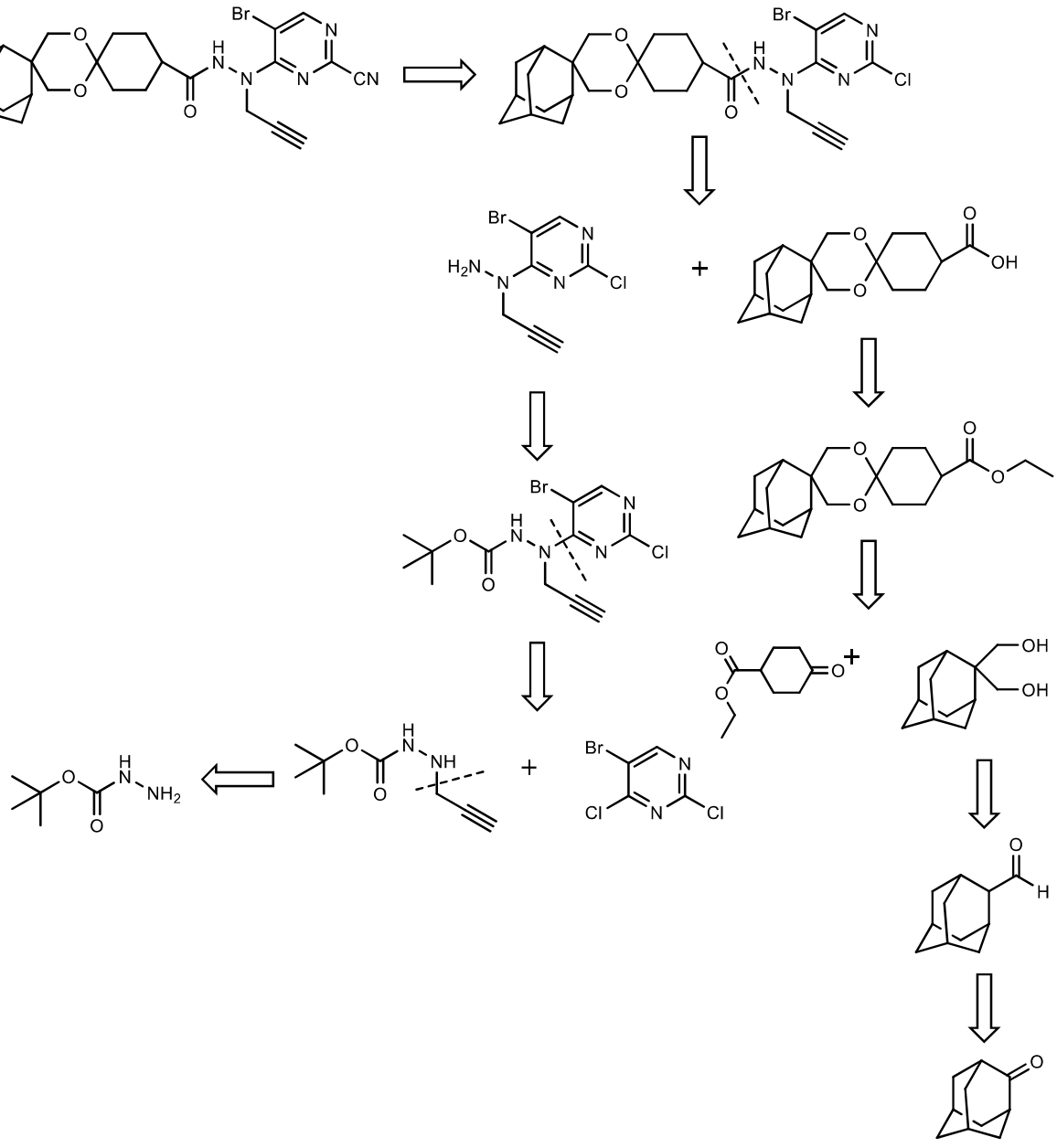

Scheme II.9 – Retrosynthetic analysis pathway for the synthesis of hybrid **31**.

In order to obtain the dioxane **51** with the carboxylic acid group, we started with 2-adamantanone **47**, according to **Scheme II.10**.

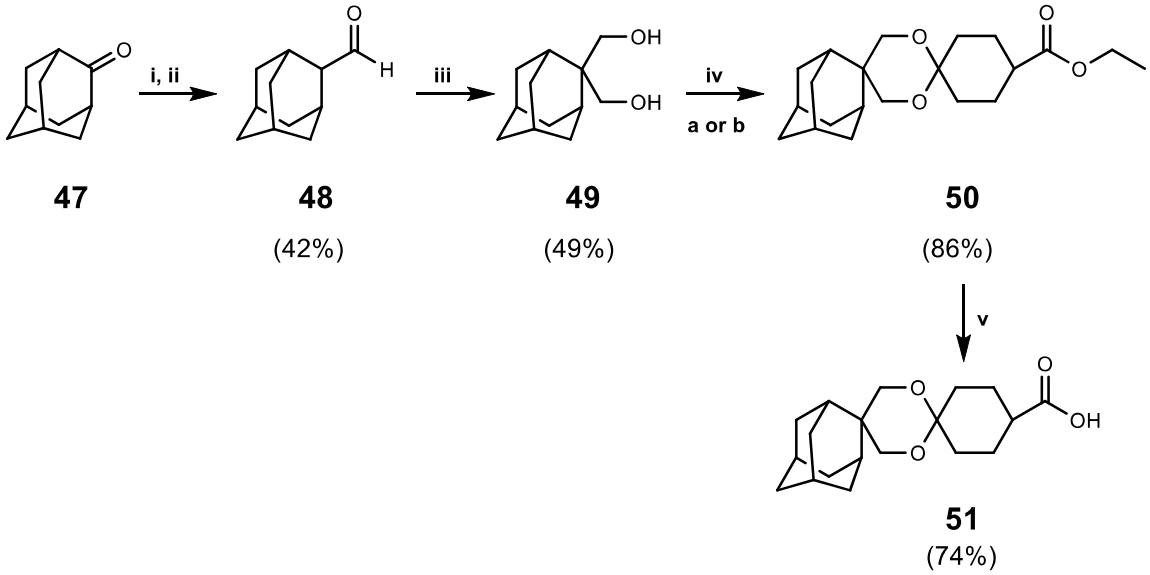

Scheme II.10 – Synthesis of dioxane **51**. Reagents and conditions: (i) KHMDS·hexane, $CH_3OCH_2PPh_3Cl$, dry THF, 0ºC, 4h, N_2; (ii) HCl, ACN, rt, ov; (iii) CH_2O, NaOH, THF:MeOH (2:3), rt, 18h; (iv) method A: **38**, *p*-TsOH, dry toluene, Dean-Stark conditions, 18h; method B: **38**, $ZrCl_4$, $(EtO)_3CH$, dry DCM, rt, 45 min, N_2; (v) NaOH, MeOH, H_2O, reflux, 2h.

Synthesis of dioxane **51** started with 2-adamantanone **47** to obtain aldehyde **48**. This reaction was made by three different methods using three different bases and a phosphonium salt in a Wittig-Horner reaction followed by hydrolysis in acidic conditions (**scheme II.11**). In method A was used potassium bis(trimethylsilyl)amide (KHMDS)[85], in method B was used n-butyllithium (*n*-BuLi)[86,87] and in method C was used sodium hydride (NaH) as base.

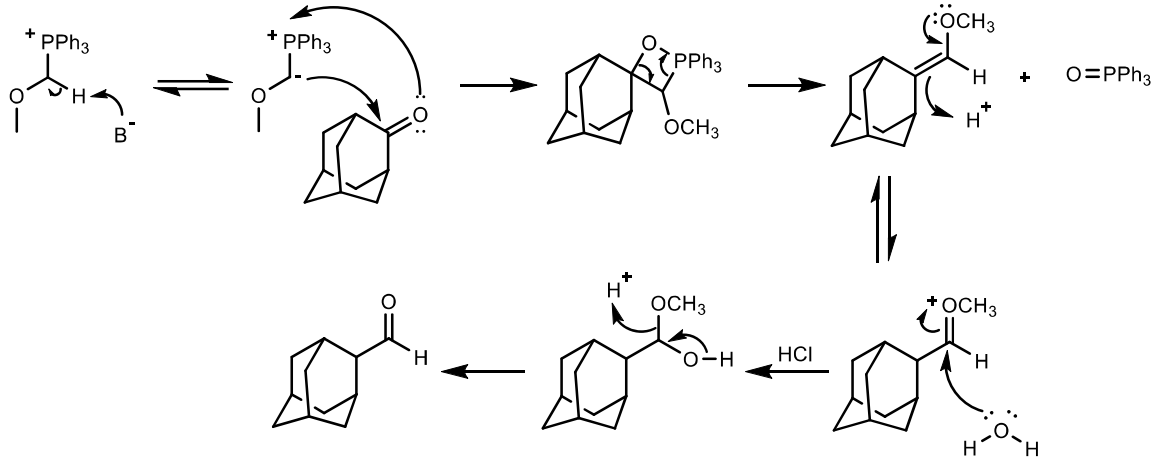

Scheme II.11 – Synthesis mechanism of aldehyde **48**.

Aldehyde **48** was not obtained using method B and method C but method A allowed the synthesis of aldehyde with moderate yields. ^{1}H-NMR spectrum (**figure VI.37**) showed the characteristic signal of the aldehyde group at 9.73 ppm and is consistent with the literature.[85] The multiplet at 2.00-1.58 ppm integrates to fourteen protons instead of twelve probably because of the presence of water in chloroform.

Diol **49** was prepared according to *Cannizzaro* (**scheme II.12**).[88,89] Treatment of the aldehyde **48** with formaldehyde in basic conditions leads to diol **49**. First, the α-hydrogen of the aldehyde reacts with formaldehyde by an aldol condensation giving a β-hydroxyaldehyde. At the same time, a second molecule of formaldehyde reacts with an hydroxide ion producing a highly unstable dianion. The dianion formed transfers a hydride to the β-hydroxyaldehyde forming the final diol **49** in moderate yields.

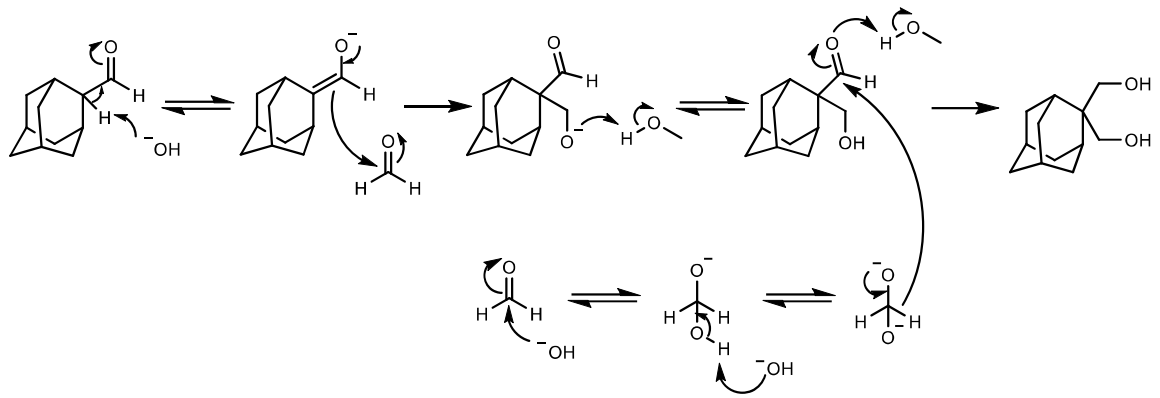

Scheme II.12 – Synthesis mechanism of diol **49**.

In ^{1}H-NMR spectrum (**figure VI.38**) it was observed the disappearance of the signal of the aldehyde proton and the appearance of a singlet integrating to four hydrogens at 3.94 ppm referent to two dimethanol groups (CH_2OH) of compound **49**.

Synthesis of dioxane ester **50** was tried by two different methods. In method A, reaction of ethyl-4-oxocyclohexane-1-carboxylate **38** with the diol **49** using Dean-Stark conditions was not successful and the product was not obtained. Method B was based in a reaction described by Firouzabadi *et al*.[90] In this method the acetalization between of ethyl-4-oxocyclohexane-1-carboxylate and the diol **49** was made using zirconium tetrachloride ($ZrCl_4$) as catalyst. Method B afforded diol **50** in good yields.

In ^{1}H-NMR spectrum of compound **50** (**figure VI.39**) was verified that the signals of the CH_2 and CH_3 of ester function appeared as a quartet at 4.11 ppm integrating to two hydrogens and a triplet at 1.23 ppm integrating to three hydrogens, respectively. The signal at 175.34 ppm in ^{13}C-NMR spectrum (**figure VI.41**) confirms the presence of the carbonyl carbon of ester function.

Dioxane ester **50** was subsequently hydrolyzed in basic conditions to afforded dioxane acid **51**. ^{1}H-NMR spectrum (**figure VI.45**) was observed the disappearance of the triplet at 1,23 ppm and the quadruplet at 4.11 ppm correspondents to CH_3 and CH_2, respectively.

For the preparation dioxane-pyrimidine nitrile hybrid **52** (**scheme II.13**) we used O-(Benzotriazol-1-yl)-N,N,N',N'-tetramethyluronium tetrafluoroborate (TBTU) at 0ºC to avoid a concentrated acid environment or high temperatures that could degrade the acetal. After the amide coupling reaction, the dioxane-pyrimidine nitrile hybrid **52** was characterized by ^{1}H-NMR and the product was not synthesized.

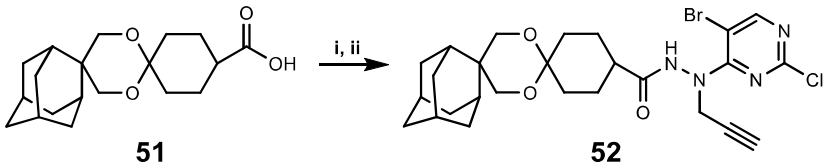

51 **52**

Scheme II.13 – Synthesis of dioxane-pyrimidine nitrile hybrid **52**. Reagents and conditions: (i) TBTU, TEA, dry DCM, 0ºC, 1h, N_2; (ii) **37**, dry DCM, rt, ov, N_2.

Chapter III

III. Concluding remarks and future perspectives

The emergence of drug-resistant pathogens is a major threat to human health, and *P. falciparum* exhibit its high propensity to develop resistance to every drug that has been deployed against it on a large scale.

In chapter I, we revealed the opportunity to develop an improved delivery system based on endoperoxide to be used as a carrier of other drugs for malaria parasites. The pharmacological potential of tetraoxanes has boosted the strategies for the synthesis of new derivatives in order to expand the libraries of new compounds for studies of pharmacological activity and to allow the identification of new drug candidates.

In order to develop a more drug-like compound, in this project we successfully designed and synthesized in moderate to good yields a new tetraoxane-pyrimidine chemical hybrid that can act by two distinct mechanisms of action, an essential feature to prevent selection of drug resistance. This compound is based in non-peptidic FP inhibitors that should be more viable for oral administration, moreover the fact they react reversibly with nucleophiles should prevent undesired toxicity.

We also successfully developed a new hybrid ABP coupled to a fluorescent tag to be used in cellular localization assays. Studying the accumulation of that compound in *Plasmodium* parasites should provide information about the delivery process of FP inhibitors by tetraoxane systems. This compound should allow us to identify the molecular targets and to understand the mechanism of action in the blood and liver stages.

Further work is needed to complete the synthesis of the negative ABP tetraoxane-pyrimidine nitrile probe. Furthermore, these compounds should be evaluated for their metabolic stability and *in vitro* and *in vivo* efficacy.

Chapter IV

IV. Synthesis

IV.1 Equipment

NMR spectra (1D and 2D) were recorded on a Brucker 300 Ultra Shield. The chemical shifts, δ, are expressed in ppm, and coupling constants (*J*) are expressed in Hz. Multiplicities are given as: s (singlet), d (duplet), t (triplet), q (quartet), quint (quintuplet) and m (multiplet).

Infrared (IR) spectra were performed on a Nicolet Impact 400 FTIR spectrophotometer using thin films between NaCl tablets and only the most significant absorption bands are reported.

Melting points were determined using a Kofler Bock Monoscop M. Camera and are uncorrected.

Mass analysis were determined using a Micromass Quattro Micro API spectrometer, equipped with Watters 2695 HPLC Module and Waters 2996 Photodiode Array Detector.

IV.2 Reagents

Reagent grade chemicals were purchased from Alfa Aesar, Sigma-Aldrich or Merck.

IV.3 Solvents

Analytical grade solvents were used. Dichloromethane was dried from calcium chloride, acetonitrile from phosphorous pentoxide, ethanol from calcium hydride and distilled at atmospheric pressure. Tetrahydrofuran and diethyl ether were dried from sodium-benzophenone system. Toluene was dried with sodium metal. All the solvents used in purification were distilled under reduced pressure.

Deutered chloroform used for NMR analysis was purchased from Merck with a degree of purity higher than 95%.

IV.4 Chromatography

Thin layer chromatography was performed on pre-coated silica gel 60 F_{254} (Merck) and visualized using a CAMAG UV cam at UV wavelength, iodine and ninhydrin, potassium permanganate, *p*-anisaldehyde and dinitrophenylhydrazine dip.

Flash chromatography was performed with silica gel 60 M, 0.400-0.063 mm (Merck). Preparative thin-layer chromatography was performed with silica gel 60 GF_{254}, 0.040-0.063 mm (Merck).

IV.5 Synthesis of tetraoxane-pyrimidine nitrile hybrid

IV.5.1 Synthesis of *tert*-butyl 2-(prop-2-yn-1-yl)hydrazine carboxylate (35)

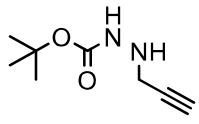

A solution of *tert*-butylcarbazate (2 mmol, 264 mg) and propargyl p-toluenesulfonate (2 mmol, 420 mg, 346 µL) in dry dichloromethane (5 mL) was stirred for 1h at 0ºC, under nitrogen atmosphere. Then, was added diisopropylethylamine (4 mmol, 517 mg, 697 µL) and the mixture was stirred for 3h in the same conditions. The mixture was concentrated and purified by flash column chromatography (10% ethyl acetate in dichloromethane). White solid (47% yield); mp: 45-47°C. ^{1}H-NMR (300 MHz, $CDCl_3$) δ = 6.17 (bs, 1H, NH), 4.09 (bs, 1H, NH), 3.63 (d, *J* = 2.5 Hz, 2H, C$\underline{H_2}$CCH), 2.25 (t, *J* = 2.5 Hz, 1H, CH_2C$\underline{H}$), 1.47 (s, 9H, Boc) ppm.

IV.5.2 Synthesis of *tert*-butyl 2-(5-bromo-2-chloropyrimidin-4-yl)-2-(prop-2-yn-1-1yl)hydrazine carboxylate (36)

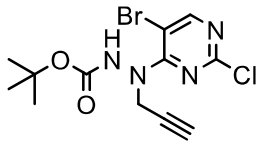

To a solution of compound **35** (1.5 mmol, 254 mg) in dry ethanol (7.5 mL), was added 5-bromo-2,4-dichloro pyrimidine (1.8 mmol, 410 mg, 230 µL) and diisopropylethylamine (3.75 mmol, 653 µL). The solution was refluxed for 5h. The solution was concentrated under reduced pressure and the crude was diluted with dichloromethane (30 mL) and washed with a saturated solution of ammonium chloride (2 x 30 mL). The combined organic extracts were dried over anhydrous sodium sulphate, filtered and concentrated under reduced pressure. The residue was purified by flash column chromatography (10% ethyl acetate in dichloromethane). Yellow solid (58% yield); mp: 140-142°C. ^{1}H-NMR (300 MHz, $CDCl_3$) δ = 8.34 (s, 1H, H_{Ar}), 6.94 (bs, 1H, NH), 4.64 (bs, 2H, $C\underline{H}_2CCH$), 2.35 (t, *J* = 2.5 Hz, 1H, $CH_2CC\underline{H}$), 1.49 (bs, 9H, Boc) ppm. ^{13}C-NMR (75 MHz, $CDCl_3$) δ = 162.48 (CO), 160.95 (Cq), 158.44 (Cq), 153.83 (C_{AR}-H), 102.07 (Cq), 83.02 ($(CH_3)_3\underline{C}$), 77.00 ($CH_2\underline{C}CH$), 74.28 ($CH_2C\underline{C}H$), 41.51 ($\underline{C}H_2CCH$), 28.65 ($OC\underline{C}H_3$) ppm.

IV.5.3 Synthesis of 1-(2-bromo-5-chlorophenyl)-1-(prop-2-yn-1-yl)hydrazine (37)

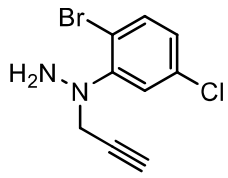

To a solution of compound **36** (0,85 mmol, 308.1 mg) in acetonitrile (6.54 mL, was added *p*-toluenesulfonic acid monohydrate (3.27 mmol, 622 mg). The reaction was stirred overnight at room temperature. Then, the solvent was removed under reduced pressure and the crude was diluted with 1M solution of sodium carbonate (30 mL) and extracted with ethyl acetate (3 x 30 mL). The combined organic phases were dried over anhydrous sodium sulphate, filtered and concentrated under reduced pressure. White solid (100% yield); ^{1}H-NMR (300 MHz, $CDCl_3$) δ = 8.32 (s, 1H, H_{Ar}), 4.59 (d, *J* = 2.4 Hz, 2H, $C\underline{H}_2CCH$), 4.30 (s, 2H, NH_2), 2.33 (t, *J* = 2.4 Hz, 1H, $CH_2CC\underline{H}$) ppm.

IV.5.4 Synthesis of tetraoxane ester (40)

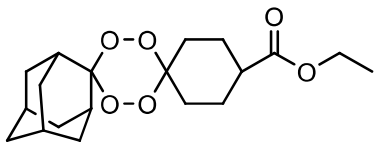

To a solution of ethyl-4-oxocyclohexane-1-carboxylate (5 mmol, 797 µL) in dry acetonitrile (5.5 mL) were added formic acid (3.7 mL) and hydrogen peroxide (1.9 mL, 50% aqueous solution) at 0ºC. After 1h of stirring at room temperature under nitrogen atmosphere the reaction mixture was diluted in dichloromethane (40 mL) and washed with distilled water (2 x 40 mL). The organic phase was dried with anhydrous sodium sulfate, filtered and concentrated under reduced pressure to give the *gem*-dihydroperoxide. The intermediate was dissolved in dry dichloromethane (5 mL) and added to a solution of 2-adamantanone (7.5 mmol, 1.126 g) and rhenium (VII) oxide (0.068 mmol %, 33 mg) in dry dichloromethane (5 mL) at 0ºC. After stirring for 3h at room temperature under nitrogen atmosphere, the reaction mixture was filtrate in vacuum with a layer of silica. The filtrate was concentrated under reduced pressure and purified by flash column chromatography (5% ethyl acetate in hexane). White solid (53% yield); mp: 67-69°C. ^{1}H-NMR (300 MHz, $CDCl_3$) δ = 4.13 (q, *J* = 7.1 Hz, 2H, C<u>H</u>$_2$CH$_3$), 2.45-2.34 (m, 1H, C<u>H</u>COOEt), 2.14-1.45 (m, 22H, adam-H and cycloh-H), 1.24 (t, *J* = 7.1 Hz, 3H, CH$_2$C<u>H</u>$_3$) ppm. ^{13}C-NMR (75 MHz, $CDCl_3$) δ = 174.60 (CO), 110.50 (adamCOO), 107.19 (OOCcycloh), 60.40 (<u>C</u>H$_2$CH$_3$), 41.68 (<u>C</u>HCOOEt), 39.26 (adam-CH$_2$ and cyclo-CH$_2$), 36.26 (adam-CH$_2$ and cycloh-CH$_2$), 33.13 (adam-CH$_2$ and cycloh-CH$_2$), 27.05 (adam-CH), 14.21 (CH$_2$<u>C</u>H$_3$) ppm.

IV.5.5 Synthesis of tetraoxane acid (41)

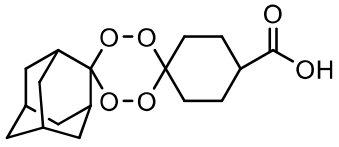

To a solution of compound **40** (0.14 mmol, 50 mg) in methanol (700 µL) was added 1M sodium hydroxide solution (700 µL) in distilled water (231 µL). The mixture was refluxed for 1h30, after which the solution was allowed to cool to room temperature and concentrated under reduced pressure. The crude was taken up in distilled water (30 mL) and extracted with diethyl ether (3 x 20 mL). The aqueous layer was acidified with concentrated hydrochloric acid to pH 1 and extracted with diethyl ether (3 x 20 mL). The combined organic phases were washed with brine solution (3 x 30 mL), dried over anhydrous sodium sulphate, filtered and concentrated under reduced pressure. White

solid (53% yield); mp: 151-153°C. ^{1}H-NMR (300 MHz, $CDCl_3$) δ = 2.52-2.41 (m, 1H, C<u>H</u>COOEt), 2.08-1.44 (m, 22H, adam-H and cycloh-H) ppm.

IV.5.6 Synthesis of tetraoxane chloride acid (42)

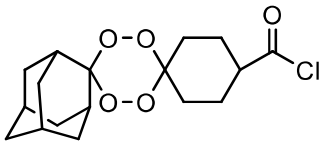

A mixture of compound **41** (0.67 mmol, 217.2 mg), thionyl chloride (59.28 mmol, 4.3 mL) and catalytic dimethylformamide was stirred for 2h in reflux. The solution was concentrated under reduced pressure. White solid (100% yield); ^{1}H-NMR (300 MHz, $CDCl_3$) δ = 2.92-2.79 (m, 1H, C<u>H</u>COOEt), 2.17-1.46 (m, 22H, adam-H and cyclo-H) ppm.

IV.5.7 Synthesis of tetraoxane-pyrimidine nitrile hybrid-Cl (43)

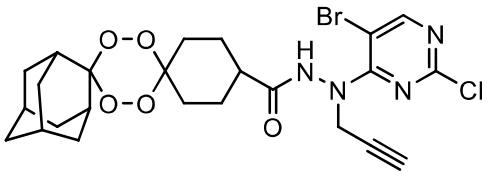

A solution of compound **37** (0.95 mmol, 248.7 mg) in dry tetrahydrofuran (4.5 mL) was added to a solution of compound **42** in dry tetrahydrofuran (2 mL). After stirring for 30 min at room temperature under nitrogen atmosphere diisopropylethylamine (2.85 mmol, 496 µL) was added. The mixture was refluxed overnight. The mixture was diluted with dichloromethane (30 mL) and washed with distilled water (30 mL) and the phases were separated. The aqueous phase was further extracted with dichloromethane (2 x 20 mL). The combined organic phases were dried over anhydrous sodium sulphate, filtered and concentrated under reduced pressure. The residue was purified by flash column chromatography (20% ethyl acetate in hexane). White solid (46 % yield); mp: 137-139°C. ^{1}H-NMR (300 MHz, $CDCl_3$) δ = 8.33 (s, 1H, H_{Ar}), 7.79 (s, 1H, NH), 4.63 (bs, 2H, C<u>H</u>$_2$CCH), 2.46-2.30 (m, 1H, C<u>H</u>CONH), 2.36 (t, *J* = 2.4 Hz, 1H, CH$_2$CC<u>H</u>), 2.09-1.49 (m, 22H, adam-H and cycloh-H) ppm. ^{13}C-NMR (75 MHz, $CDCl_3$) δ = 172.42 (CO), 161.92 (C_{Ar}-H), 160.79 (Cq), 158.20 (Cq), 110.70 (adamCOO), 106.75 (OOCcycloh), 102.21 (Cq), 77.00 (CH$_2$<u>C</u>CH), 74.38 (CH$_2$C<u>C</u>H), 41.57 (<u>C</u>HCOOEt), 40.72 (<u>C</u>H$_2$CCH), 36.88 (adam-CH$_2$ and cycloh-CH$_2$), 33.12 (adam-CH$_2$ and cycloh-CH$_2$), 26.99 (adam-CH) ppm.

IV.5.8 Synthesis of tetraoxane-pyrimidine nitrile hybrid-CN (30)

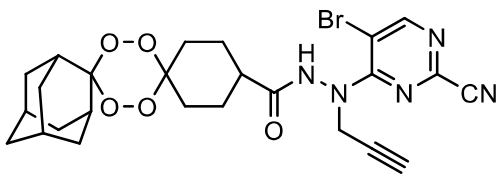

To a solution of compound **43** (0.377 mmol, 214.3 mL) and 1,4-diazabicyclo[2,2,2]octane (0.377 mmol, 42.29 mg) in dimethylsulfoxide/water (9:1, 3.77 mL) was added potassium cyanide (0.415 mmol, 27 mg). After 4h30 of stirring at room temperature the reaction mixture was poured into ice water (40 mL) and extracted with ethyl acetate (3 x 40 mL). The combined organic phases were washed with saturated sodium bicarbonate (2 x 30 mL), dried over anhydrous sodium sulphate, filtered and concentrated under reduced pressure. White solid (69% yield); mp: 143-145ºC. ^{1}H-NMR (300 MHz, $CDCl_3$) δ = 8.53 (s, 1H, H_{Ar}), 7.95 (s, 1H, NH), 4.62 (bs, 2H, C$\underline{H}_2$CCH), 2.48-2.32 (m, 1H, C$\underline{H}$CONH), 2.39 (t, *J* = 2.4 Hz, 1H, $CH_2C\underline{C}H$), 2.11-1.42 (m, 22H, adam-H and cycloh-H) ppm. ^{13}C-NMR (75 MHz, $CDCl_3$) δ = 172.52 (CO), 160.93 (C_{Ar}-H), 160.18 (Cq), 141.55 (Cq), 115.16 (CN), 110.72 (adamCOO), 107.20 (OOCcycloh), 106.69 (Cq), 76.57 ($CH_2\underline{C}CH$), 74.77 ($CH_2C\underline{C}H$), 41.50 (cyclohCHCO), 40.96 ($\underline{C}H_2CCH$), 36.87 (adam-CH_2 and cycloh-CH_2), 33.11 (adam-CH_2 and cyclo-CH_2), 26.98 (adam-CH) ppm.

IV.6 Synthesis of tetraoxane-pyrimidine nitrile probe

IV.6.1 Synthesis of N-(3-azidopropyl)-7-nitrobenzo[C][1,2,5] oxadiazol-4-amine (46)

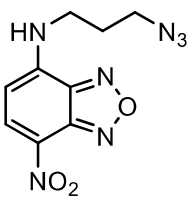

To a solution of 3-bromopropylamine hydrobromide (0.55 mmol, 120.4 mg) in tetrahydrofuran/water (3:1, 1 mL) was added sodium azide (1.1 mmol, 71.5 mg) and catalytic potassium iodide. The mixture was refluxed overnight and then cooled to room temperature. After was added 10N sodium hydroxide solution until pH 11. The mixture was diluted with brine solution (30 mL) and washed with dichloromethane (3 x 30 mL). The combined organic phases were dried with anhydrous sodium sulphate, filtered and partially concentrated under reduced pressure at low temperature. The resultant solution was diluted in methanol (3.5 mL) and

0.1N sodium hydrogen carbonate solution (10 mL). After was added 4-chloro-7-nitrobenzoxadiazole (1.5 mmol) in methanol (5 mL) and the mixture was refluxed 3h. The solution was concentrated under reduced pressure and purified by flash column chromatography (50% ethyl acetate in hexane). Brown solid (33 % yield); mp: 59-61°C. ^{1}H-NMR (300 MHz, $CDCl_3$) δ = 8.47 (s, 1H, H_{Ar}), 6.64 (s, 1H, NH), 6.22 (d, *J* = 8.7 Hz, 1H, H_{Ar}), 3.66 (dd, *J* = 6.5, 12.8 Hz, 2H, NHC$\underline{H}_2$), 3.59 (t, *J* = 12.3 Hz, 2H, C$\underline{H}_2N_3$), 2.07 (quint, *J* = 6.4 Hz, 2H, $CH_2C\underline{H}_2CH_2$) ppm. MS-ESI m/z: 264.1 $[M + H]^+$.

IV.6.2 Synthesis of tetraoxane-pyrimidine nitrile probe (32)

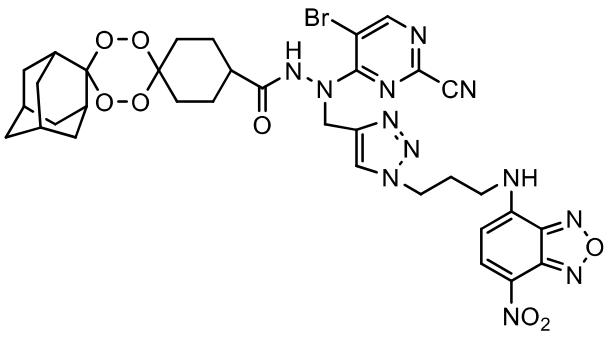

To a stirring solution of compound **30** (0.09 mmol, 50 mg) in dry dimethylformamide (900 µL) at room temperature under nitrogen atmosphere, cooper sulphate (92 µL, aqueous solution 25 mg/ 1 mL) and sodium ascorbate (92 µL, aqueous solution 40 mg/ 1 mL) were added dropwise. After 5 min, compound **46** was also added dropwise and the reaction was stirred at room temperature overnight. After 22h was added a solution of triethylamine (0.098 mmol, 13.7 µL) and the reaction was stirred for more 3h. The mixture was concentrated under reduced pressure, diluted with distilled water (15 mL) and extracted with ethyl acetate (4 x 15 mL). The combined organic phases were dried over anhydrous sodium sulphate, filtered and concentrated. The resulting residue was purified by preparative thin-layer chromatography (40 % ethyl acetate in hexane). Brown oil (32 % yield). ^{1}H-NMR (300 MHz, $CDCl_3$) δ = 9.13 (s, 1H, C$\underline{H}_{triazole}$), 8.43 (s, 1H, $H_{Ar\text{-}pyr}$), 8.35 (d, *J* = 8.7 Hz, 1H, $H_{Ar\text{-}NBD}$), 7.88 (s, 1H, cyclohCON$\underline{H}$), 7.20 (m, 1H, $CH_2CH_2CH_2N\underline{H}$), 6.16 (d, *J* = 8.7 Hz, 1H, $H_{Ar\text{-}NBD}$), 5.03 (s, 2H, NHNC$\underline{H}_2$), 4.70-4.55 (m, 2H, C$\underline{H}_2CH_2CH_2$), 3.65-3.50 (m, 2H, $CH_2CH_2C\underline{H}_2$), 2.55-2.35 (m, 3H, C$\underline{H}$CONH and $CH_2C\underline{H}_2CH_2$), 2.15-1.42 (m, 22H, adam-H and cycloh-H) ppm. ^{13}C-NMR (75 MHz, $CDCl_3$) δ = 173.86 (CO), 160.67 ($C_{Ar\text{-}pyr}$), 159.84 (Cq), 144.22 (Cq), 143.83 (Cq), 141.95 (Cq), 141.21 (Cq), 136.70 ($C_{Ar\text{-}NBD}$), 134.18 ($C_{Ar\text{-}triazole}$), 129.21, 128.24, 124.95, 123.57 (Cq), 115.43 (CN), 110.63 (adamCOO), 107.06 (OOCcycloh), 106.78 (Cq), 99.22 ($C_{Ar\text{-}NBD}$), 47.72 ($\underline{C}H_2CH_2CH_2$), 47.04 (NHN$\underline{C}H_2$), 41.01 ($\underline{C}$HCONH), 40.80 ($CH_2CH_2\underline{C}H_2$), 36.82 (adam-CH_2 and

cycloh-CH_2), 33.07 (adam-CH_2 and cycloh-CH_2), 28.48 ($CH_2\underline{C}H_2CH_2$), 26.97 (adam-CH) ppm. MS-ESI m/z: 821.0 $[M + H]^+$.

IV.6 Synthesis of dioxane-pyrimidine nitrile hybrid

IV.6.1 Synthesis of adamantane-2-carbaldehyde (48)

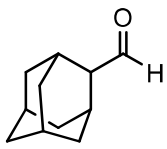

Method A: A solution of methoxymethyltriphenylphosphonium (5.83 mmol, 1.9985 g) and potassium bis(trimethylsilyl)amide (0.5M in hexane, 11.66 mL) in dry tetrahydrofuran (7.5 mL) was stirred for 15 min at 0ºC under nitrogen atmosphere. Then was added a solution of 2-adamantanone (4.16 mmol, 625 mg) in dry tetrahydrofuran (2.5 mL) and the mixture was stirred for 2h in the same conditions. The solution was diluted with distilled water (30 mL) and extracted with diethyl ether (3 x 30 mL). The combined organic phases were dried with anhydrous sodium sulphate, filtered and concentrated under reduced pressure. The crude was dissolved in acetonitrile (25 mL) and hydrochloric acid (1M, 6,25 mL) was added and stirred for 21h at room temperature. The solution was diluted with brine soltution (30 mL) and extracted with diethyl ether (3 x 30 mL). The combined organic phases were dried over anhydrous sodium sulphate, filtered and concentrated under reduced pressure. White solid (42% yield); mp: 129-131°C. ^{1}H-NMR (300 MHz, $CDCl_3$) δ = 9.73 (s, 1H, COH), 2.43-2.36 (m, 3H), 2.00-1.58 (m, 12H) ppm.

Method B: A two-necked round-flask was charged with methoxymethyltriphenyl phosphonium (5 mmol, 1.717 g) and purged with nitrogen. Then was added dry diethyl ether (11.5 mL) and stirred at 0ºC for 10 min. n-buthyllithium was slowly added and the mixture changed from yellow to dark orange and stirred for 1h at 0ºC under nitrogen atmosphere. In another flask, 2-adamantanone (4.3 mmol, 646 mg) was dissolved in dry diethyl ether (7.12 mL) and the mixture was added dropwise to the previous flask. The mixture was allowed to stir for 16h30 at room temperature under nitrogen atmosphere. The solution was stirred vigorously while zinc chloride was added to complex with the suspended triphenylphosphine oxide. The ether layer was filtrated and concentrated under reduced pressure to yield the enol ether. The crude was dissolved in dry diethyl ether (8 mL) and were added perchloric acid (70%, 799 µL) and distilled water (444 µL). After

stirring for 1h in reflux, the mixture was poured into distilled water (50 mL). The organic layer was extracted with distilled water (2 x 50 mL), dried over anhydrous sodium sulphate, filtered and concentrated under reduced pressure. The desired product was not isolated.

Method C: A solution of methoxymethyltriphenylphosphonium (5 mmol, 1.714 g) and sodium hydride (7.5 mmol, 179.9 mg) in dry tetrahydrofuran (6.43 mL) was stirred for 15 min at 0ºC under nitrogen atmosphere. Then was added a solution of 2-adamantanone (3.57 mmol, 536.3 mg) in dry tetrahydrofuran (2.14 mL) and the mixture was stirred for 4h at room temperature. The solution was diluted with distilled water (30 mL) and washed with diethyl ether (3 x 30 mL). The combined organic phases were dried over anhydrous sodium sulphate, filtered and concentrated under reduced pressure. The crude was dissolved in acetonitrile (21,44 mL) and hydrochloric acid (1M, 5,36 mL) was added and stirred for 22h at room temperature. The solution was diluted with brine solution (30 mL) and extracted with diethyl ether (3 x 30 mL). The combined organic phases were dried over anhydrous sodium sulphate, filtered and concentrated under reduced pressure. The desired product was not isolated.

IV.6.2 Synthesis of adamantane-2,2-diyldimethanol (49)

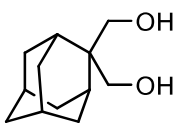

To a solution of compound **48** (0.82 mmol, 134.8 mg) in tetrahydrofuran (161 µL) and methanol (241 µL) was added formaldehyde 37% (2.21 mmol, 178 µL) at 0ºC. Sodium hydroxide (1.28 mmol, 204 µL, aqueous solution 25%) was carefully added and the solution was stirred at room temperature for 19h. The mixture was poured into brine solution (20 mL) and extracted with tetrahydrofuran/ethyl acetate (1:1, 3 x 30 mL). The combined organic phases were dried with anhydrous sodium sulphate, filtered and concentrated under reduced pressure. Crude was purified by recrystallization from diethyl ether/hexane. White solid (49% yield); mp: 161-163 ºC. ^{1}H-NMR (300 MHz, $CDCl_3$) δ = 3.94 (s, 4H, 2 x C$\underline{H}_2$OH), 2.72 (bs, 2H, 2 x $CH_2O\underline{H}$), 2.06-1.95 (m, 4H, adam-H), 1.93-1.85 (m, 2H, adam-H), 1.80-1.68 (m, 4H, adam-H), 1.65-1.55 (m, 4H, adam-H) ppm. MS-ESI m/z: 197.1 $[M + H]^+$.

IV.6.3 Synthesis of dioxane ester (50)

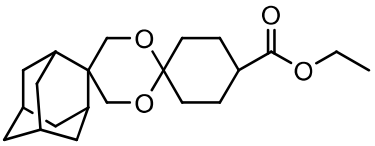

Method A: A solution of compound **49** (0.11 mmol, 22.5 mg), ethyl-4-oxocyclohexane-1-carboxylate (0.11 mmol, 17.5 µL) and ρ-toluenesulfonic acid (0.11 mmol, 18.9 mg) in dry toluene (1.5 mL) was heated at 125ºC in Dean-Stark conditions for 18h. The mixture was concentrated under reduced pressure. The desired product was not isolated.

Method B: To a solution of compound **49** (0.73 mmol, 150 mg) in dry dichloromethane (4.45 mL) were added ethyl-4-oxocyclohexane-1-carboxylate (0.49 mmol, 77.7 µL), $(EtO)_3CH$ (0.49 mmol, 81.5 µL) and catalytic zirconium tetrachloride. The solution was stirred at room temperature for 75 min. The mixture was poured into 10% sodium hydroxide solution (20 mL) and extracted with dichloromethane (3 x 20 mL). The combined organic phases were washed with distilled water (3 x 40 mL), dried over anhydrous sodium sulphate, filtered and concentrated under reduced pressure. Crude was purified by flash column chromatography (20% ethyl acetate in hexane). Clear oil (86 % yield); ^{1}H-NMR (300 MHz, $CDCl_3$) δ = 4.11 (q, *J* = 7.1 Hz, 2H, CH_2CH_3), 3.85 (s, 2H, CH_2OH), 3.81 (s, 2H, CH_2OH), 2.37-2.25 (m, 1H, CHCOOEt), 2.20-2.09 (m, 2H), 1.98-1.63 (m, 14H), 1.62-1.52 (m, 4H), 1.47-1.34 (m, 2H), 1.23 (t, *J* = 7.1 Hz, 3H, CH_2CH_3) ppm. ^{13}C-NMR (75 MHz, $CDCl_3$) δ = 175.34 (CO), 97.05 (adamC$(CH_2)_2$), 66.39 and 66.22 (adamC$(CH_2)_2$), 60.19 (CH_2CH_3), 42.19 (dioxCHCONH), 38.88 (adam-CH2 and cycloh), 37.62 (adam-CH2 and cycloh), 32.42 (adam-CH2 and cycloh), 31.20 (adam-CH2 and cycloh), 30.91 (adam-CH), 28.01 (adam-CH), 25.07 OOCcycloh), 14.23 (CH_2CH_3) ppm.

IV.6.4 Synthesis of dioxane acid (51)

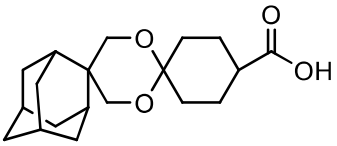

To a solution of compound **50** (0.144 mmol, 50 mg) in methanol (720 µL) was added 10 M sodium hydroxide solution (72 µL) in distilled water (231 µL). The mixture was refluxed for 1h30, after which was allowed to cool to room temperature and concentrated under reduced pressure. The crude was taken up in distilled water (20 mL) and extracted with dichloromethane (3 x 20 mL). The aqueous layer was acidified with concentrated perchloric acid and extracted with dichloromethane (3 x 20 mL). The combined organic phases were washed with brine solution (2 x 40 mL), dried with anhydrous sodium sulphate

and concentrate under reduced pressure. Clear oil (74 %); ^{1}H-NMR (300 MHz, $CDCl_3$) δ = 3.86 (s, 2H, C<u>H</u>$_2$OH), 3.82 (s, 2H, C<u>H</u>$_2$OH), 2.43-2.31 (m, 1H, C<u>H</u>COOEt), 2.22-2.10 (m, 2H), 1.98-1.37 (m, 20H) ppm

IV.7 Synthesis of dioxane-pyrimidine nitrile hybrid (52)

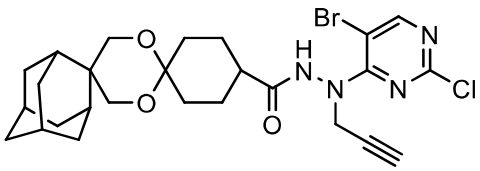

A mixture of compound **51** (0.31 mmol, 98 mg), triethylamine (0.465 mmol, 64.7 µL) and 2-(1H-benzotriazole-1-yl)-1,1,3,3-tetramethylaminium tetrafluoroborate (0.31 mmol, 99 mg) in dry dichloromethane (9.12 mL) was stirred at 0ºC for 2h under nitrogen atmosphere. In another flask, compound **37** (0.31 mmol, 81.1 mg) was dissolved in dichloromethane (9.12 mL) and the mixture was added dropwise to the previous flask. The mixture was allowed to stir for 15 min at 0ºC under nitrogen atmosphere and then for 19h at room temperature. The mixture was poured into distilled water (25 mL) and extracted with ethyl acetate (3 x 30 mL). The combined organic phases were washed with brine solution (3 x 40 mL), dried over anhydrous sodium sulphate and concentrate under reduced pressure. The desired product was not isolated.

Chapter V

V. References

1. Coslédan, F., Fraisse, L., Pellet, A., Guillou, F., Mordmüller, B., Kremsner, P. G., Moreno, A., Mazier, D., Maffrand, J., Meunier, B. Selection of a trioxaquine as an antimalarial drug candidate. *Proc. Natl. Acad. Sci.* 105, 17579–17584 (2008).

2. White, N. J., Pukrittayakamee, S., Hien, T. T., Faiz, M. A., Mokuolu, O. A., Dondorp, A. M. Malaria. *Lancet* 383, 723–735 (2014).

3. Tarun, A. S., Peng, X., Dumpit, R. F., Ogata, Y., Silva-Rivera, H., Camargo, N., Daly, T. M., Bergman, L. W., Kappe, S. H. I. A combined transcriptome and proteome survey of malaria parasite liver stages. *Proc Natl Acad Sci U S A.* 105, 305–310 (2008).

4. Tangpukdee, N., Duangdee, C., Wilairatana, P., Krudsood, S. Malaria diagnosis: A brief review. *Korean J Parasitol.* 47, 93–102 (2009).

5. Sherman, I. W. Biochemistry of Plasmodium (Malarial Parasites). *Microbiol. Rev.* 43, 453–495 (1979).

6. World Health Organization, World Malaria Report 2016. (2016).

7. Schlitzer, M. Malaria Chemotherapeutics Part I: History of Antimalarial Drug Development, Currently Used Therapeutics, and Drugs in Clinical Development. *ChemMedChem.* 2, 944–986 (2007).

8. Pasvol, G. Protective hemoglobinopathies and Plasmodium falciparum transmission. *Nat Genet.* 42, 284–285 (2010).

9. Markus, M. B. The hypnozoite concept, with particular reference to malaria. *Parasitol Res.* 108, 247–252 (2011).

10. WHO Media Centre. Malaria Fact sheet N°94. http://www.who.int/mediacentre/factsheets/fs094/en/ (accessed Aug 18, 2017).

11. Foley, M., Tilley, L. Quinoline Antimalarials: Mechanisms of Action and Resistance and Prospects for New Agents. *Pharmacol Ther.* 79, 55–87 (1998).

12. Achan, J., Talisuna, A. N., Erhart, A., Yeka, A., Tibenderana, J. K., Baliraine, F. N., Rosenthal, P. J., D'Alessandro, U. Quinine, an old anti-malarial drug in a modern world: role in the treatment of malaria. *Malar J.* 10, 144 (2011).

13. Salako, L. A., Sowunmi, A. Disposition of quinine in plasma, red blood cells and saliva after oral and intravenous administration to healthy adult Africans. *Eur J Clin Pharmacol.* 42, 171–174 (1992).

14. White, N. J. The Treatment of Malaria. *N. Engl. J. Med.* 335, 800–806 (1996).

15. White, N. J., Chanthavanich, P., Krishna, S., Bunch, C., Silamut, K. Quinine Disposition Kinetics. *Br J Clin Pharmacol.* 16, 399–403 (1983).

16. Baird, J. K., Hoffman, S. L. Primaquine Therapy for Malaria. *Clin Infect Dis.* 39, 1336–1345 (2004).

17. White, N. J. Determinants of relapse periodicity in Plasmodium vivax malaria. *Malar J.* 297, 1–35 (2011).

18. Spiller, D. G., Bray, P. G., Hughes, R. H., Ward, S. A., White, M. R. H. The pH of the Plasmodium falciparum digestive vacuole: holy grail or dead-end trail? *Trends in Parisotology* 18, 441–444 (2002).

19. Deu, E., Chen, I. T., Lauterwasser, E. M. W., Valderramos, J., Li, H., Edgington, L. E., Renslo, A. R., Bogyo, M. Ferrous iron-dependent drug delivery enables controlled and selective release of therapeutic agents in vivo. *Proc Natl Acad Sci U S A.* 110, 18244–18249 (2013).

20. O'Neill, P. M., Barton, V. E., Ward, S. A. The Molecular Mechanism of Action of Artemisinin—The Debate Continues. *Molecules.* 15, 1705–1721 (2010).

21. Burgess, S. J., Selzer, A., Kelly, J. X., Smilkstein, M. J., Riscoe, M. K., Peyton, D. H. A Chloroquine-like Molecule Designed to Reverse Resistance in Plasmodium falciparum. *J. Med. Chem.* 49, 5623–5625 (2006).

22. Ginsburg, H., Golenser, J. Glutathione is involved in the antimalarial action of chloroquine and its modulation affects drug sensitivity of human and murine species of Plasmodium. *Redox Rep* 8, 276–279 (2003).

23. Vanderesse, R., Colombeau, L., Frochot, C., Acherar, S. Inactivation of Malaria Parasites in Blood: PDT vs Inhibition of Hemozoin Formation. *Curr. Top. Malar.* 7, 205–233 (2016).

24. Abdul-ghani, R., Farag, H. F., Allam, A. F. Sulfadoxine-pyrimethamine resistance in Plasmodium falciparum: A zoomed image at the molecular level within a geographic context. *Acta Trop.* 125, 163–190 (2013).

25. Basco, L. K., Tahar, R., Ringwald, P. Molecular Basis of In Vivo Resistance to Sulfadoxine-Pyrimethamine in African Adult Patients Infected with Plasmodium falciparum Malaria Parasites. *Antimicrob Agents Chemother.* 42, 1811–1814 (1998).

26. Aubouy, A., Jafari, S., Huart, V., Migot-Nabias, F., Mayombo, J., Durand, R., Bakary, M., Bras, J., Deloron, P. DHFR and DHPS genotypes of Plasmodium falciparum isolates from Gabon correlate with in vitro activity of pyrimethamine and cycloguanil , but not with sulfadoxine–pyrimethamine treatment efficacy. *J Antimicrob Chemother.* 52, 43–49 (2003).

27. Ehmke, V., Kilchmann, F., Heindl, C., Cui, K., Huang, J., Schirmeister, T., Diederich, F. Peptidomimetic nitriles as selective inhibitors for the malarial cysteine protease falcipain-2. *Med. Chem. Commun.* 2, 800–804 (2011).

28. Oliveira, R., Guedes, R. C., Bronze, M. R., Gut, J., Rosenthal, P. J., Prudêncio, M., Moreira, R., O'Neill, P. M., Lopes, F. Tetraoxane−Pyrimidine Nitrile Hybrids as Dual Stage Antimalarials. *J Med Chem.* 57, 4916–4923 (2014).

29. Oliveira, R., Newton, A. S., Guedes, R. C., Miranda, D., Amewu, R. K., Srivasta, A., Gut, J., Rosenthal, P. J., O'Neill, P. M., Ward, S. A., Lopes, F., Moreira, R. An Endoperoxide-Based Hybrid Approach to Deliver Falcipain Inhibitors Inside Malaria Parasites. *ChemMedChem.* 8, 1528–1536 (2013).

30. Rosenthal, P. J. Cysteine proteases of malaria parasites. *Int J Parasitol.* 34, 1489–1499 (2004).

31. Coterón, J. M., Catterick, D., Castro, J., Chaparro, M. J, Díaz, B., Fernández, E., Ferrer, S., Gamo, F. J., Gordo, M., Gut, J., Heras, Laura, Legac, J., Marco, M., Miguel, J., Muñoz, V., Rosenthal, P. J., Fiandor, J. M. Falcipain Inhibitors: Optimization Studies of the 2-Pyrimidinecarbonitrile Lead Series. *J Med Chem.* 53, 6129–6152 (2010).

32. Rosenthal, P. J., Sijwali, P. S., Singh, A., Shenai, B. R. Cysteine Proteases of Malaria Parasites: Targets for Chemotherapy. *Curr Pharm Des.* 8, 1659–1672 (2002).

33. Kerr, I. D., Lee, J. H, Pandey, K. C., Harrison, A., Sajid, M., Rosenthal, P. J., Brinen, L. S. Structures of Falcipain-2 and Falcipain-3 Bound to Small Molecule Inhibitors: Implications for Substrate Specificity. *J Med Chem.* 52, 852–857 (2009).

34. Subramanian, S., Hardt, M., Choe, Y., Niles, R. K., Johansen, E. B., Legac, J., Gut, J., Kerr, I. D., Craik, C. S., Rosenthal, P. J. Hemoglobin Cleavage Site-Specificity of the Plasmodium falciparum Cysteine Proteases Falcipain-2 and Falcipain-3. *PLoS One.* 4, e5156 (2009).

35. Dasaradhi, P. V. N., Mohmmed, A., Kumar, A., Hossain, M. J., Bhatnagar, R. K., Chauhan, V. S., Malhotra, P. A role of falcipain-2, principal cysteine proteases of Plasmodium falciparum in merozoite egression. *Biochem Biophys Res Commun.* 336, 1062–1068 (2005).

36. Omotuyiabc, I. O., Hamada, T. Dynamical footprint of falcipain-2 catalytic triad in hemoglobin-β-bound state. *J Biomol Struct Dyn.* 33, 1027–1036 (2015).

37. Sabnis, Y. A., Desai, P. V, Rosenthal, P. J., Avery, M. A. Probing the structure of falcipain-3, a cysteine protease from Plasmodium falciparum: Comparative protein modeling and docking studies. *Protein Sci.* 12, 501–509 (2003).

38. Hogg, T., Nagarajan, K., Herzberg, S., Chen, L., Shen, X., Jiang, H., Wecke, M., Blohmke, C., Hilgenfeld, R., Schmidt, C. L. Structural and Functional Characterization of Falcipain-2 , a Hemoglobinase from the Malarial Parasite Plasmodium falciparum. *J Biol Chem.* 281, 25425–25437 (2006).

39. Mallari, J. P., Shelat, A. A., Obrien, T., Caffrey, C. R., Kosinski, A., Connelly, M., Harbut, M., Greenbaum, D., McKerrow, J. H., Guy, R. K. Development of Potent Purine-Derived Nitrile Inhibitors of the Trypanosomal Protease TbcatB. *J. Med. Chem.* 51, 545–552 (2008).

40. Palmer, J. T., Bryant, C., Wang, D., Davis, D. E., Setti, E. L., Rydzewski, R. M., Venkatraman, S., Tian, Z., Burril, L. C., Janc, J. W., McGrath, M., Somoza, J. R., Enriquez, P., Yu, Z. W., Strickley, R. M., Liu, L., Venuti, M. C., Parcival, M. D., Falgueyret, J., Prasit, P., Oballa, R., Riendeau, D., Young, R. N., Wesolowski, G., Rodan, S. B., Johnson, C., Kimmel, D. B., Rodan, G. Design and Synthesis of Tri-Ring P3 Benzamide-Containing Aminonitriles as Potent, Selective, Orally Effective Inhibitors of Cathepsin K. *J. Med. Chem.* 48, 7520–7534 (2005).

41. Robert, A., Benoit-Vical, F., Meunier, B. The key role of heme to trigger the antimalarial activity of trioxanes. *Coord. Chem. Rev.* 249, 1927–1936 (2005).

42. Meshnick, S. R. Artemisinin: mechanisms of action, resistance and toxicity. *Int J Parasitol* 32, 1655–1660 (2002).

43. Hartwig, C. L., Rosenthal, A. S., D'Angelo, J., Griffin, C. E., Posner, G. H., Cooper, R. A. Accumulation of artemisinin trioxane derivatives within neutral lipids of Plasmodium falciparum malaria parasites is endoperoxide-dependent. *Biochem Pharmacol.* 77, 322–336 (2009).

44. Ridder, S. De, Kooy, F. Van Der, Verpoorte, R. Artemisia annua as a self-reliant treatment for malaria in developing countries. *J Ethnopharmacol.* 120, 302–314 (2008).

45. Cui, L., Su, X. Discovery, mechanisms of action and combination therapy of artemisinin. *Expert Rev Anti Infect Ther.* 7, 999–1013 (2009).

46. Muraleedharan, K. M., Avery, M. A. Progress in the development of peroxide-based anti-parasitic agents. *Drug Discov Today.* 14, 793–803 (2009).

47. Tonmunphean, S., Parasuk, V., Kokpol, S. Theoretical investigations on reaction mechanisms of artemisinin compounds: effect of structure on kinetic energy profile and antimalarial activity. *J. Mol. Struct.* 724, 99–105 (2005).

48. Meshnick, S. R., Yang, Y., Lima, V., Kuypers, F., Kamchonwongpaisan, S., Yuthavong, Y. Iron-Dependent Free Radical Generation from the Antimalarial Agent Artemisinin (Qinghaosu). *Antimicrob Agents Chemother.* 37, 1108–1114 (1993).

49. Jones, M., Mercer, A. E., Stocks, P. A., Pensée, L. J. I., Cosstick, R., Park, B. K., Rawe, S. L., Baird, J., Charidza, T., Janneh, O., O'Neill, P. M. Antitumour and antimalarial activity of artemisinin–acridine hybrids. *Bioorg. Med. Chem. Lett.* 19, 2033–2037 (2009).

50. Haynes, R. K., Chan, C., Lung, C., Uhlemann, C., Eckstein, U., Taramelli, D., Parapini, S., Monti, D., Krishna, S. The Fe^{2+} - Mediated Decomposition, PfATP6 Binding, and Antimalarial Activities of Artemisone and Other Artemisinins: The Unlikelihood of C-Centered Radicals as Bioactive Intermediates. *ChemMedChem.* 2, 1480–1497 (2007).

51. Meunier, B., Robert, A. Heme as Trigger and Target for Trioxane-Containing Antimalarial Drugs. *Acc Chem Res.* 43, 1444–1451 (2010).

52. Dondorp, A. M., Nosten, F., Yi, P., Das, D., Phyo, A. P., Taming, J., Lwin, K. M., Ariey, F., Hanpithakpong, W., Lee, S. J., Ringwald, P., Silamut, K., Imwong, M., Chotivanich, K., Lim, P., Herdman, T., An, S. S., Yeung, S., Singhasivanon, P., Day, N. P. J., Lindegardh, N., Socheat, D., White, N. J. Artemisinin Resistance in

Plasmodium falciparum Malaria. *N Engl J Med.* 361, 455–467 (2009).

53. Noedl, H., Se, Y., Schaecher, K., Smith, B. L., Socheat, D., Fukuda, M. M. Evidence of Artemisinin-Resistant Malaria in Western Cambodia. *N Engl J Med.* 359, 2619–2620 (2008).

54. Fairhurst, R. M., Dondorp, A. M. Artemisinin-Resistant Plasmodium falciparum Malaria. *Microbiol Spectr* 4, 1–16 (2016).

55. Garah, F. B., Wong, M. H., Amewu, R. K., Muangnoicharoen, S., Maggs, J. L., Stigliani, J., Park, B. K., Chadwick, J., Ward, S. A., O'Neill, P. M. Comparison of the Reactivity of Antimalarial 1,2,4,5-Tetraoxanes with 1,2,4-Trioxolanes in the Presence of Ferrous Iron Salts, Heme, and Ferrous Iron Salts/Phosphatidylcholine. *J. Med. Chem. 2011* 54, 6443–6455 (2011).

56. Borstnik, K., Paik, I., Shapiro, T. A., Posner, G. H. Antimalarial chemotherapeutic peroxides: artemisinin , yingzhaosu A and related compounds. *Int J Parasitol* 32, 1661–1667 (2002).

57. Kumar, N., Singh, R., Rawat, D. S. Tetraoxanes: Synthetic and Medicinal Chemistry Perspective. *Med Res Rev.* 32, 581–610 (2012).

58. Ploypradith, P. Development of artemisinin and its structurally simplified trioxane derivatives as antimalarial drugs. *Acta Trop.* 89, 329–342 (2004).

59. O'Neill, P. M., Amewu, R. K., Nixon, G. L., ElGarah, F. B., Mungthin, M., Chadwick, J., Shone, A. E., Vivas, L., Lander, H., Barton, V., Muangnoicharoen, S., Bray, P. G., Davies, J., Park, B. K., Wittlin, S., Brun, R., Preschel, M., Zhang, K., Ward, S. A. Identification of a 1,2,4,5-Tetraoxane Antimalarial Drug-Development Candidate (RKA182) with Superior Properties to the Semisynthetic Artemisinins. *Angew Chem Int Ed Engl.* 49, 5693–5697 (2010).

60. Amewu, R., Stachulski, A. V., Ward, S. A., Berry, N. G., Bray, P. G., Davies, J., Labat, G., Vivasc, L., O'Neill, P. M. Design and synthesis of orally active dispiro 1,2,4,5-tetraoxanes; synthetic antimalarials with superior activity to artemisinin. *Org. Biomol. Chem* 4, 4431–4436 (2006).

61. Muregi, F. W., Ishih, A. Next-Generation Antimalarial Drugs: Hybrid Molecules as a New Strategy in Drug Design. *Drug Dev Res.* 71, 20–32 (2010).

62. Walsh, J. J., Bell, A. Hybrid Drugs for Malaria. *Curr Pharm Des.* 15, 2970–2985

(2009).

63. Meunier, B. Hybrid Molecules with a Dual Mode of Action: Dream or Reality? *Acc Chem Res.* 41, 69–77 (2008).

64. Varotti, F. P., Botellho, A. C. C., Andrade, A. A., Paula, R. C., Fagundes, E. M. S., Valverde, A., Mayer, L. M. U., Mendonça, J. S., Souza, M. V. N., Boechat, N., Krettli, A. U. Synthesis, Antimalarial Activity, and Intracellular Targets of MEFAS, a New Hybrid Compound Derived from Mefloquine and Artesunate. *Antimicrob Agents Chemother.* 52, 3868–3874 (2008).

65. Zhang, M., Wilkinson, B. Drug discovery beyond the 'rule-of-five'. *Curr Opin Biotechnol.* 18, 478–488 (2007).

66. Quesne, M. G., Ward, R. A., Sam, P., Visser, D. Cysteine protease inhibition by nitrile-based inhibitors: a computational study. *Front Chem*. 1, 1–10 (2013).

67. O'Neill, P. M., Posner, G. H. A Medicinal Chemistry Perspective on Artemisinin and Related Endoperoxides. *J Med Chem* 47, 2945–2964 (2004).

68. Dong, Y., Chollet, J., Matle, H., Charman, S. A., Chiu, F. C. K., Charman, W. N., Scorneaux, B., Urwyler, H., Tomas, J. S., Scheurer, C., Snyder, C., Dorn, A., Wang, X., Karle, J. M., Tang, Y., Wittlin, S., Brun, R., Vennerstrom, J. L. Spiro and Dispiro-1,2,4-trioxolanes as Antimalarial Peroxides: Charting a Workable Structure - Activity Relationship Using Simple Prototypes. *J Med Chem* 48, 4953–4961 (2005).

69. Ellis, G. L., Amewu, R., Sabbani, S., Stocks, P. A., Shone, A., Stanford, D., Gibbons, P., Davies, J., Vivas, L., Charnaud, S., Bongard, E., Hall, C., Rimmer, K., Lozanom, S., Jesús, M., Gargallo, D., Ward, S. A., O'Neill, P. M. Two-Step Synthesis of Achiral Dispiro-1,2,4,5-tetraoxanes with Outstanding Antimalarial Activity, Low Toxicity, and High-Stability Profiles. *J Med Chem.* 51, 2170–2177 (2008).

70. Ingram, K., Yaremenko, I. A., Krylov, I. B., Hofer, L., Terent'ev, A. O., Keiser, J. Identification of Antischistosomal Leads by Evaluating Bridged 1,2,4,5-Tetraoxanes, Alphaperoxides, and Tricyclic Monoperoxides. *J Med Chem.* 55, 8700–8711 (2012).

71. Fonović, M., Bogyo, M. Activity Based Probes as a tool for Functional Proteomic Analysis of Proteases. *Espert Rev Proteomics* 5, 721–730 (2010).

72. Li, N., Overkleeft, H. S., Florea, B. I. Activity-based protein profiling: an enabling

technology in chemical biology research. *Curr Opin Chem Biol.* 16, 227–233 (2012).

73. Ismail, H. M., Barton, V., Phanchana, M., Charoensutthivarakul, S., Wong, M. H. L., Hemingway, J., Biagini, G. A., O'Neill, P. M., Ward, S. A. Artemisinin activity-based probes identify multiple molecular targets within the asexual stage of the malaria parasites Plasmodium falciparum 3D7. *Proc Natl Acad Sci U S A.* 113, 2080–2085 (2016).

74. Ismail, H. M., Barton, V. E., Phanchana, M., Charoensutthivarakul, S., Biagini, G. A., Ward, S. A., O'Neill, P. M. A Click Chemistry-Based Proteomic Approach Reveals that 1,2,4-Trioxolane and Artemisinin Antimalarials Share a Common Protein Alkylation Profile. *Angew Chem Int Ed Engl.* 55, 6401–6405 (2016).

75. Horisawa, K. Specific and quantitative labeling of biomolecules using click chemistry. 5, 1–7 (2014).

76. Agalave, S. G., Maujan, S. R., Pore, V. S. Click Chemistry: 1,2,3-Triazoles as Pharmacophores. *Chem Asian J.* 6, 2696–2718 (2011).

77. Hein, C. D., Liu, X., Wang, D. Click Chemistry, A Powerful Tool for Pharmaceutical Sciences. *Pharm Res.* 25, 2216–2230 (2008).

78. Sanman, L. E., Bogyo, M. Activity-Based Profiling of Proteases. *Annu Rev Biochem.* 83, 249–273 (2014).

79. Carvalho, L. A. R., Ruivo, E. F. P., Lucas, S. D., Moreira, R. Activity-Based Probes as Molecular Tools for Biomarker Discovery. *Med. Chem. Commun.* 6, 536–546 (2015).

80. Singh, M. S., Chowdhury, S., Koley, S. Advances of azide-alkyne cycloaddition-click chemistry over the recent decade. *Tetrahedron* 72, 5257–5283 (2016).

81. Ghorai, P., Dussault, P. H. A broadly applicable synthesis of unsymmetrical 1,2,4,5-tetraoxanes. *Org. Lett.* 11, 213–216 (2008).

82. Ruivo, E. F. P., Gonçalves, L. M., Carvalho, L. A. R., Guedes, R. C., Hofbauer, S., Brito, J. A., Archer, M., Moreira, R., Lucas, S. D. Clickable 4-Oxo-b-lactam-Based Selective Probing for Human Neutrophil Elastase Related Proteomes. *ChemMedChem.* 11, 2037–2042 (2016).

83. Presolski, S. I., Hong, V. P., Finn, M. G. Copper-Catalyzed Azide–Alkyne Click Chemistry for Bioconjugation. *Curr Protoc Chem Biol.* 3, 153–162 (2012).

84. Slavin, S., Burns, J., Haddleton, D. M., Becer, C. R. Synthesis of glycopolymers via click reactions. *Eur. Polym. J.* 47, 435–446 (2011).

85. Chadwick, J., Amewu, R. K., Marti, F., Bousera-ElGarah, F., Sharma, R., Berry, N. G., Stocks, P. A., Burrel-Saward, H., Wittlin, S., Ward, S. A., O'Neill, P. M. Antimalarial Mannoxanes: Hybrid Antimalarial Drugs with Outstanding Oral Activity Profiles and A Potential Dual Mechanism of Action. *ChemMedChem.* 6, 1357–1361 (2011).

86. Alberts, A. H., Wynberg, H., Strating, J. Synthesis of 2-Adamantane Carboxylic Acid. *Synth. Commun.* 2, 79–81 (1971).

87. Natarajan, A., Joy, A., Kaanumalle, L. S., Scheffer, J. R., Ramamurthy, V. Enhanced Enantio- and Diastereoselectivity via Confinement and Cation Binding: Yang Photocyclization of 2-Benzoyladamantane Derivatives within Zeolites. *J Org Chem.* 67, 8339–8350 (2002).

88. Geissman, T. A. The Cannizzaro Reaction. *Org. React.* 3, 94–113 (2011).

89. Cannizzaro, S. Ueber Den Der Benzoësäure Entsprechenden Alkohol. *Justus Liebigs Ann. Chem.* 88, 129–130 (1853).

90. Firouzabadi, H., Iranpoor, N., Karimi, B. Zirconium Tetrachloride ($ZrCl_4$) Catalyzed Highly Chemoselective and Efficient Acetalization of Carbonyl Compounds. *Synlett* 4, 321–323 (1999).

Chapter VI

VI. Annexes

VI.1 *Tert*-butyl 2-(prop-2-yn-1-yl)hydrazine carboxylate (35)

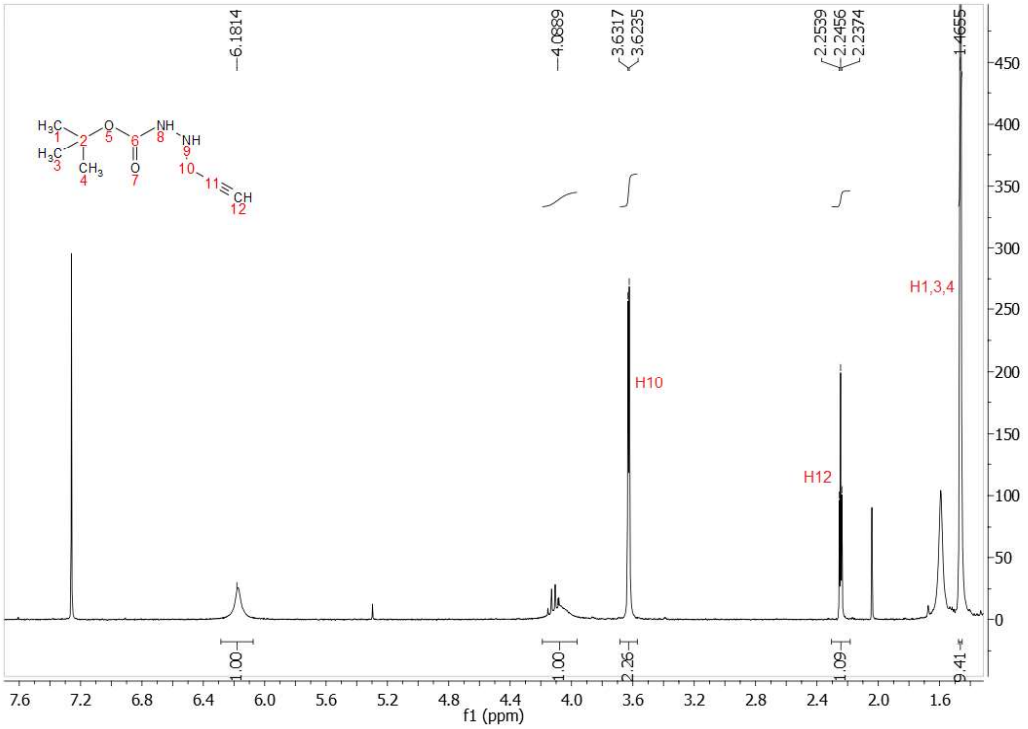

Figure VI.1 - ^{1}H-NMR spectrum ($CDCl_3$) of compound **35**.

VI.2 *Tert*-butyl 2-(5-bromo-2-chloropyrimidin-4-yl)-2-(prop-2-yn-1-yl)hydrazine carboxylate (36)

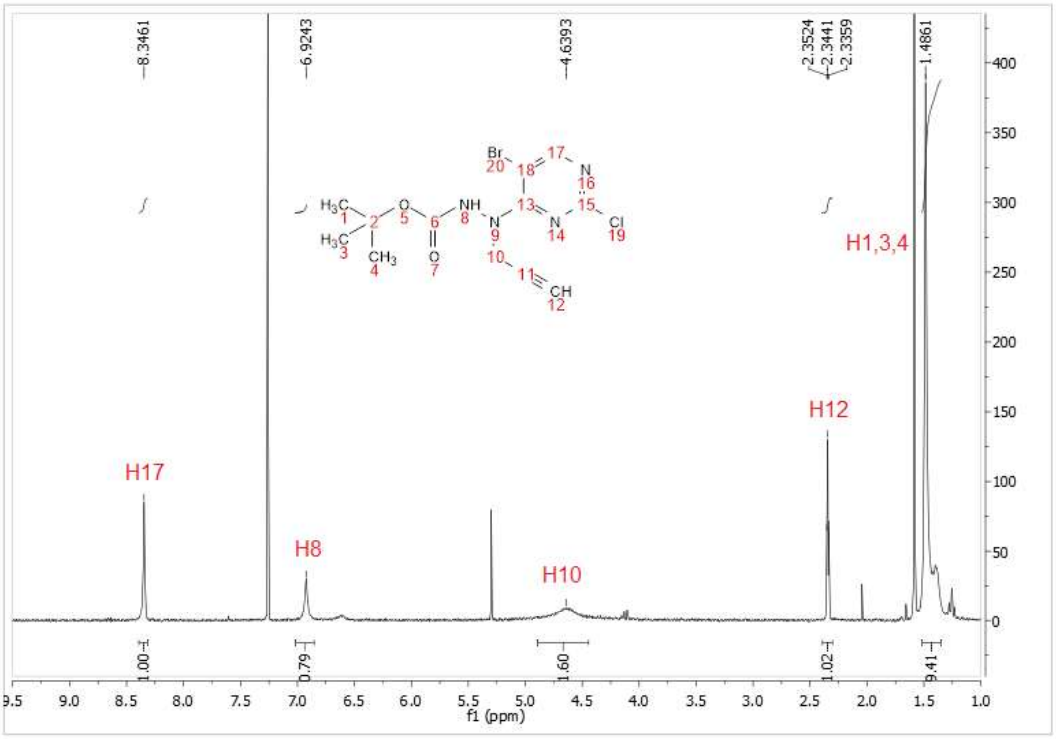

Figure VI.2 - ^{1}H-NMR spectrum ($CDCl_3$) of compound **36**.

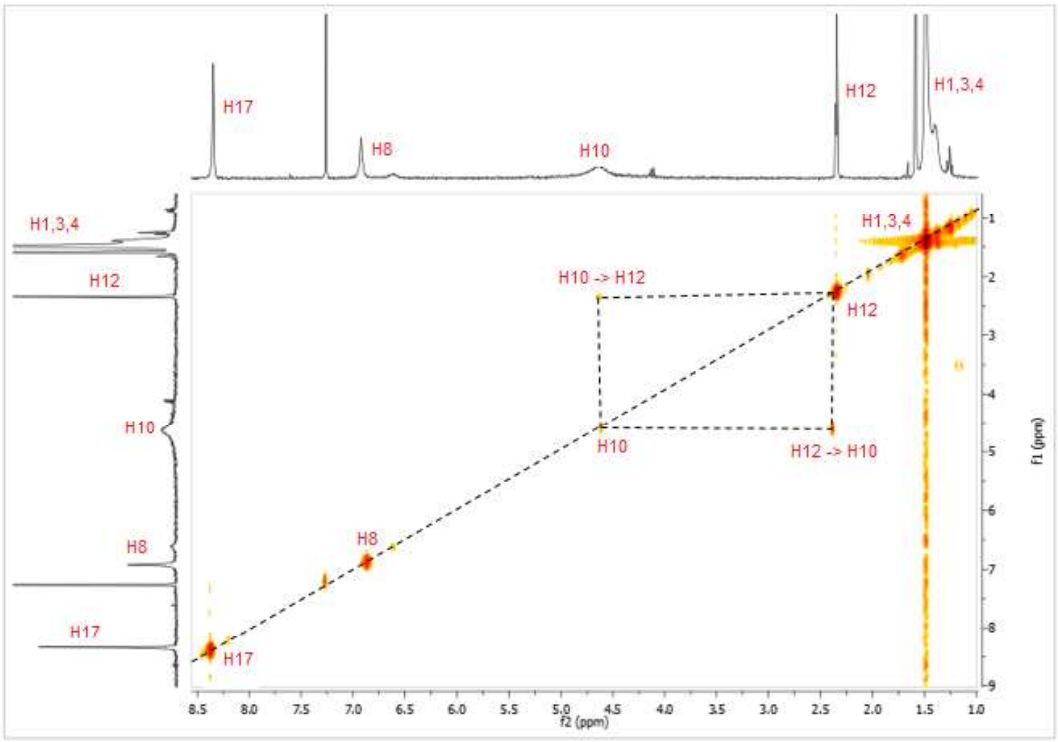

Figure VI.3 - COSY spectrum ($CDCl_3$) of compound **36**.

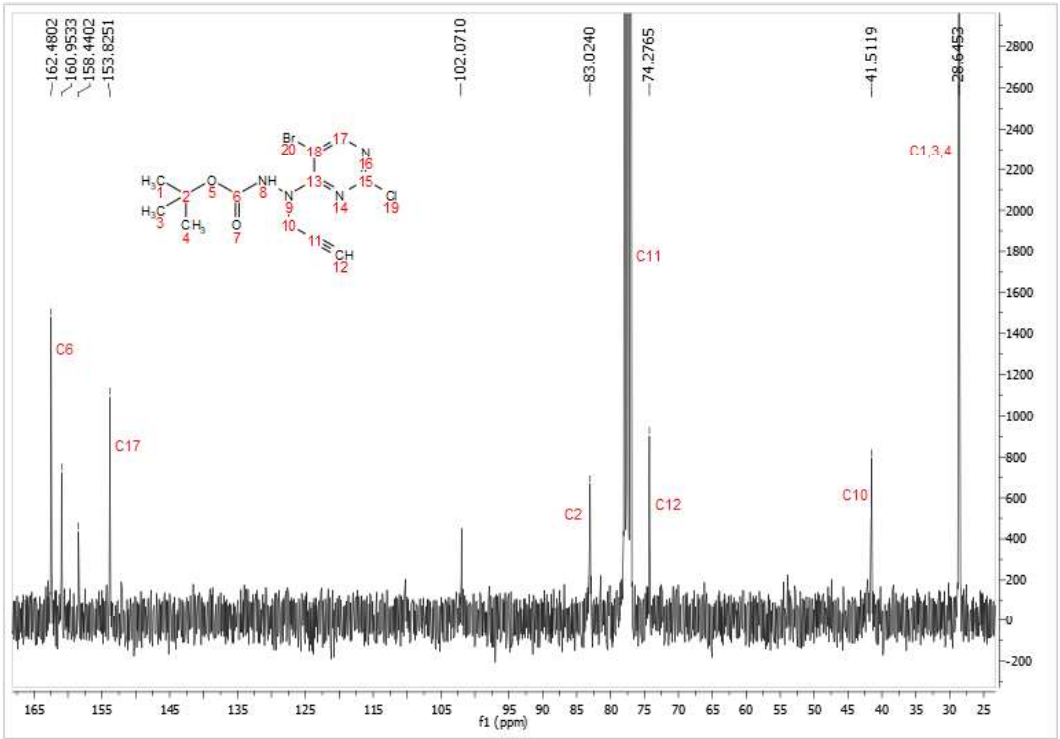

Figure VI.4 - ^{13}C-NMR spectrum ($CDCl_3$) of compound **36**.

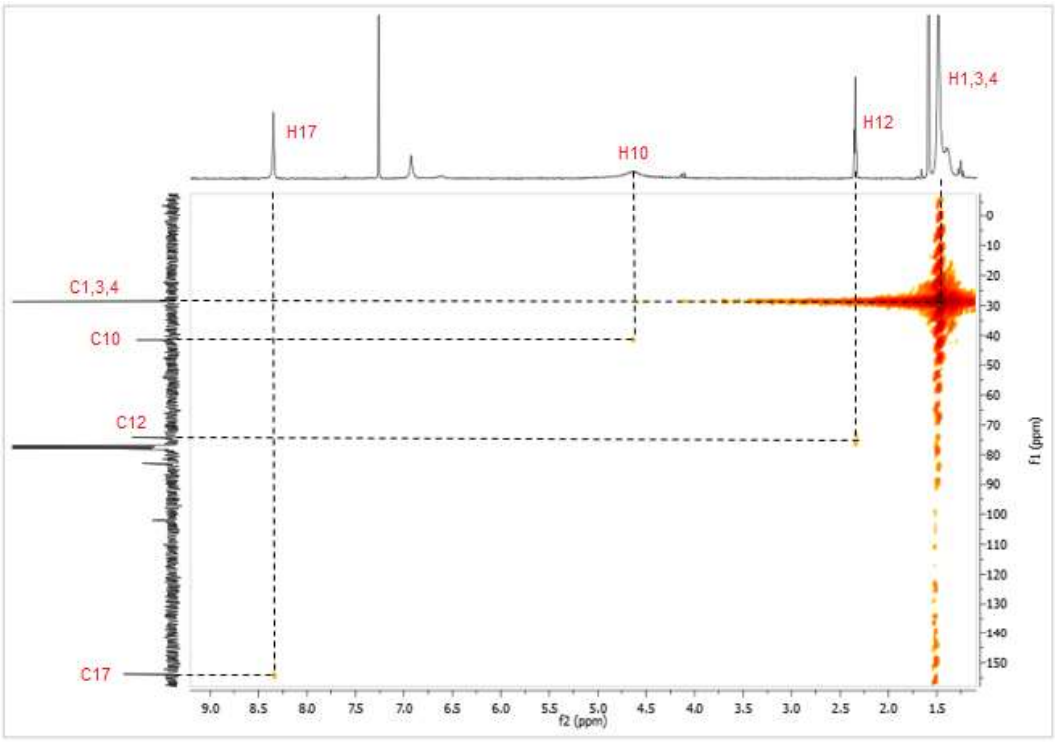

Figure VI.5 - HMQC spectrum ($CDCl_3$) of compound **36**.

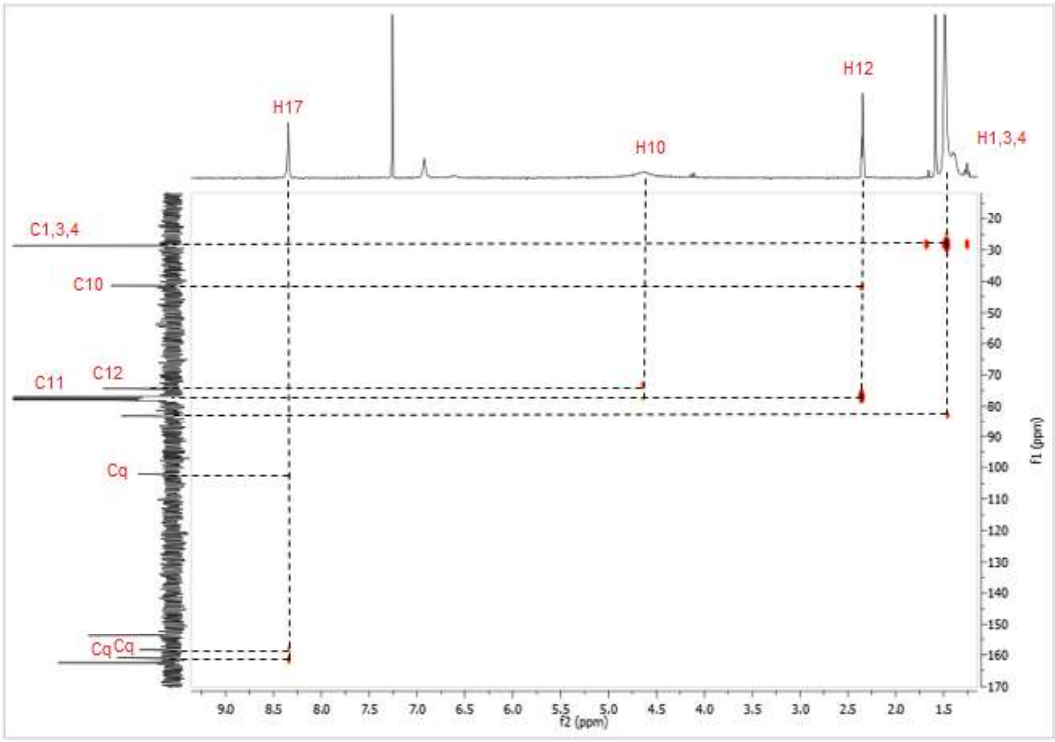

Figure VI.6 - HMBC spectrum ($CDCl_3$) of compound **36**.

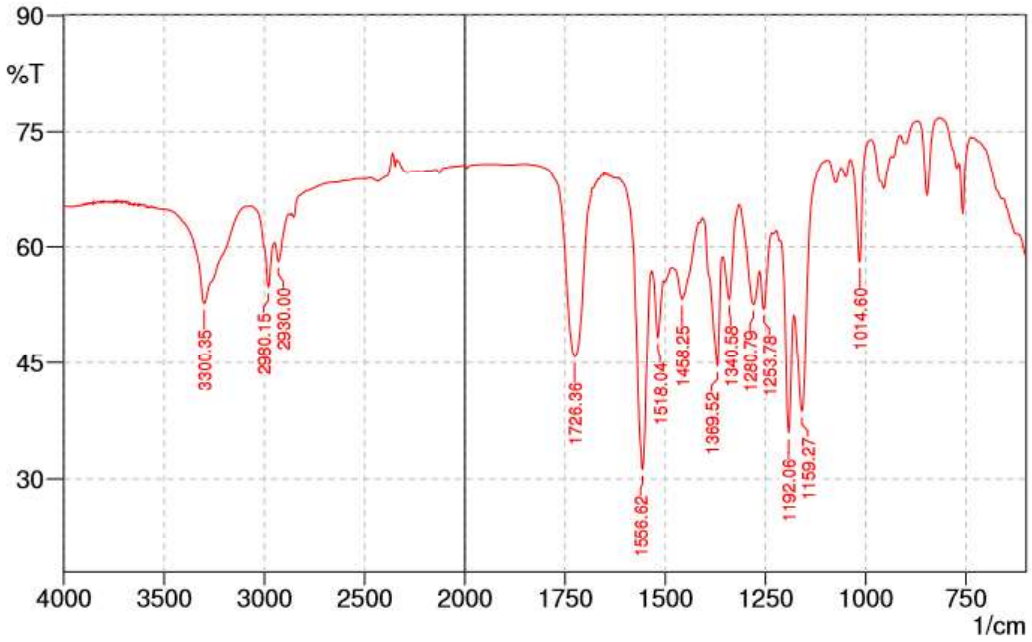

Figure VI.7 - IR spectrum of compound **36**.

VI.3 1-(2-bromo-5-chlorophenyl)-1-(prop-2-yn-1-yl)hydrazine (37)

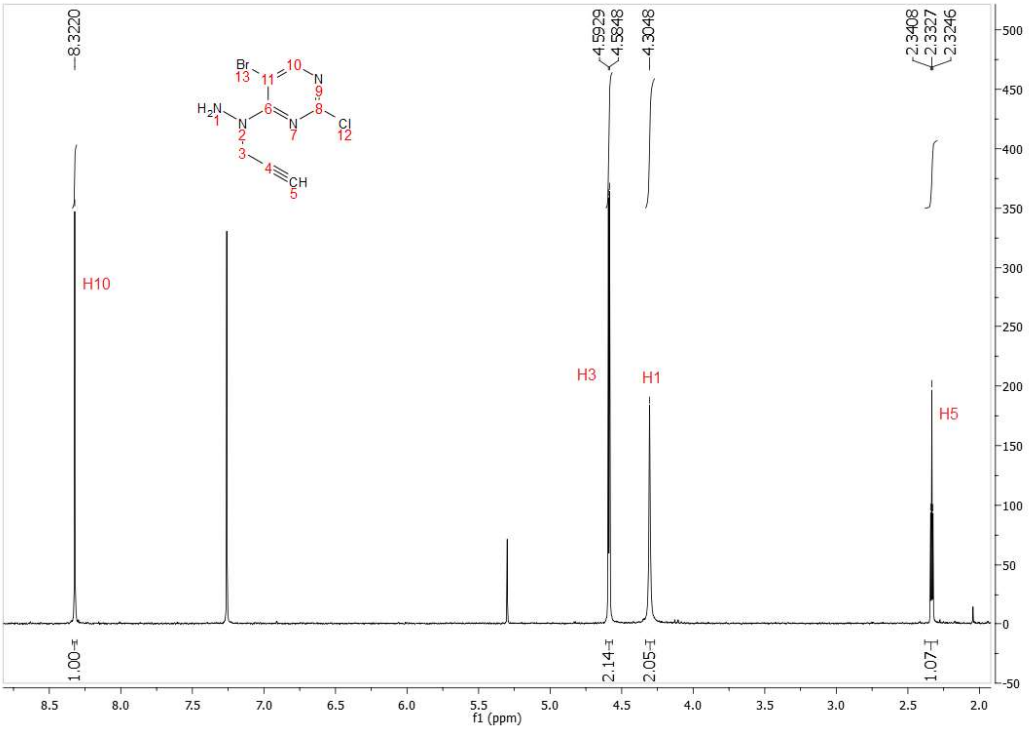

Figure VI.8 - ^{1}H-NMR spectrum ($CDCl_3$) of compound **37**.

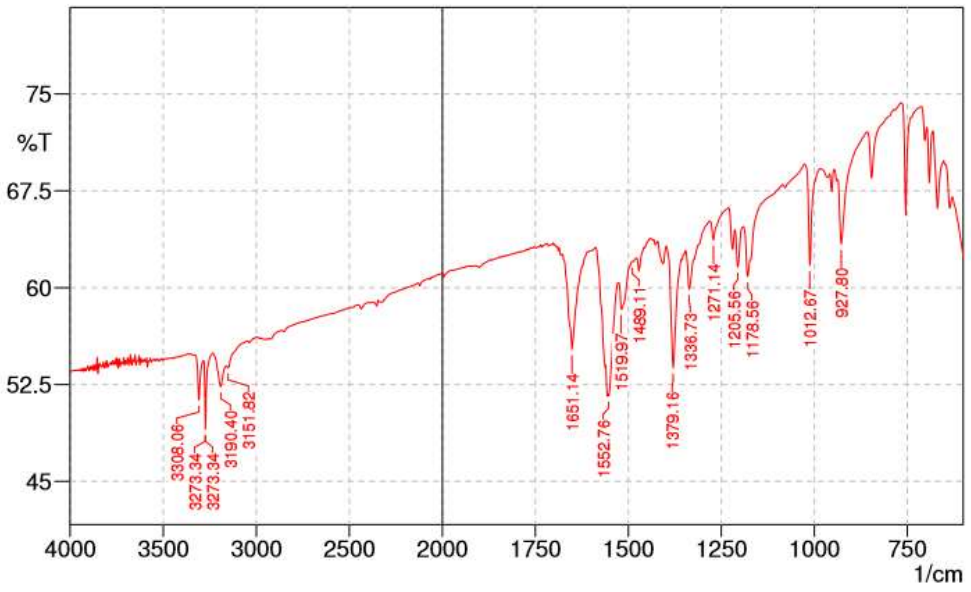

Figure VI.9 – IR spectrum of compound **37**.

VI.4 Tetraoxane ester (40)

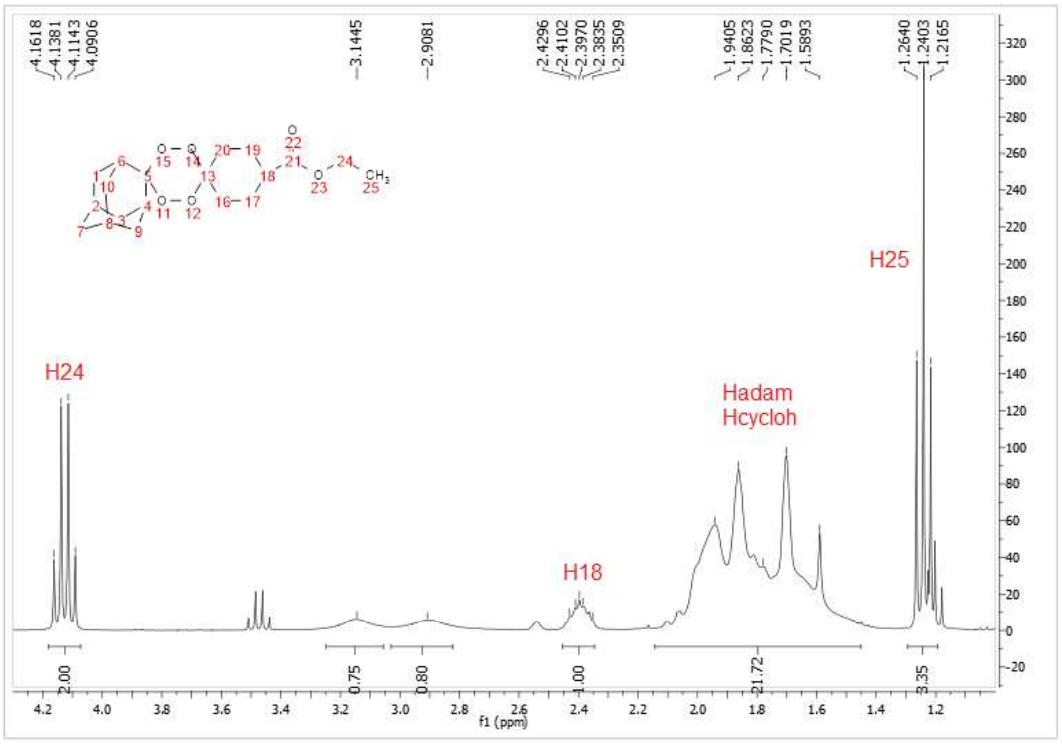

Figure VI.10 - ^{1}H-NMR spectrum ($CDCl_3$) of compound **40**.

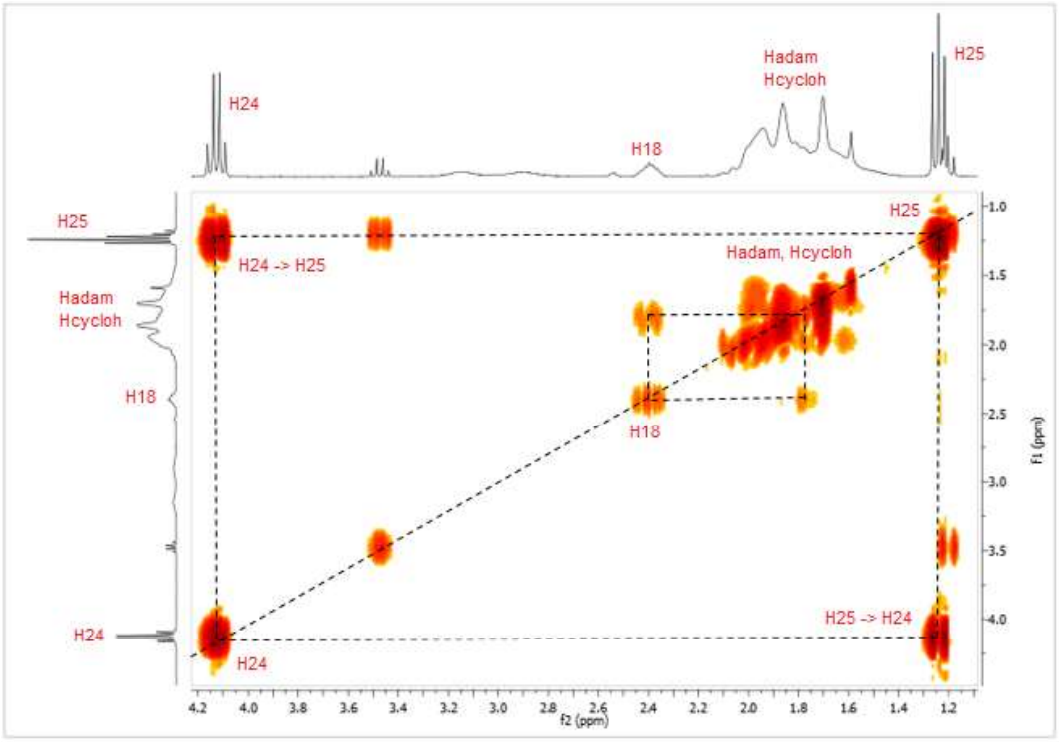

Figure VI.11 – COSY spectrum ($CDCl_3$) of compound **40**.

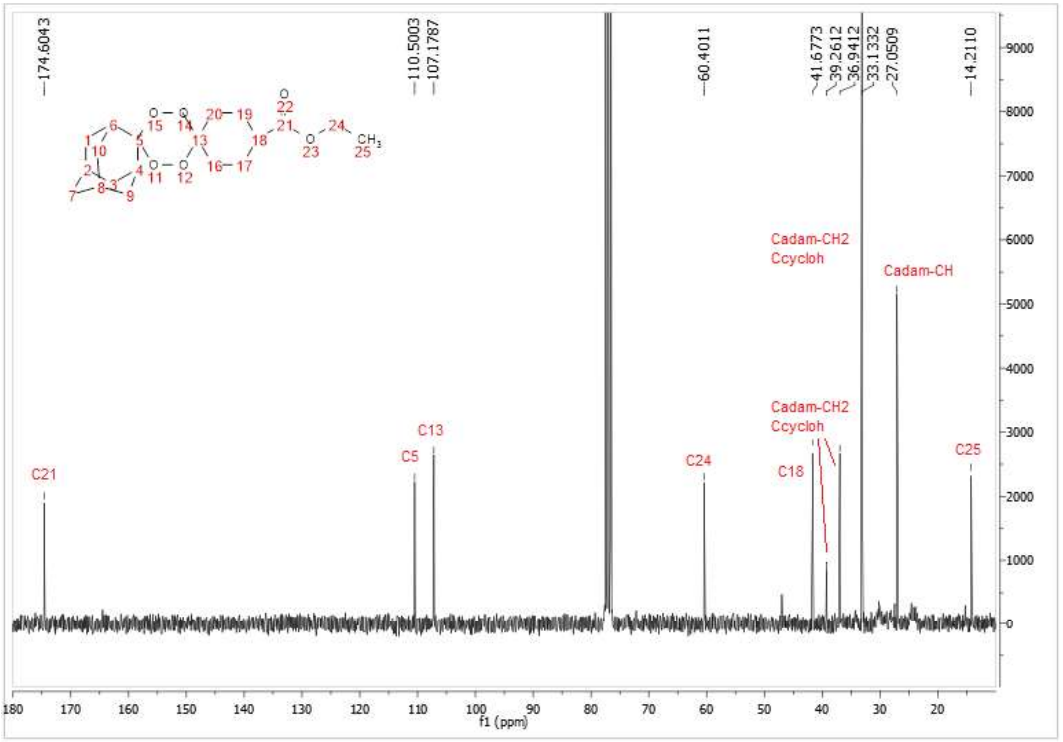

Figure VI.12 - ^{13}C-NMR spectrum ($CDCl_3$) of compound **40**.

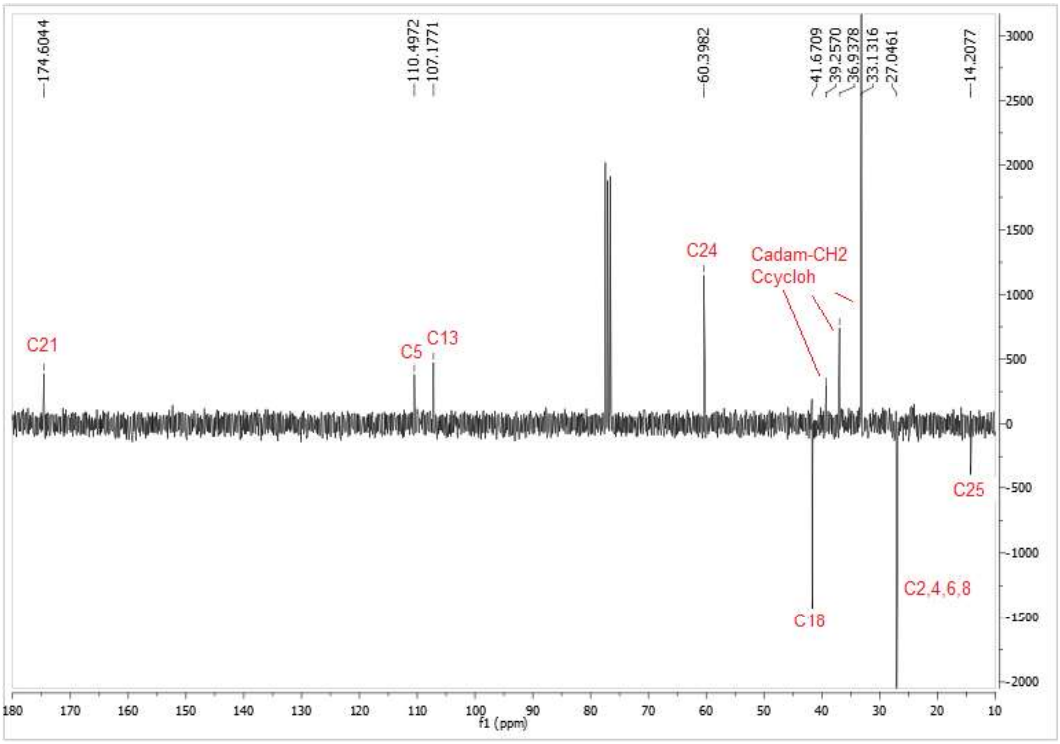

Figure VI.13 – APT spectrum ($CDCl_3$) of compound **40**.

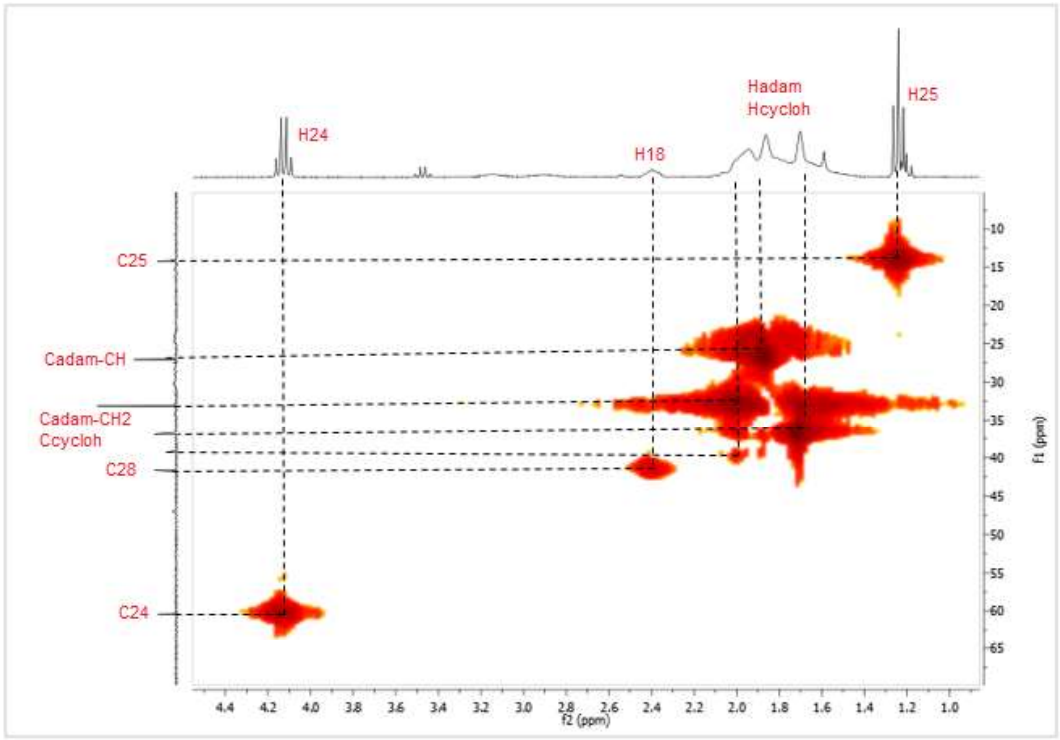

Figure VI.14 – HMQC spectrum ($CDCl_3$) of compound **40**.

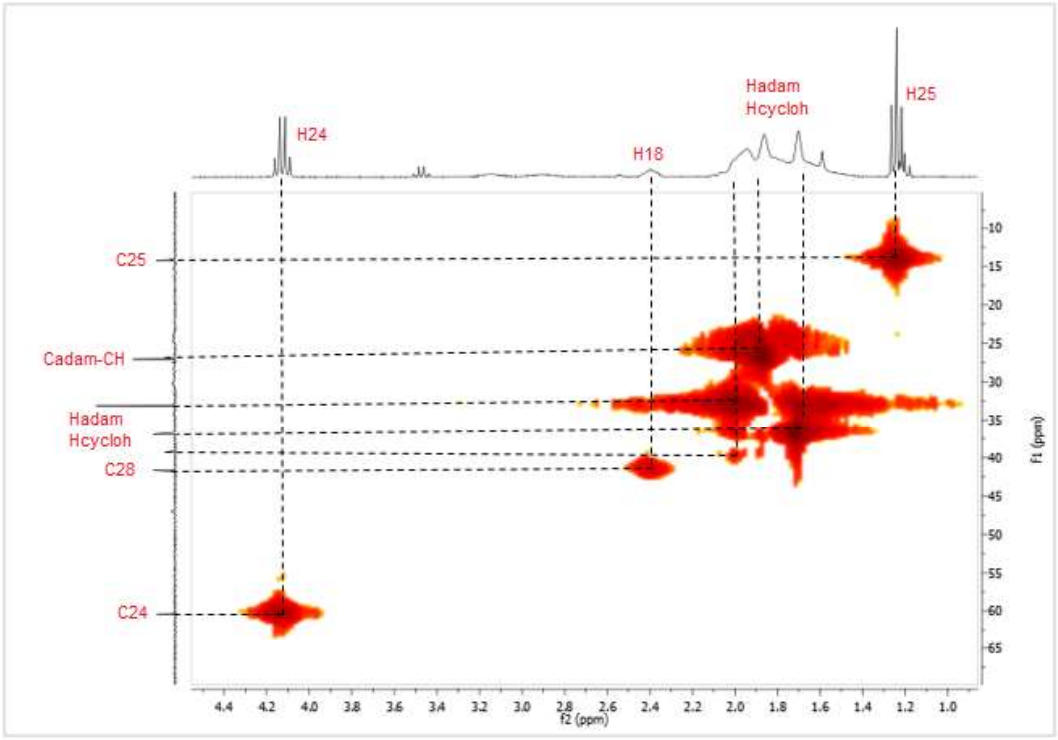

Figure VI.15 – HMBC spectrum ($CDCl_3$) of compound **40**.

VI.5 Tetraoxane acid (41)

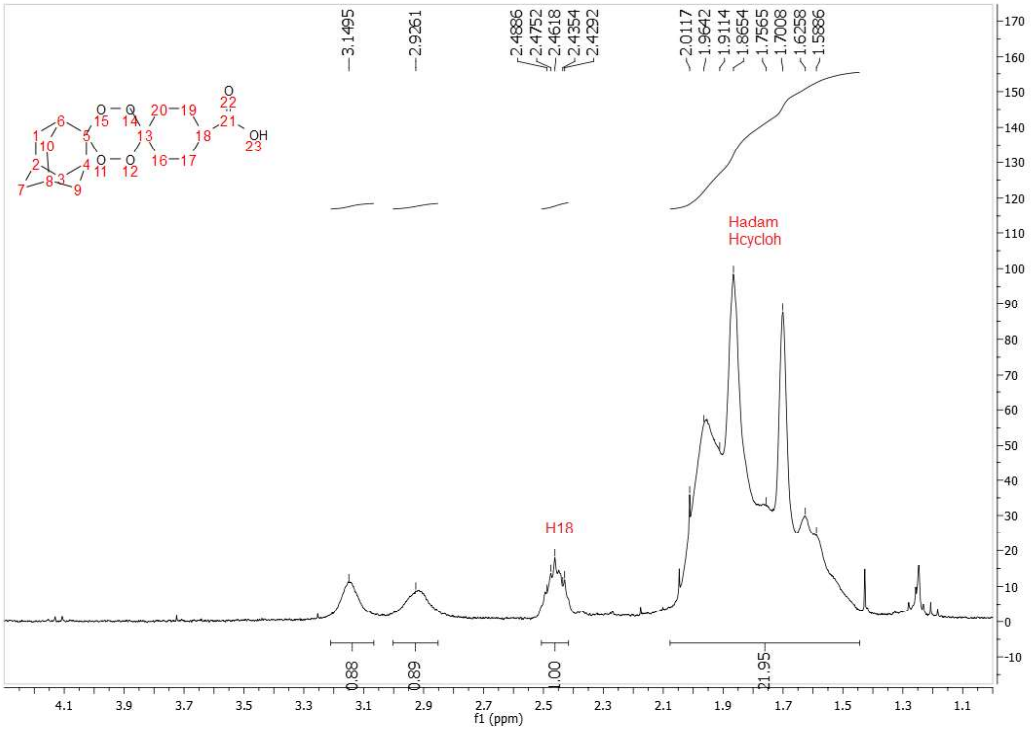

Figure VI.16 - ^{1}H-NMR spectrum ($CDCl_3$) of compound **41**.

VI.6 Tetraoxane chloride acid (42)

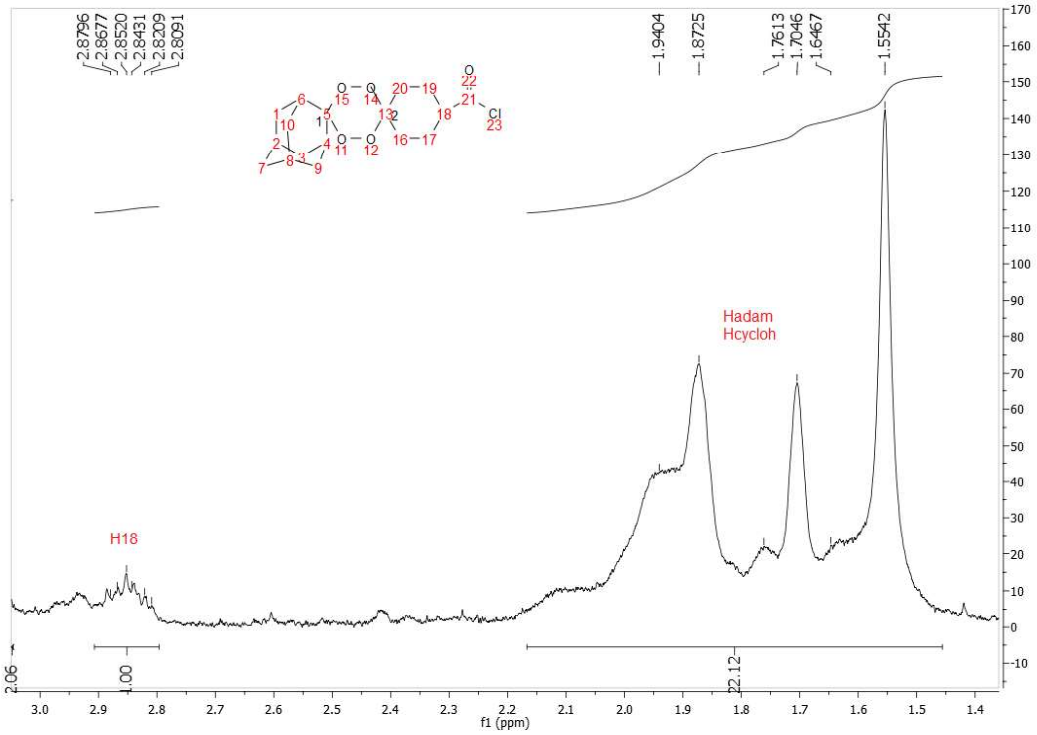

Figure VI.17 - ^{1}H-NMR spectrum ($CDCl_3$) of compound **42**.

VI.7 Tetraoxane-pyrimidine nitrile hybrid-Cl (43)

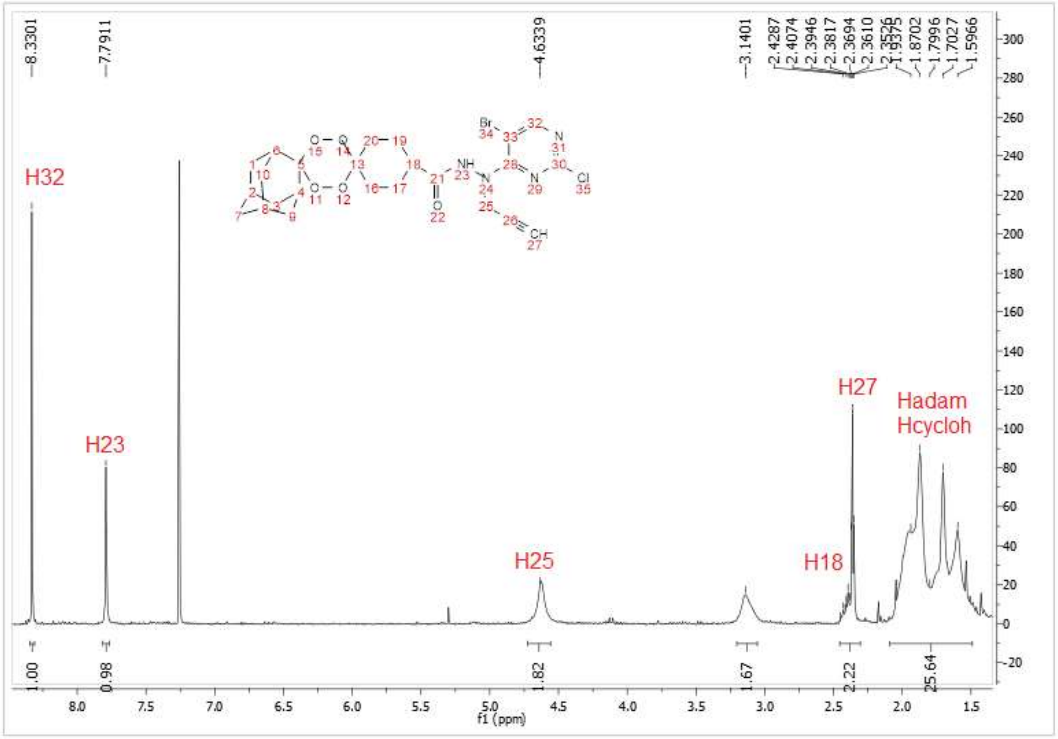

Figure VI.18 - ^{1}H-NMR spectrum ($CDCl_3$) of compound **43**.

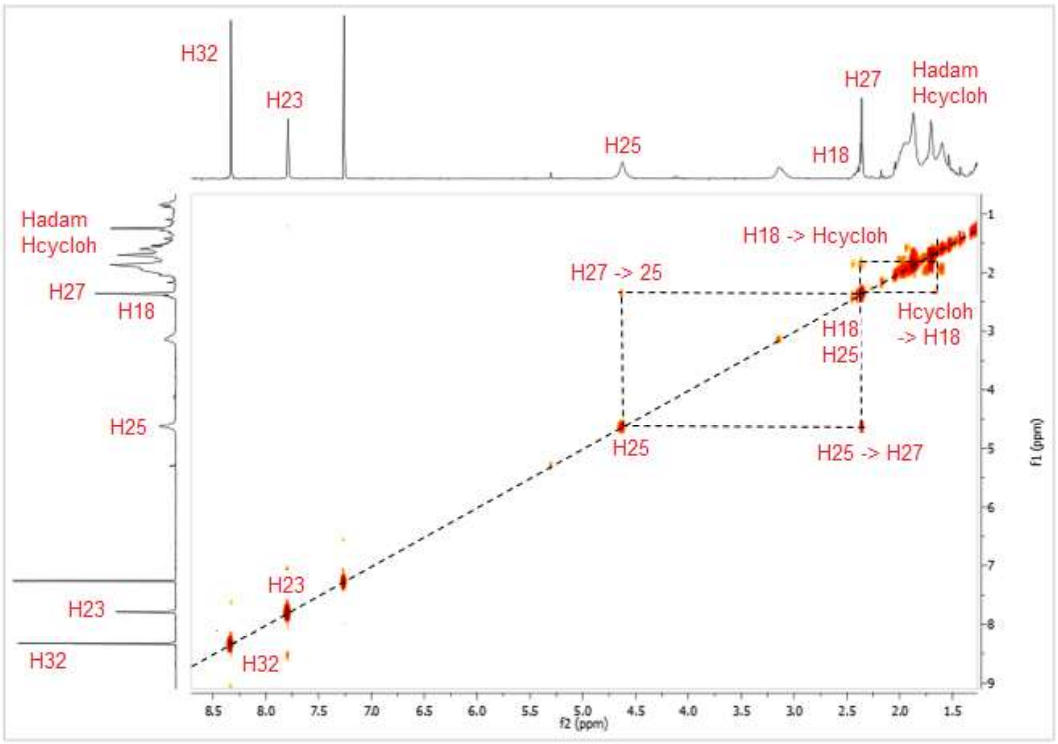

Figure VI.19 – COSY spectrum ($CDCl_3$) of compound **43**.

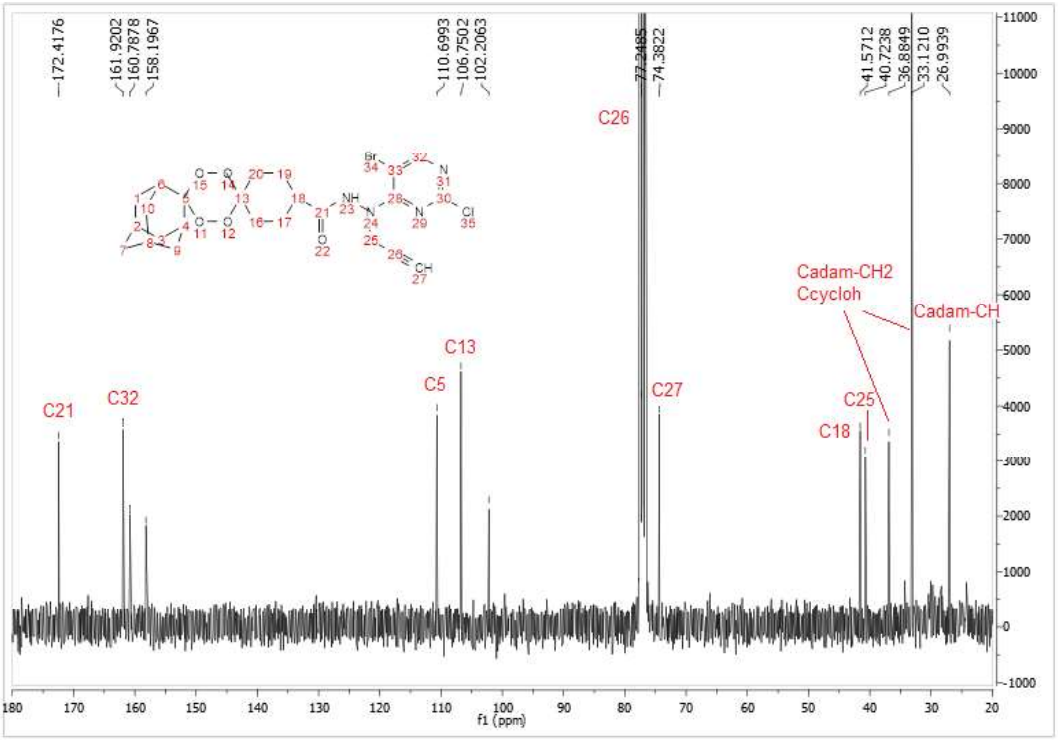

Figure VI.20 - ^{13}C-NMR spectrum ($CDCl_3$) of compound **43**.

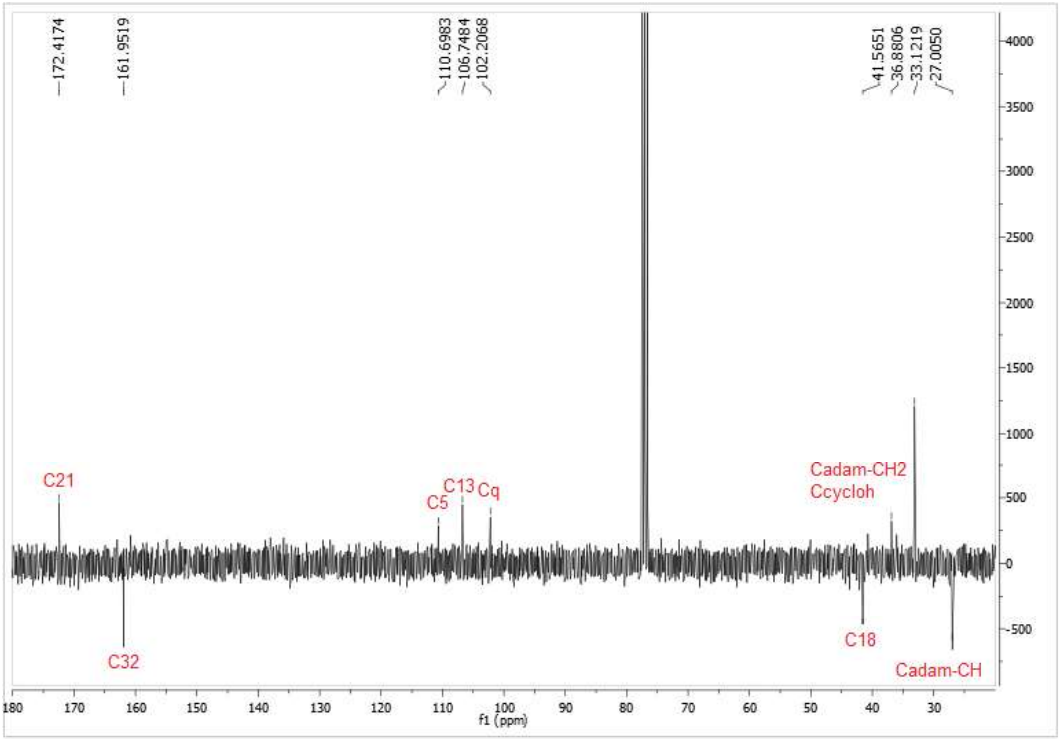

Figure VI.21 – APT spectrum ($CDCl_3$) of compound **43**.

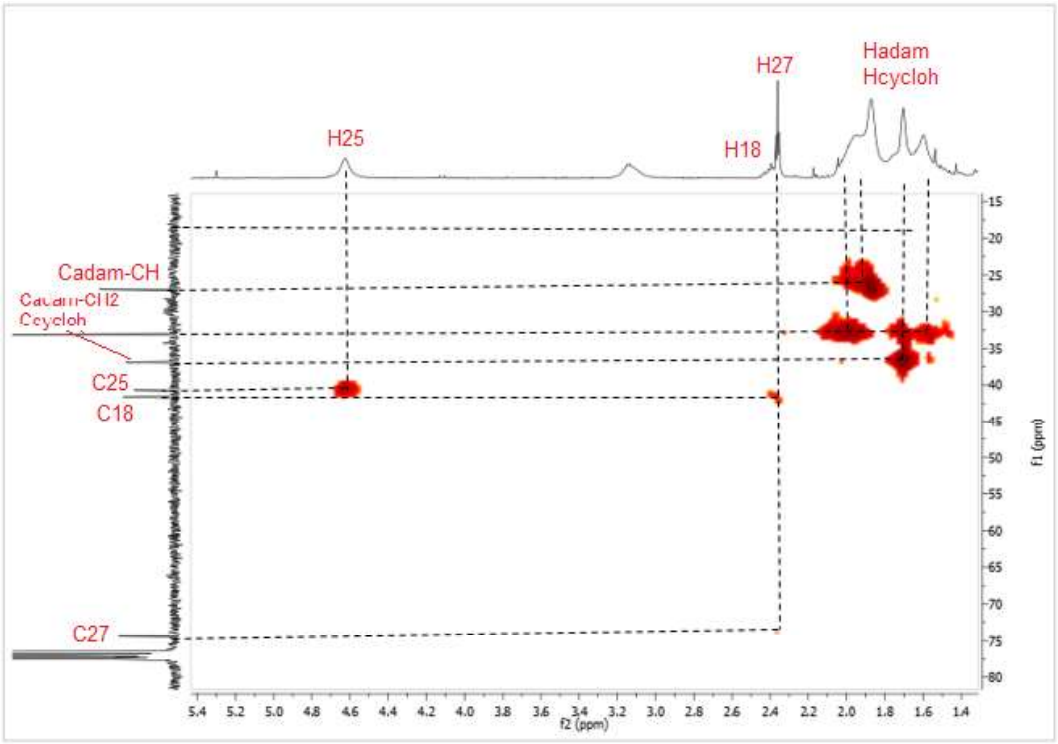

Figure VI.22 – HMQC spectrum ($CDCl_3$) of compound **43**.

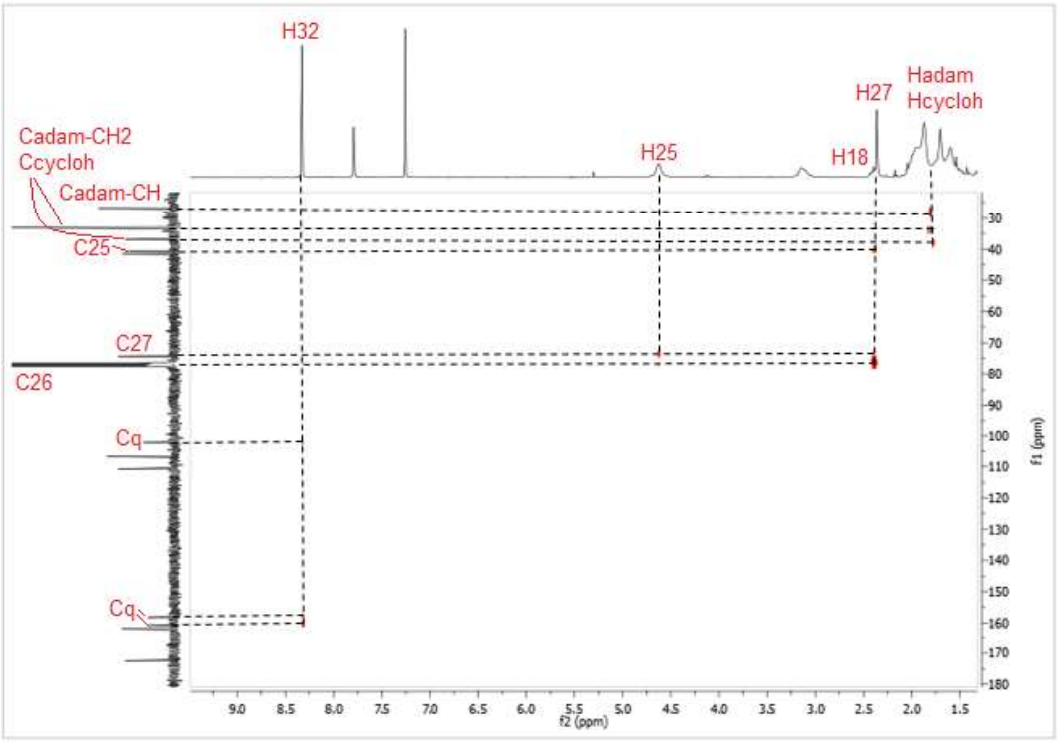

Figure VI.23 – HMBC spectrum ($CDCl_3$) of compound **43**.

VI.8 Tetraoxane-pyrimidine nitrile hybrid-CN (30)

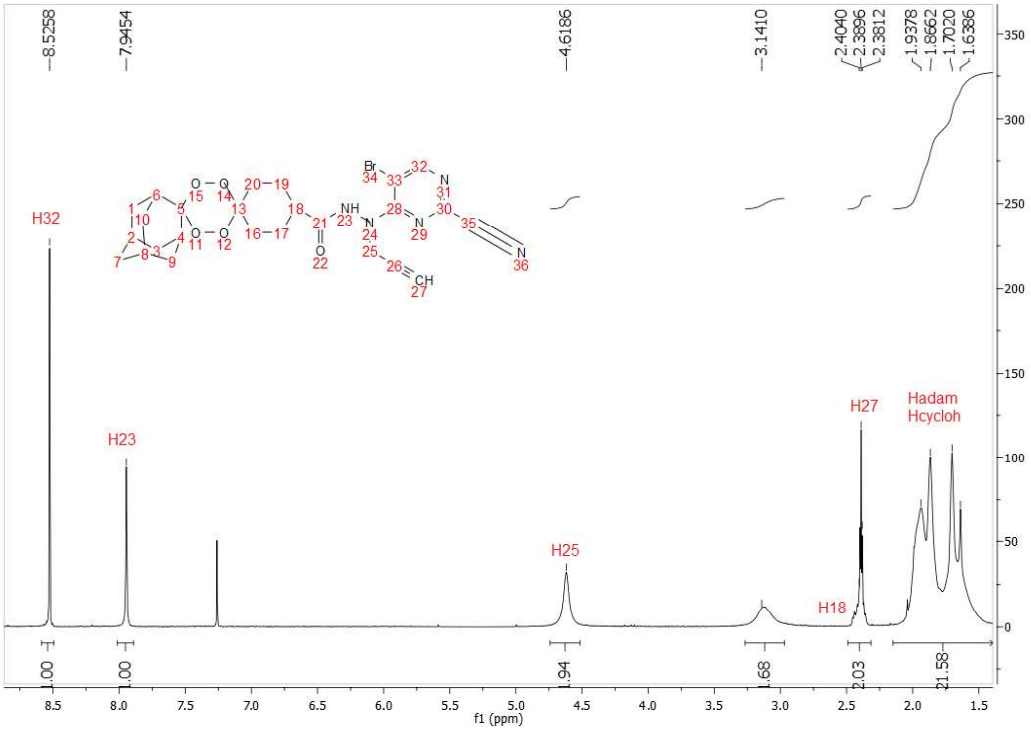

Figure VI.24 - ^{1}H-NMR spectrum ($CDCl_3$) of compound **30**.

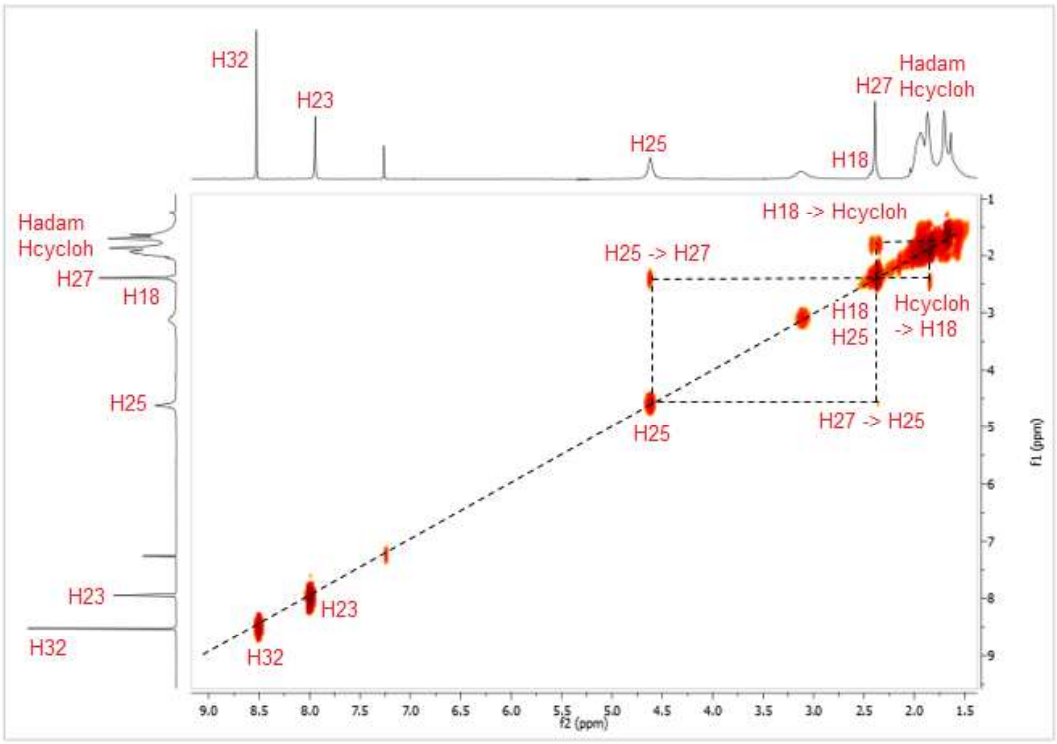

Figure VI.25 – COSY spectrum ($CDCl_3$) of compound **30**.

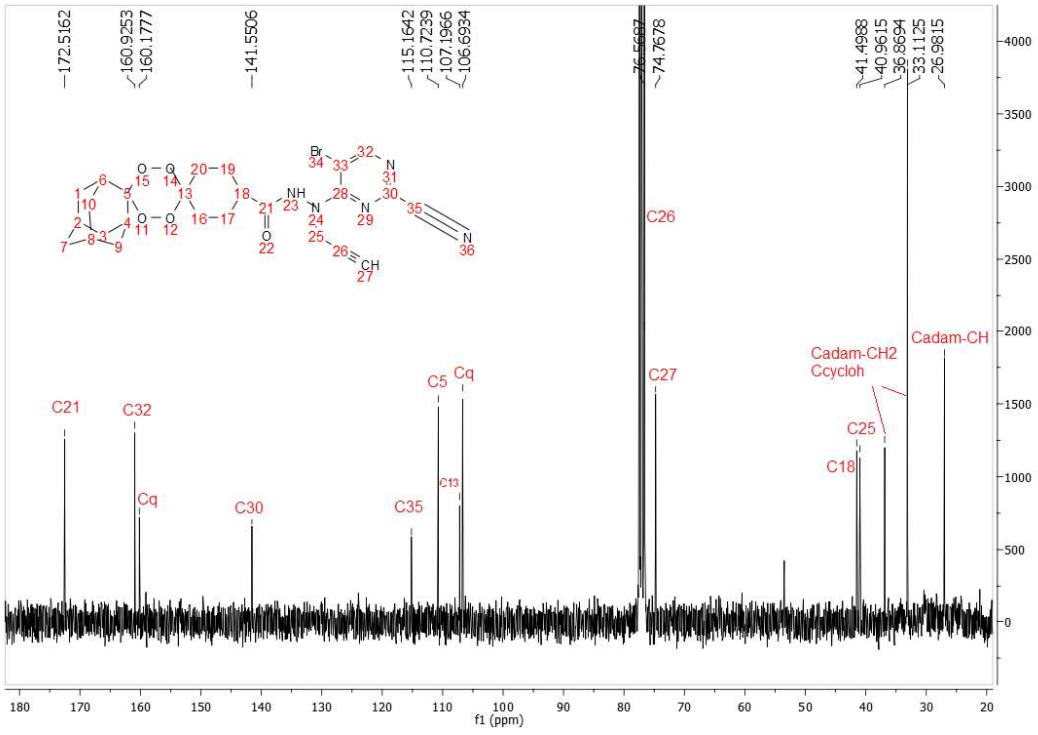

Figure VI.26 - ^{13}C-NMR spectrum ($CDCl_3$) of compound **30**.

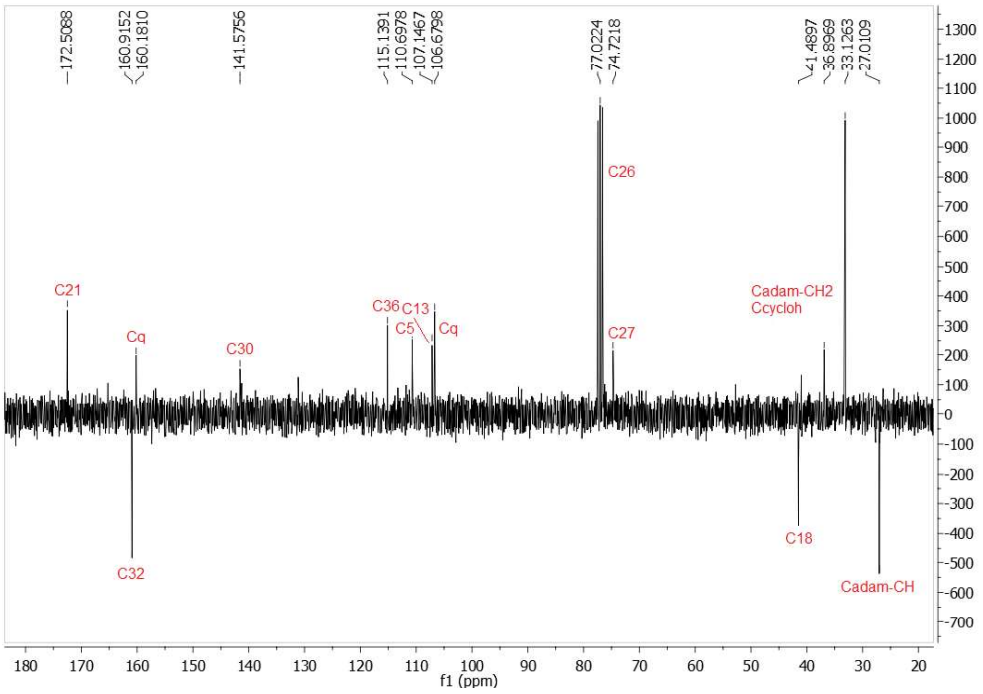

Figure VI.27 – APT spectrum ($CDCl_3$) of compound **30**.

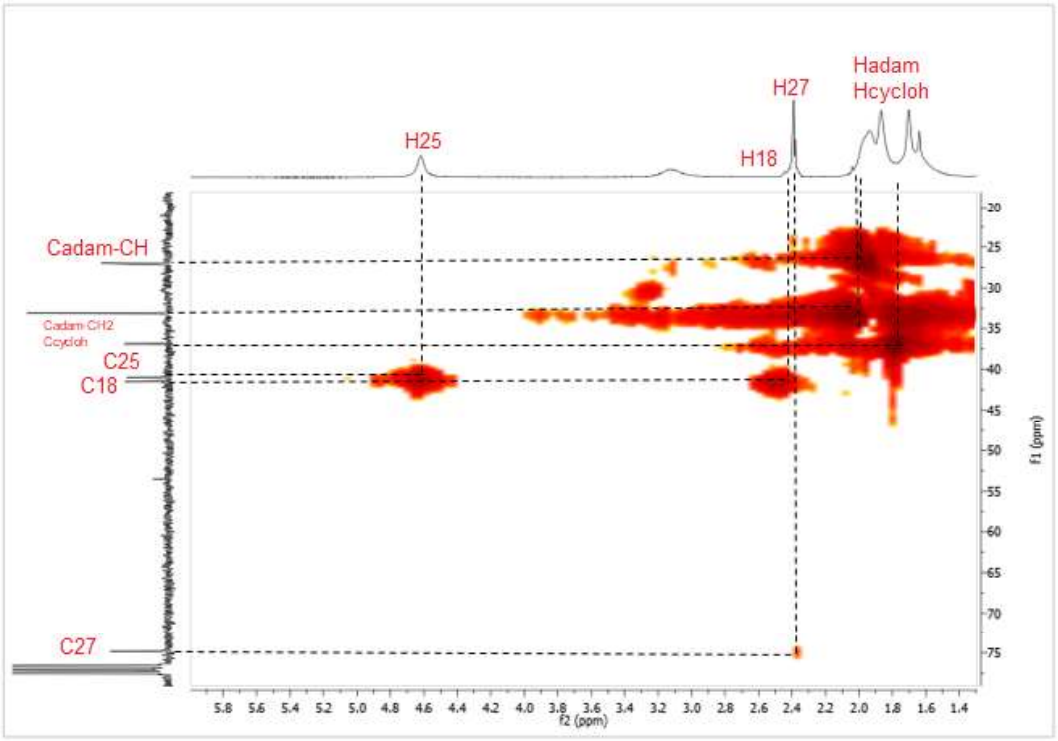

Figure VI.28 – HMQC spectrum ($CDCl_3$) of compound **30**.

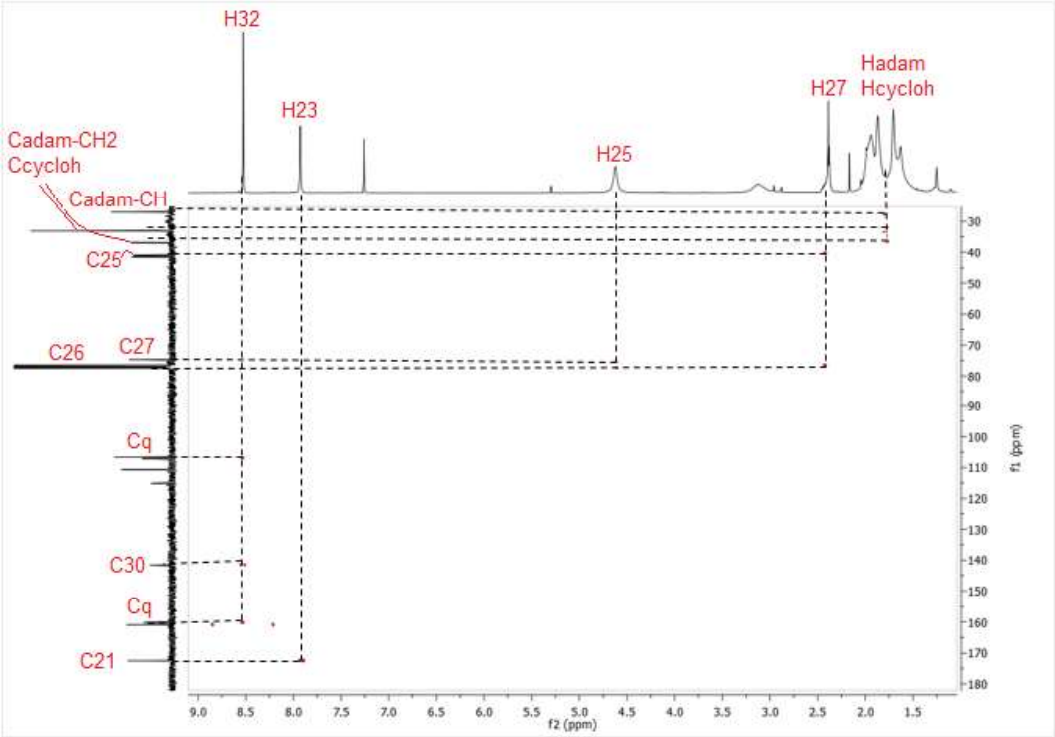

Figure VI.29 – HMBC spectrum ($CDCl_3$) of compound **30**.

VI.9 Chemical probe NBD (46)

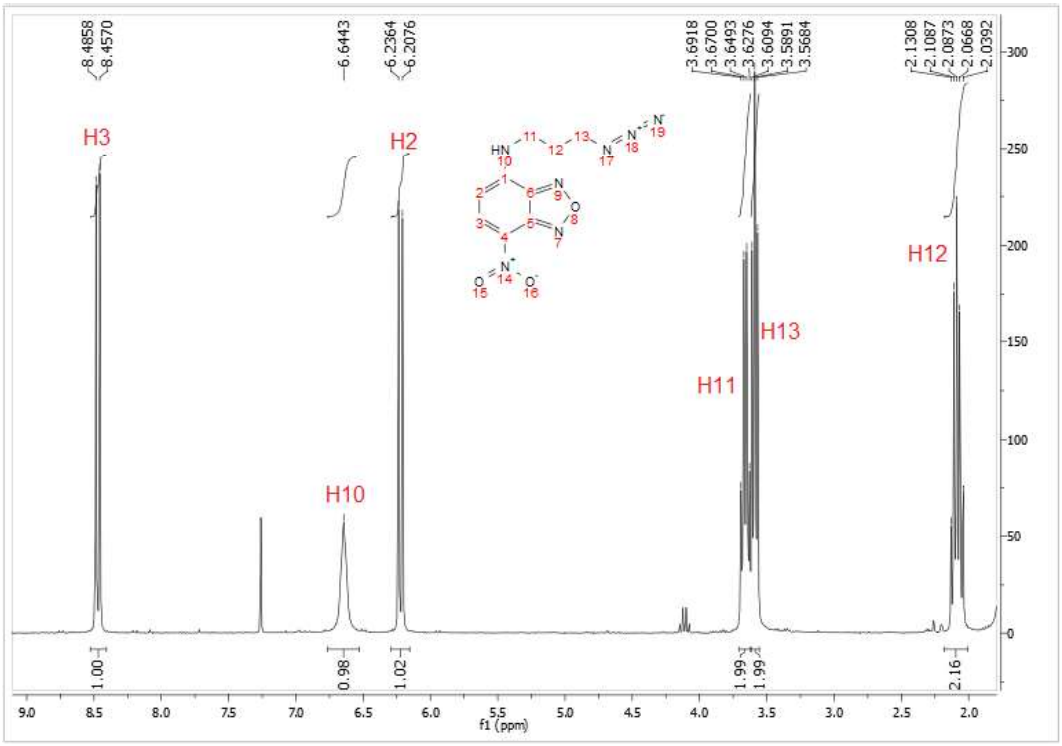

Figure VI.30 - ^{1}H-NMR spectrum ($CDCl_3$) of compound **46**.

VI.10 Tetraoxane-pyrimidine nitrile probe (32)

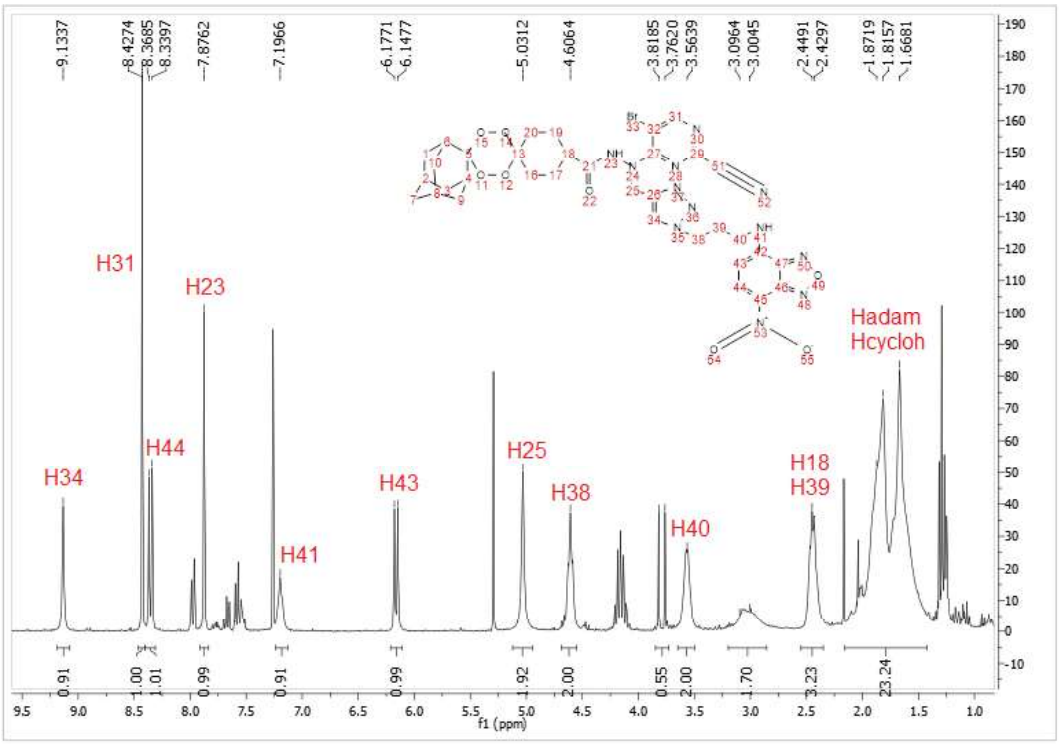

Figure VI.31 - ^{1}H-NMR spectrum ($CDCl_3$) of compound **32**.

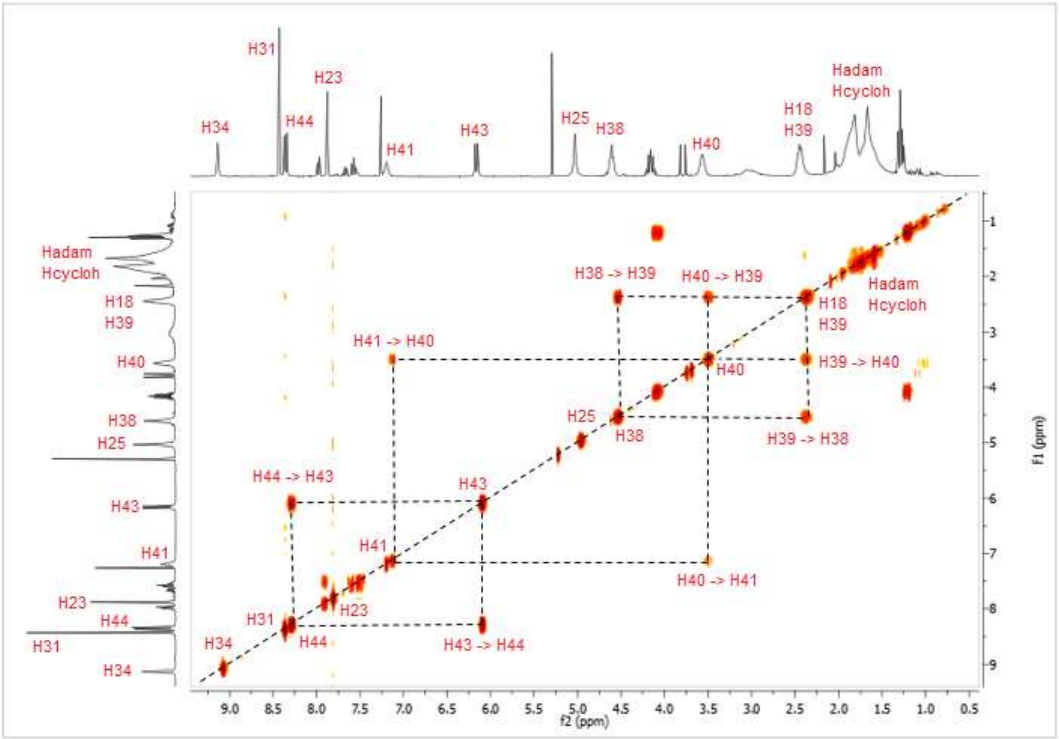

Figure VI.32 – COSY spectrum ($CDCl_3$) of compound **32**.

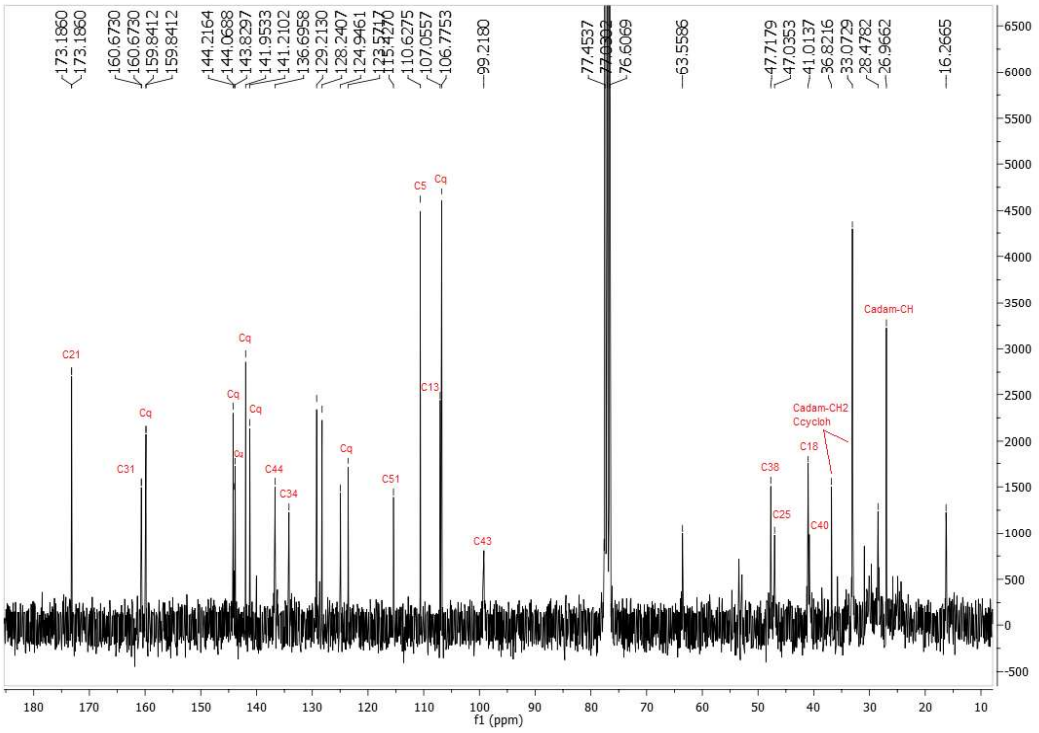

Figure VI.33 - ^{13}C-NMR spectrum ($CDCl_3$) of compound **32**.

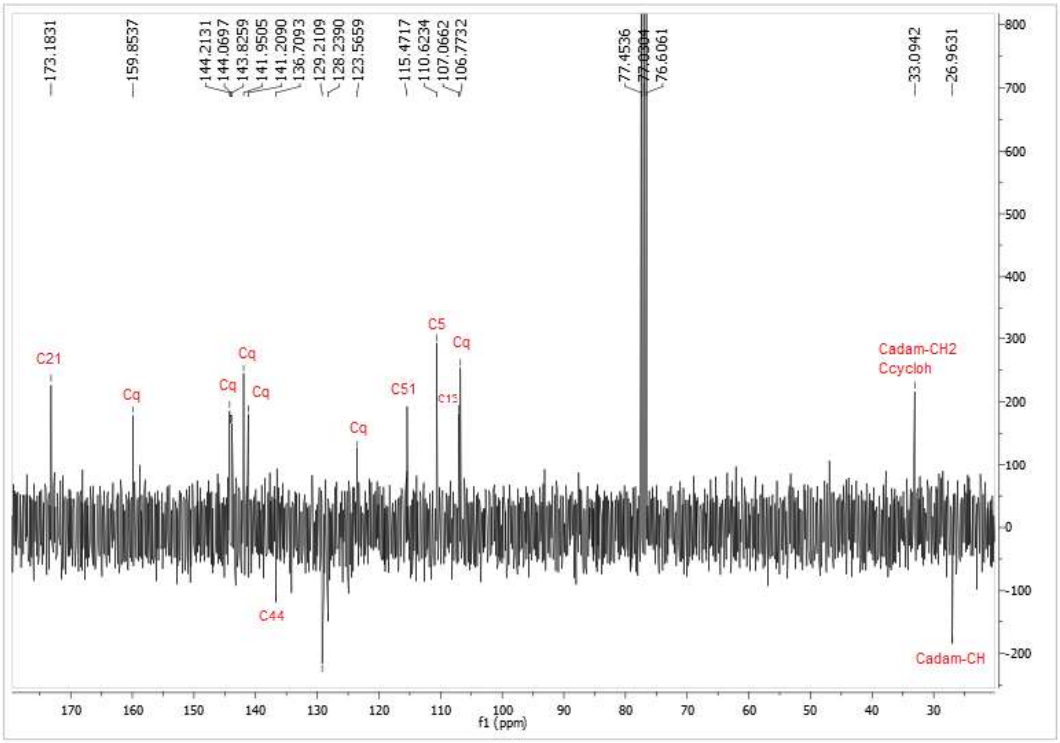

Figure VI.34 – APT spectrum ($CDCl_3$) of compound **32**.

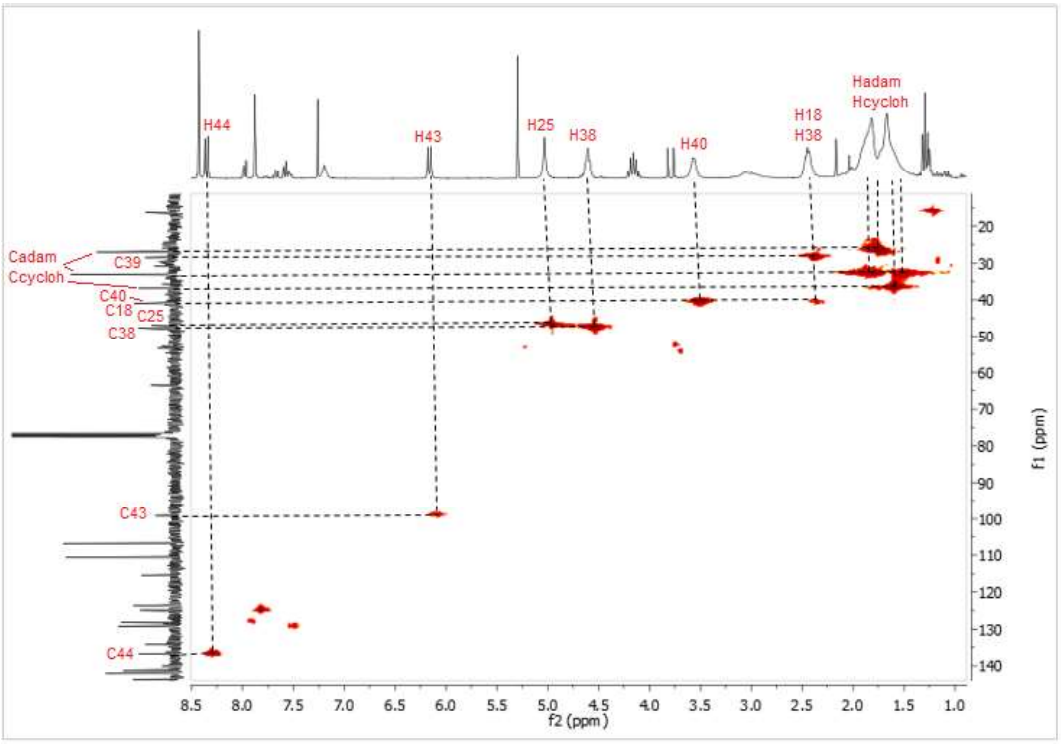

Figure VI.35 – HMQC spectrum ($CDCl_3$) of compound **32**.

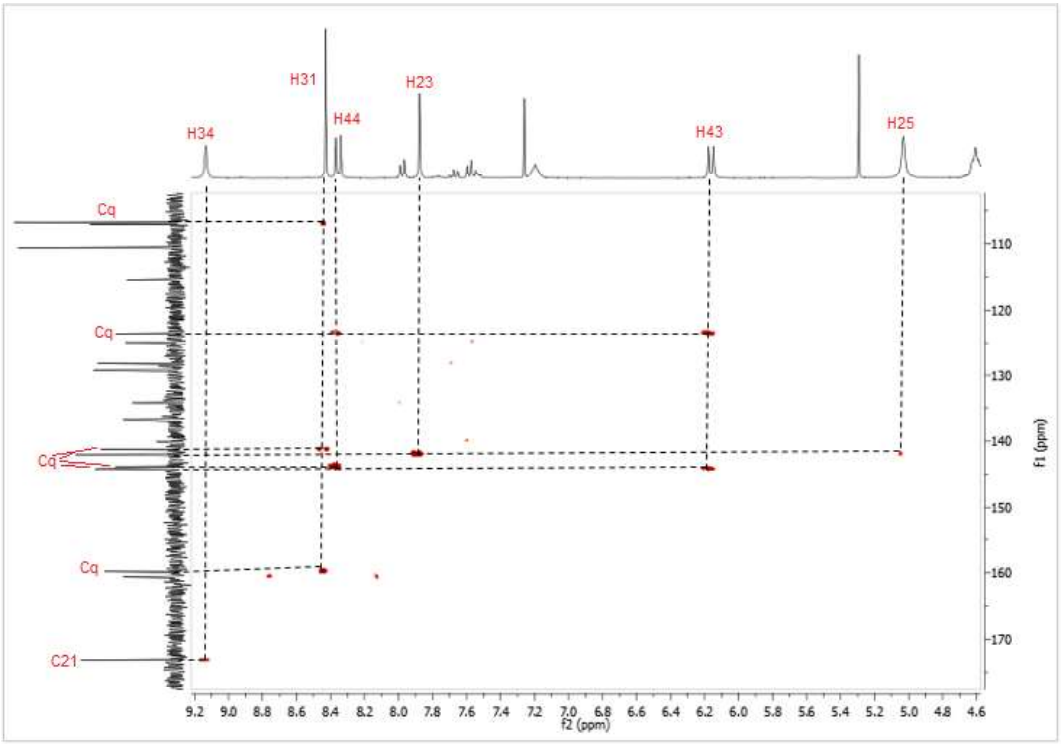

Figure VI.36 – HMBC spectrum ($CDCl_3$) of compound **32**.

VI.11 Adamantane-2-carbaldehyde (48)

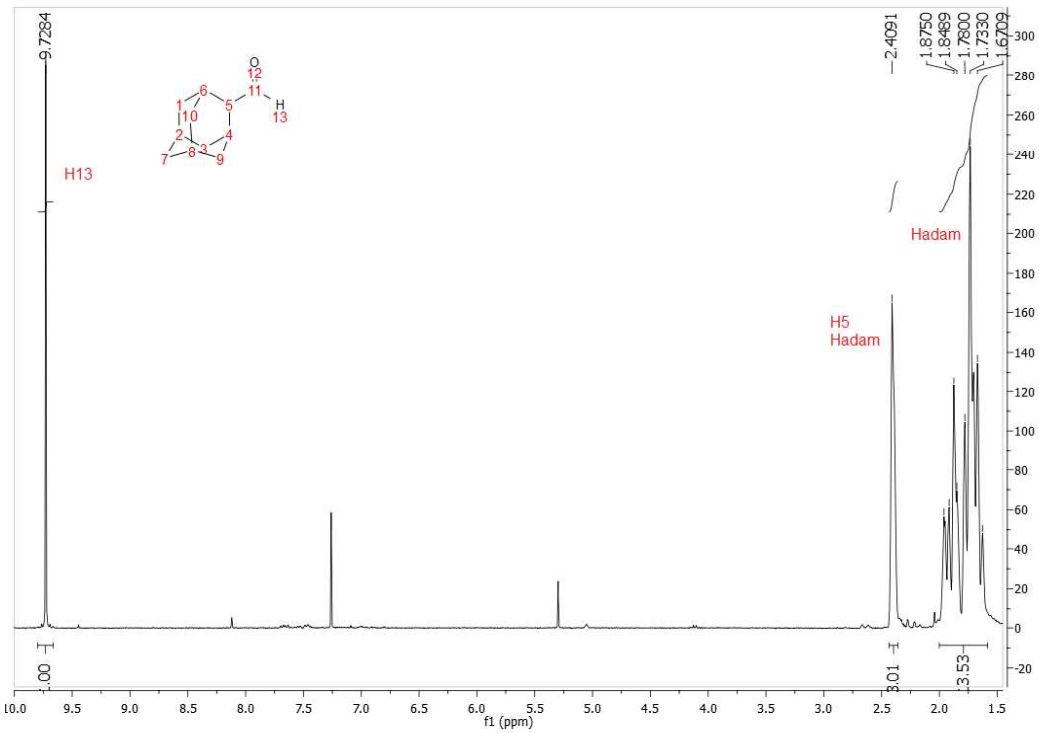

Figure VI.37 - ^{1}H-NMR spectrum ($CDCl_3$) of compound **48**.

VI.12 Adamantane-2,2-diyldimethanol (49)

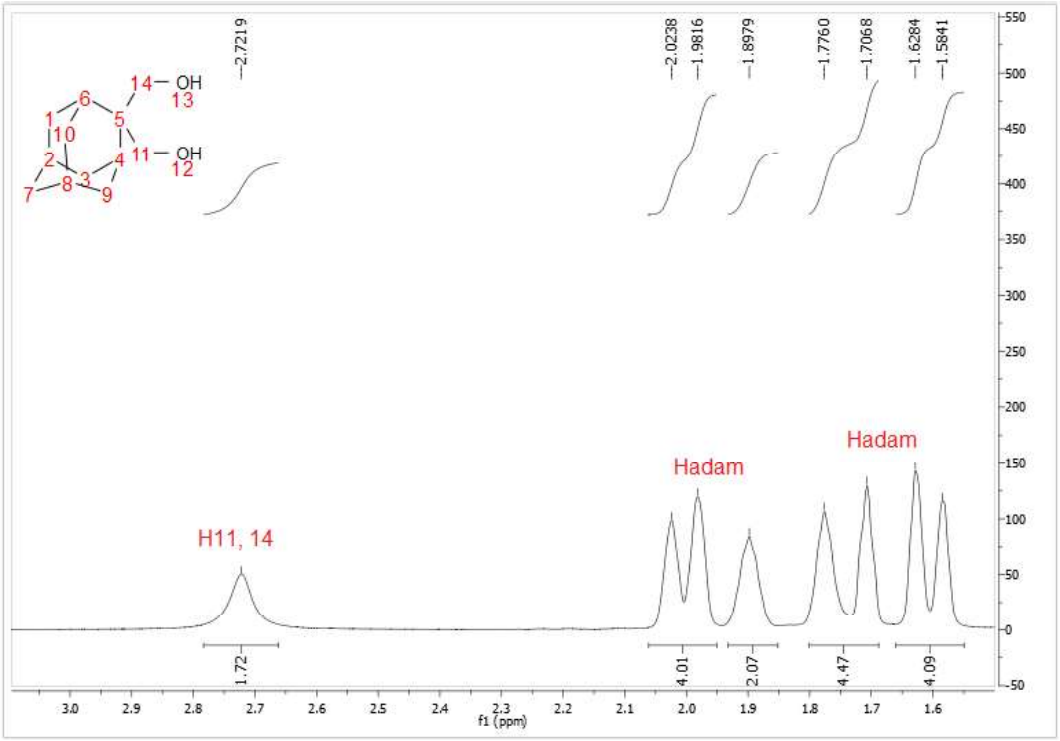

Figure VI.38 - ^{1}H-NMR spectrum ($CDCl_3$) of compound **49**.

VI.13 Dioxane ester (50)

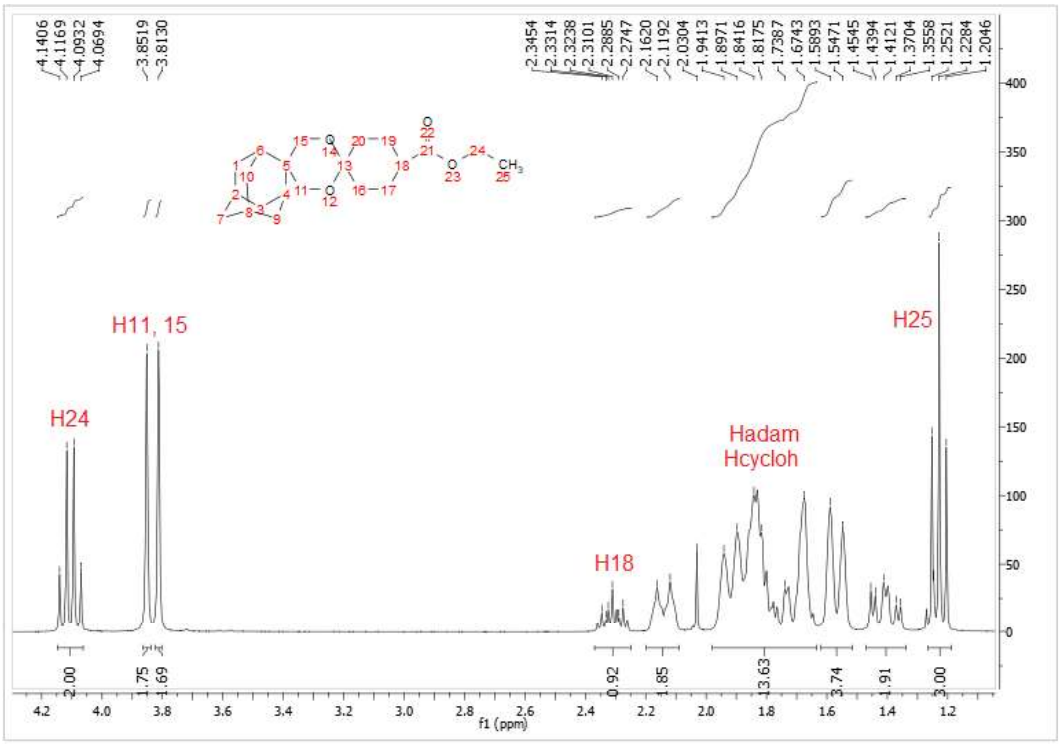

Figure VI.39 - ^{1}H-NMR spectrum ($CDCl_3$) compound **50**.

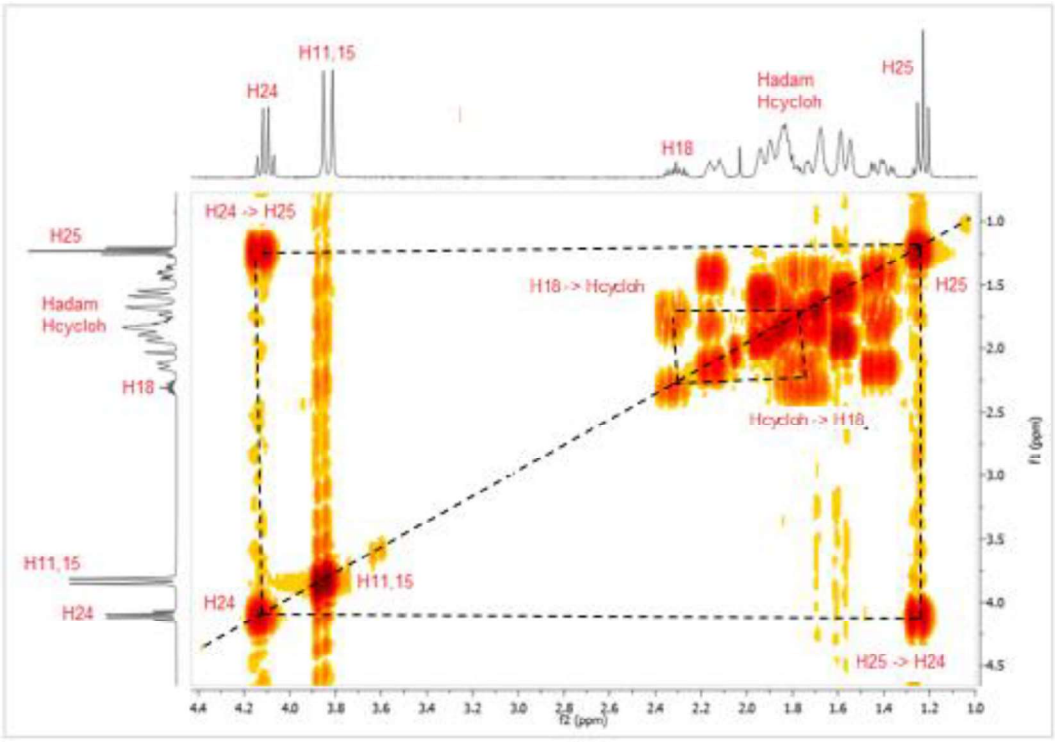

Figure VI.40 – COSY spectrum ($CDCl_3$) of compound **50**.

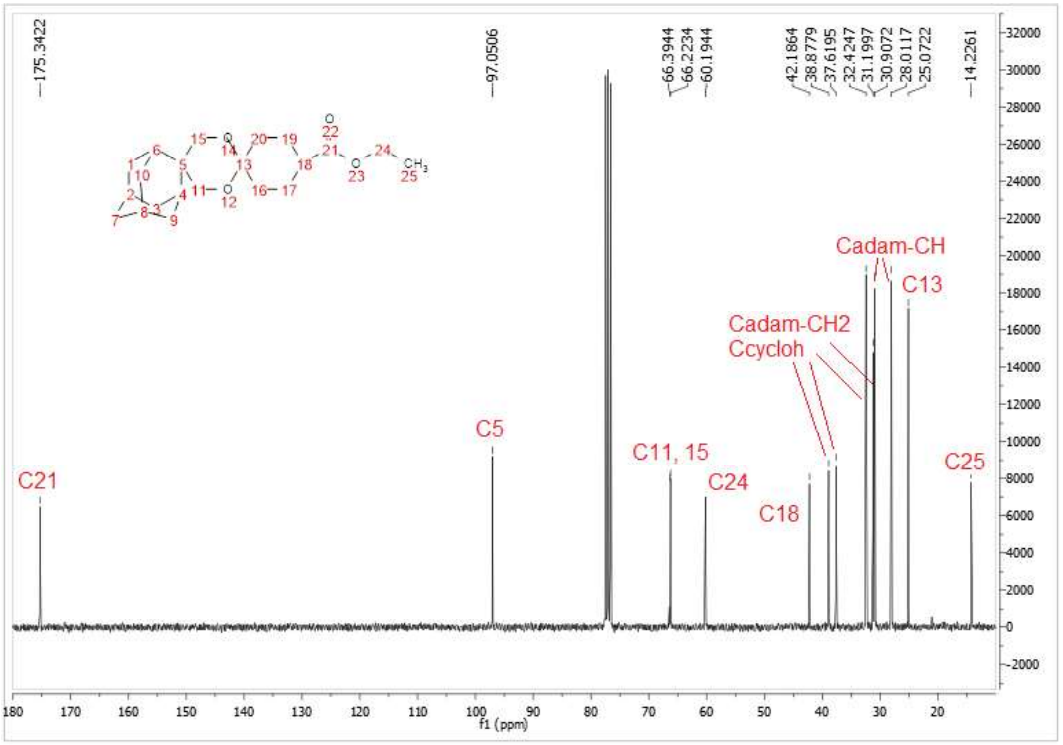

Figure VI.41 - ^{13}C-NMR spectrum ($CDCl_3$) of compound **50**.

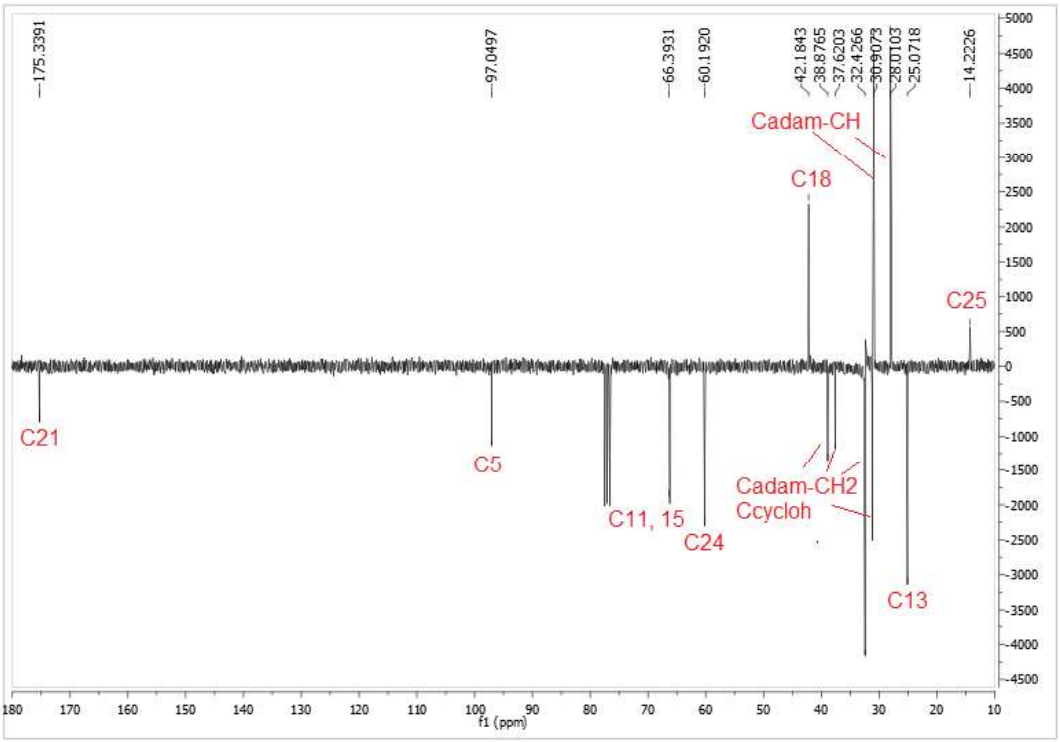

Figure VI.42 – APT spectrum ($CDCl_3$) of compound **50**.

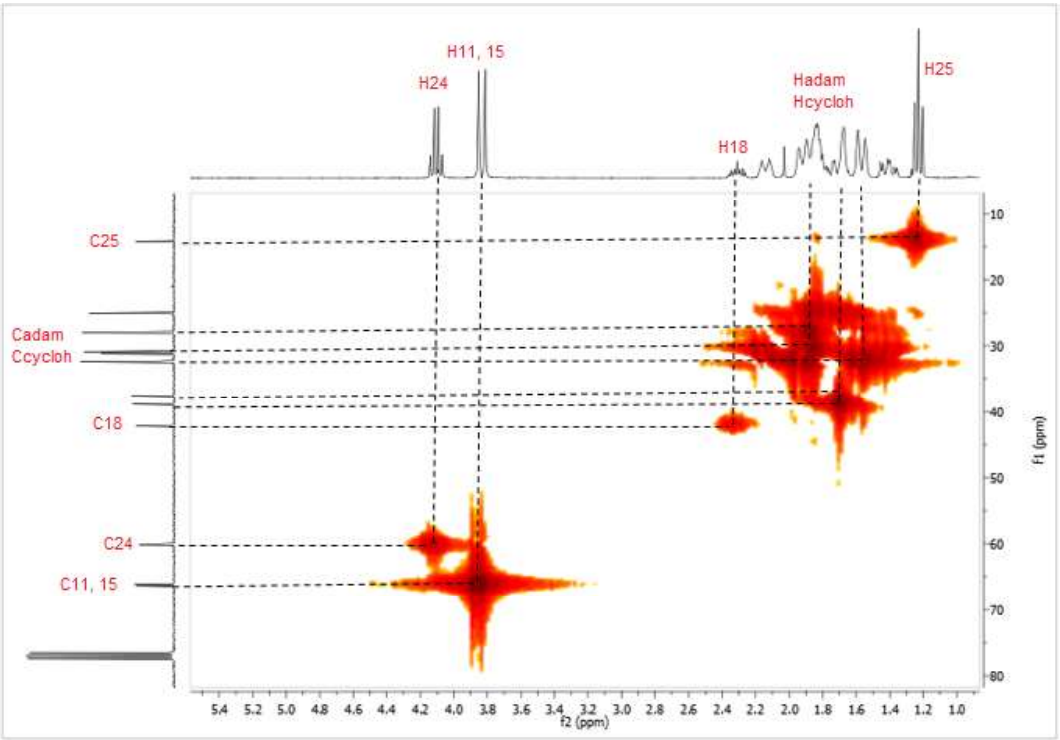

Figure VI.43 – HMQC spectrum ($CDCl_3$) of compound **50**.

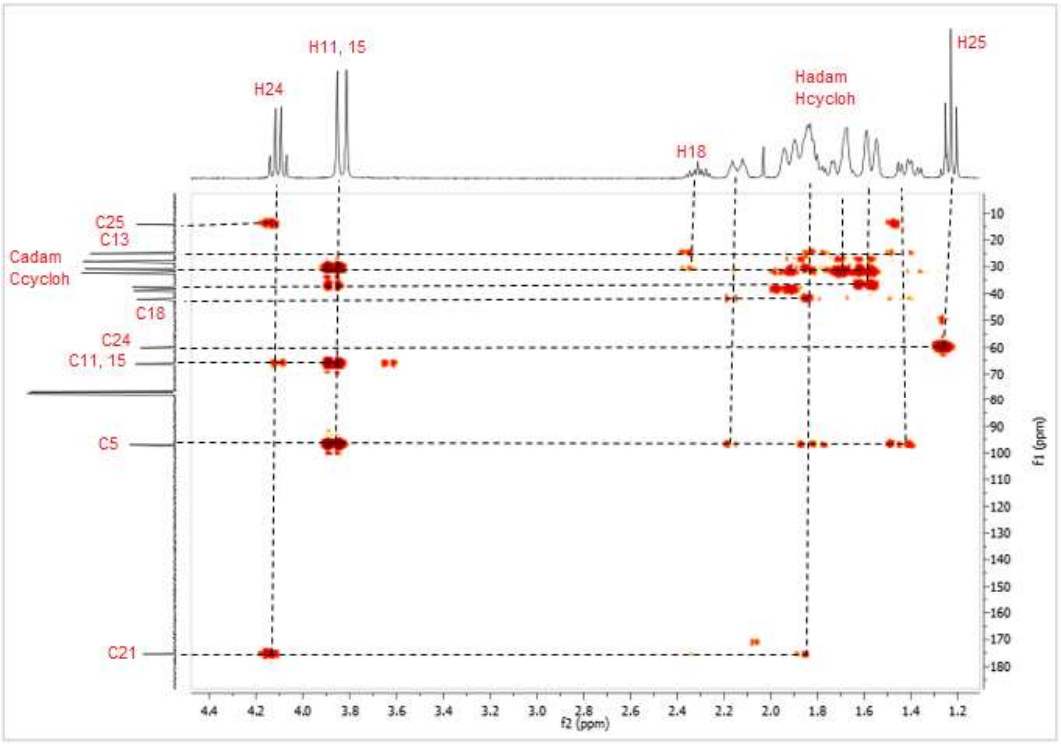

Figure VI.44 – HMBC spectrum ($CDCl_3$) of compound **50**.

VI.13 Dioxane acid (51)

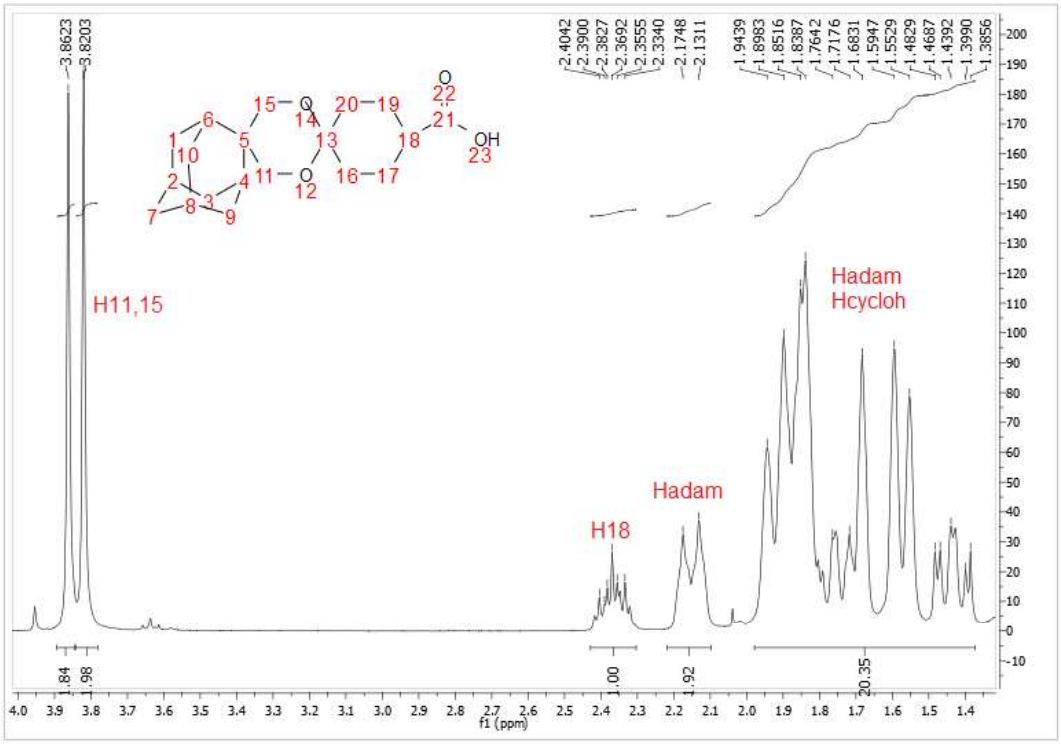

Figure VI.45 - ^{1}H-NMR spectrum ($CDCl_3$) compound **51**.